

Review

Hydrophones, fundamental features, design considerations, and various structures: A review



Hamid Saheban, Zoheir Kordrostami*

Department of Electrical Engineering, Shiraz University of Technology, Shiraz, Iran

ARTICLE INFO

Article history:

Received 18 October 2020

Received in revised form 23 March 2021

Accepted 24 April 2021

Available online 29 April 2021

Keywords:

Hydrophone

Sensitivity

Bandwidth

Piezoelectric

Piezoresistive

MEMS

Low frequency

Ultrasonic

ABSTRACT

This paper presents a comprehensive review of hydrophones, their design considerations, physical aspects, and structures by reviewing many publications that have been published over the last two decades. The investigation of the fundamental aspects and essential considerations of hydrophones in the literature are distributed in different papers and have not been brought together in a conclusive manner. This paper has collected and classified all the information about hydrophones including the parameters that affect their performance as well as their features. We have categorized the hydrophones according to their mechanism of operation, structure design, frequency response, and application. The literature has been summarized in a way that enables the readers' easy referral to appropriate designs for their desired application scenarios.

© 2021 Elsevier B.V. All rights reserved.

Contents

1. Introduction	2
2. Key features of hydrophones.....	3
2.1. Active element size	4
2.2. Spatial averaging: Interference with the acoustic field	4
2.3. Sensitivity	5
2.4. Noise	6
2.4.1. Background acoustic noise	6
2.4.2. Mechanical noise of platform	6
2.4.3. Electrical noise - minimum (noise equivalent) acoustic signal/pressure	6
2.5. Signal to noise ratio.....	7
2.6. Maximum acoustic signal/pressure	7
2.7. Dynamic range (D/DNR).....	8
2.8. Frequency response (Bandwidth).....	8
2.9. Directional response (Directivity).....	8
2.10. Cable effect	9
2.11. Consistency & durability against hydrostatic pressure	10
2.12. Acoustic impedance matching	10
2.13. Influence of water electrical conductivity/dielectric constant	10
2.14. Fragility	10
2.15. Immersion.....	10
2.16. Cost	10

* Corresponding author.

E-mail address: kordrostami@sutech.ac.ir (Z. Kordrostami).

3.	Piezo material for hydrophones	10
3.1.	Piezo-ceramics	11
3.2.	Piezo-polymers.....	12
3.3.	PVDF polymer	12
3.4.	Piezo-composites	12
3.5.	Single-crystal.....	13
3.6.	Piezoelectric metamaterial.....	13
4.	MEMS hydrophones	13
4.1.	FET based hydrophone	15
5.	Piezoelectric/piezoresistive and fiber-optic hydrophones	16
6.	Vector hydrophones	18
6.1.	Cilia-type four-beam vector hydrophone	19
6.1.1.	Sensitivity enhancement approach	19
6.1.2.	Technology improvement approach	21
6.1.3.	3-D redesigning approach.....	21
6.1.4.	Left-right ambiguity resolving approach	21
6.1.5.	Vibration/acceleration suppressing approach	21
6.2.	T-shape vector hydrophone	22
6.3.	Co-vibrating vector hydrophone	22
7.	Hydrophones for different frequency ranges.....	24
7.1.	Hydrophones for infrasonic applications	24
7.2.	Hydrophones for ultrasonic applications	25
7.3.	Hydrophones for low-frequency applications	27
8.	Hydrophones geometries	27
8.1.	Needle hydrophones	27
8.2.	Membrane hydrophone	27
9.	Hydrophone operation mechanism	29
9.1.	Operating at the resonance frequency	29
9.2.	Multimode hydrophone	29
9.3.	Inertia type hydrophone	29
10.	Applications	30
11.	Summery and conclusion.....	31
	Acknowledgments.....	31
	References	31
	Biography.....	41

1. Introduction

Research and development of underwater electroacoustic transducers have grown rapidly in the 20th century and is still an increasingly studied field [1–5]. Studying the electroacoustic transducers, which have found various applications, needs to combine different sciences such as mechanics, electronics, optics, magnetics, semiconductors, and acoustics. Generally, acoustic transducers convert the acoustic pressure to electronic/optical signals and vice versa. Familiar names and accessories such as speaker and microphone which are used as the transmitter and receiver in the air are replaced by the projector and the hydrophone underwater.

The word hydrophone is composed of 'hydro' meaning water and 'phone' meaning sound. In a simple word, a hydrophone is a device for measuring sound in the water - an underwater microphone.

Because the propagation distances of acoustic waves are much larger than that of the electromagnetic waves in water, acoustic waves are the most effective carriers for underwater applications and transmitting information over long-distances [6–8]. Also, the use of communications based on electromagnetic waves is severely limited underwater due to the problems of multipath propagation, time variations of the communication channel, small bandwidth, and the requirement for strong signals [9]. That's why the sound has been widely used in the field of underwater so far [10].

Hydrophones are used to obtain scalar or vector information of the underwater acoustic field and have received wide attention from researchers around the world. Today, depending on the application requirements various designs are available. Hydrophones and other underwater sensors are conventionally involved with

critical technologies including robust mechanical design, acoustic pressure sensing, and advanced electronics [11].

The hydrophone was invented in the year 1929 by a Canadian inventor, 'Reginal Fessenden'. Earlier, the hydrophone was known as Fessenden oscillator. Then, the technology was taken over and the hydrophone was re-designed by France to identify and detect German sappers during World War II.

Generally, micro-machined capacitive microphones - designed to work in the air - can be used as hydrophones. However, the mass loading induced by the heavy fluid environment greatly reduces the bandwidth and degrades the efficiency so that conventional microphones are not suitable for use in hydrophones [12].

The ideas of measuring the acoustic vector, the acoustic particle velocity, and the acoustic particle acceleration have been around for at least 50 years. These are the aspects that the sensing elements of the acoustic sensors usually interact with.

Studies for simultaneous detection of the magnitude and direction of acoustic waves have been carried out since the publication of the research results that measured the velocity of underwater particles in 1956 [13]. Leslie et al. fabricated a hydrophone that measured the flow velocity of water by installing a velocity pickup inside a rigid spherical housing. It was quite directional at low frequencies. The key concept of his design was the mass-spring system, which would convert the particle velocity into a change in magnetic flux. Following this idea, researchers have developed several modified sensors [14–16]. They casted the composites around geophones, making them suitable for underwater application. By replacing the 'spring' with applicable and compliant layers of piezoelectric materials, a similar structure of acoustic vector sensors was designed [14,17–19]. In this case, the output generated by the

acoustic vector sensor is proportional to the particle acceleration, which is itself related to the strain of the piezoelectric material. At the same time, researchers have proposed another type of acoustic vector sensor that used two spatially close acoustic pressure sensor [20]. The underlying principle of sensing in these sensors is based on the Newton's law in fluid, which states that the particle acceleration is proportional to the gradient of acoustic pressure. Although this method is essentially plagued by the errors related to subtracting two almost equal signals that it is not prone to platform vibration but it has been of interest to researchers [21–24].

After more than 10 years, a directional and a low-frequency pressure gradient hydrophone were developed for underwater acoustic fields [25,26].

In 1998, the first piezoelectric, flexural-disk was designed that was inherently a buoyant underwater accelerometer [27]. By evolving the microelectromechanical (MEMS) technology, in 1999, a MEMS hydrophone was presented by Boston University that could detect the acoustic field variations by detecting a reflected laser beam [28].

In the 2000s, rapid advances were made in the area of particle velocity hydrophones and these developments still continue [29].

Traditional vector hydrophones generally adopt the principle of moving-coil or piezoelectric [30]. For example, Britain and France have used a hydrophone made from Polyvinylidene fluoride (PVDF) film in their submarines in the past [31]. There have been many developments in recent years and the detection of underwater acoustic signals with a variety of new sensing mechanisms has been reported. Many countries especially China have developed a variety of vector hydrophones based on different mechanisms, e.g. moving-coil, velocity, piezoelectric (vibrating), piezoresistive and fiber-optic hydrophones. These have led to the realization of various scalar and vector acoustic sensors and a diversity of functions [30].

Different hydrophones structures with different operation mechanisms are used to meet the different needs of the situation in the field of the underwater acoustic measurement. These devices range from conventional commercial use to SONAR (Sound navigation and ranging) apparatus and underwater military weapons.

Instead of a single hydrophone, a 2D or 3D array or network of hydrophones can be used to improve the performance and create new capabilities in each of the active and passive modes based on specific techniques and algorithms.

Some reasons and motivations for the development of hydrophones in recent years can be summarized below:

- 1 In recent years, with the development of high-speed and large-scale ships, accident between ships, collision, stranding, and grounding happens frequently. Underwater acoustic technology by using the scalar and vector hydrophone which acquire the target location by organizing array can improve transport efficiency and traffic safety [32–37].
- 2 With the emergence of smaller size and lower cost hydrophones as well as development of their capabilities such as detection and identification of targets, estimating their distance, direction, and position underwater, they have found wide application in the civil and military domain [13,38,39].
- 3 With the development of underwater acoustic warfare and techniques, high-frequency noise emitted by underwater platforms has greatly reduced each year [40,41]. Due to the reduction of the efficiency of the traditional methods for underwater sound detection, modern hydrophones with high spatial gain, small scale, precise azimuth tracking, and low-frequency operation are considered the best choices in many countries [42–44].
- 4 Almost 71 % of the earth's surface is covered with water. In the future, humans will be heavily dependent on ocean resources. Hence the high performance underwater acoustic detection

equipment is urgently required and the hydrophone is considered as the core component.

5 One of the main challenges that we are facing today is maritime security. Consider that large volumes of our nation's overseas cargo travel through ports and that internationally billions of tons of goods, billions of gallons of petroleum products, and millions of passengers are carried by sea every year. Seaborne and undersea threats from smugglers and terrorists at ports, public waterways, and coastal areas put our safety and economy at risk [45]. Hydrophones are the main technology for safety improvement.

6 Today, "calculus of kidney and ureters" is listed as the major diseases of society [46]. Shock-wave lithotripsy (SWL) is the primary treatment modality of these types of diseases because SWL is effective, non-invasive, and can be used for outpatient treatment. Improving the understanding of stone fragmentation and the risk of tissue damage depends on accurate acoustic field characterization that cannot be realized without hydrophones [47].

Acoustic waves are fundamentally sound waves in any medium. Water is an elastic medium and any disturbance in the water is propagated from its origin as a wave. When water molecules are pushed or broken apart, they apply a restoring force that resists the motion. The force is locally felt as pressure/force per unit. The fundamental parameters of an acoustic wave are pressure and frequency [48]. Functionally, the pressure variations of acoustic waves along with the ambient sea or other noises in the detectable frequency bandwidth reach the vector hydrophone or hydrophone array, then they are converted to electric/optical signals by the hydrophone. By processing the acoustic (field) information received by the hydrophone, the existence of the target and its other status features can be determined. It may also be useful to characterize the distribution of an acoustic field. Consequently, the required information about the target or field can be provided.

Investigating the literature shows that over the last decades, published works on performance improvement in have generally focused on the algorithm or signal processing and innovations or changes in the hydrophone physics. Improving measurement techniques is another favorite subject that has its own research papers [49,50]. But our main approach in this paper is to comprehensively review the design, development, and fabrication of various types of hydrophones and we do not address signal processing issues. This paper begins with key considerations and features for hydrophone development. Then it examines the process of piezoelectric material development for being used in hydrophone. Descriptions of different hydrophone divisions based on scalar/vector, frequency range and transduction mechanism such as piezoelectric or fiber optic as well as various geometries under development such as needle or membrane types are presented. Our approach in each section is to compare and express the main features of each type. It should be noted that the vast majority of hydrophones used worldwide are based on piezoelectric in essence. Consequently, the literature corresponding to the modeling, fabrication, characterization and application of piezoelectric hydrophones is extensive. That's why the main focus of this paper is on recent non-optical hydrophones, especially piezoelectric and MEMS hydrophones. The importance of this paper is in presenting the outline of various structures of hydrophones and the comparison of the hydrophone capabilities in different applications.

2. Key features of hydrophones

The characteristics of each underwater transducer are not completely determined unless its performance is measured practically. This is known as the calibration procedure [51]. This section

provides a general overview of hydrophones' important issues, physical aspects, and performance features and parameters that are necessary to be considered and determined. Understanding these features helps the users in making the right choices when selecting a particular type of hydrophone for a definite application. For more detailed information and understanding of other parameters, the readers are encouraged to refer to the textbooks by Bobber [52], Stansfield [53] or Wilson [54]. There are many parameters to consider when designing hydrophones. These parameters and their desired values for a high performance hydrophone are as follows: Low size, high sensitivity, high free-field voltage sensitivity (FFVS), high noise resolution, large signal to noise ratio (SNR), large dynamic range, high bandwidth, good linearity, and high spatial resolution. Also, important physical aspects that affect the device performance such as the spatial averaging, cable effect, hydrostatic pressure, and acoustic impedance matching to the liquid medium need to be paid attention. Fabrication method simplicity, using off-the-shelf components and hand tools which translates into ease of fabrication and reduction in the unit cost are also essential considerations in the design and manufacture of hydrophones. The designer should be familiar with the newly developed modeling and optimization methods to determine the responses before entering the fabrication process (especially for micro-acoustic transducers) [55–57]. Using efficient fabrication methods instead of processes that are chiefly responsible for the cost and difficulty is another requirement [58]. Packaging or encapsulation is also one of the essential issues in the development of hydrophones that has a direct impact on the sensitivity.

The most important factors in the development and design of hydrophones are explained below.

2.1. Active element size

The size of the active element of a hydrophone is an important parameter because of the following reasons. First, when a typical hydrophone is placed in a real acoustic field, it must cause less influence on the original acoustic field. However hydrophones suffer from unwanted noise created as the result of their presence in real fields. Ideally, the measured data should close the true value but the impacts of this type of noise makes some problems and particularly in fast flows it becomes more problematic [59]. Bharath et al. [60] using COMSOL turbulence modeling software, simulated and quantified the design features of the Ocean Sonics hydrophone and showed how it leads to adverse acoustic noise. (See Fig. 1)

According to the acoustic theory, the scattering of an incident acoustic wave caused by hydrophones can be ignored whenever condition $k\alpha \ll 1$ is true. (k is acoustic wavenumber and α is the hydrophone radial size). Accordingly in the far field condition, the hydrophone is equivalent to water particles, as shown in Fig. 1 [31].

When the physical dimensions of the hydrophone (usually probe) are smaller than the acoustic wavelength of the studied field, the hydrophone operates approximately like a point receiver and the received acoustic field has a planar wave front [61]. Second, many applications such as therapeutic ultrasound and sonar with small aperture need small size hydrophones to provide the required features. Particularly when it is composed of an array it can have a large size and this easily leads to scattering and the consistency and stability cannot be guaranteed [62]. Third, if the sensor size (diameter) is decreased, random errors increase. This is because the capacitive component of the output impedance of the hydrophone is reduced while the capacitance of its fittings is constant. Simultaneously, the systematic errors caused by averaging the acoustic pressure over the surface of the hydrophone with finite size (in terms of wavelength) reduces [63].

Keith A. Wear et al. [64,65] have provided a guide to show the effect of sensitive element size on the distortions caused by mea-

suring the pressure of the nonlinear ultrasound signals for a variety of hydrophones. The authors have also introduced some inverse filters to correct these distortions [66–68]. Generally, needle type hydrophone has the smallest size and this is followed by the encapsulation design, but membrane-type hydrophones are very large in terms of the active element.

2.2. Spatial averaging: Interference with the acoustic field

In some applications like characterizing of medical ultrasound devices the safety and effectiveness are extremely vital. This can be done by a hydrophone which senses the pressure distribution incident on its sensitive element [69,70]. Unfortunately, like most measurement devices, the measurement of the incident pressure wave by hydrophones is associated with distortion. This distortion has two main origins: frequency-dependent sensitivity and spatial averaging across the sensitive element.

When a hydrophone scans an acoustic field, the measured beam profile is the convolution of the hydrophone aperture with the true acoustic pressure distribution. If the hydrophone aperture is too larger than the spatial variation of the acoustic field, the accurate location of the spatial peak will not be resolved. That is, its peak amplitude will be underestimated whilst beam width becomes overestimated. This effect is known as spatial averaging [71]. An indication of the overall trends of this effect is illustrated in Fig. 2. Note that this graph represents the subject only as one-dimensional, whereas hydrophone spatial averaging is a two-dimensional effect. Therefore, the convolutional nature of spatial averaging means that any change in the shape or dimension of the hydrophone aperture and/or the source pressure distribution causes different results.

Generally, as the size of the hydrophone's sensitive element is increased, sensitivity tends to be optimally increased but the spatial averaging also increases. Needle and fiber optic hydrophones are now available in a wide range of sensitive element sizes from 7 μm to 1 mm and above, making the choice difficult and field-dependent [64]. Spatial averaging has the potential to affect calibration that must be watched.

One simple method to resolve this impasse is to apply a spatial equivalent of the Nyquist–Shannon sampling. Considering that the dimensions of the hydrophone are not greater than half the smallest wavelength present in the field, the spatial averaging can be ignored for most cases.

A more rigorous approach has been proposed by Radulescu et al. [72] in 2004 that uses a mathematical model to simulate the hydrophone's spatial response. They derived the necessary spatial averaging correction algorithm. Recently, Eleanor Martin and Bradley Treeby [73] have shown that at low frequencies, effective element sizes of hydrophones are much larger than their nominal element sizes. This should be considered for evaluating a field with small pressure spatial variation. Their study suggests that, at least in the cases tested, the spatial averaging is the largest source of measurement error. When spatial averaging is not significant or appropriate corrections have been applied, broadband acoustic/pressure fields are measured with differences of less than 10 % with a set of hydrophones, as long as their frequency response over the required bandwidth is known and variations are captured at the correct scale.

Spatial averaging can be a more complicated problem in quantifying high amplitude acoustic waveforms. With the emergence of nonlinearity properties in ultrasonic propagation, the acoustic signal spectrum at some distance away from the source comprises harmonics in much higher frequencies (shorter wavelengths). Non-linear acoustic signals have wide frequency bands covered with multiple harmonics from the fundamental frequency. Therefore distortions tend to increase with signal nonlinearity. As harmonic

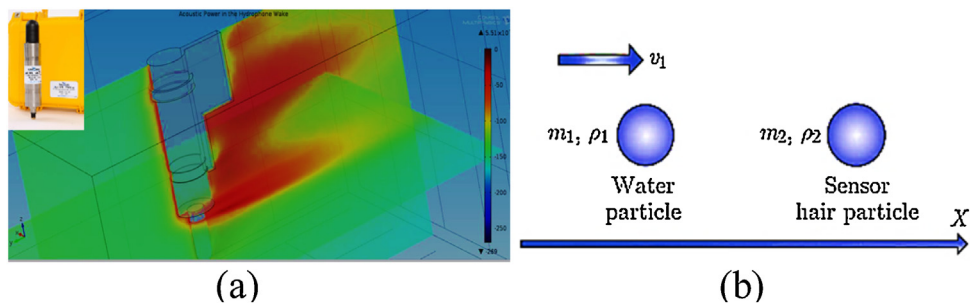


Fig. 1. (a) Acoustic Power in the wake following the hydrophone (dB) (An Ocean Sonics ic Listen 3500 hydrophone and CAD model. Source: <http://oceansonics.com/iclisten-smarthydrophones>) and (b) Water particle with sensor hair particle.

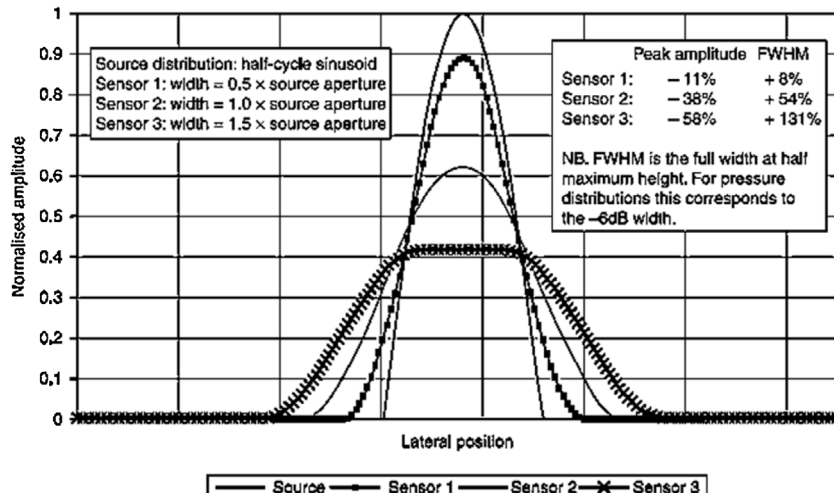


Fig. 2. The effect of spatial averaging on measured beam profile [71]. For three typical configurations the integrated signal amplitude is the same. The smallest sensor provides a reasonable estimation of the source distribution with error in both peak amplitude and full width at half maximum (FWHM) being approximately 10 %. However, the pressure profile derived from the largest sensor contains gross errors, with the peak amplitude being less than half of its true value and the FWHM being more than double that of the source distribution. In this case, the user may be oblivious to the spatial averaging, since the erroneously large FWHM would imply the field much broader than the sensor used to measure it.

frequency increases because of the nonlinearity effect, the harmonic beam width decreases, and the harmonic spatial averaging potential increases [65]. In 2011 Cooling et al. proposed a numerical method using non-linear Khokhlov-Zabolotskaya-Kuznetsov (KZK) equation to quantify the spatial averaging factor as a function of the frequency of the source, pressure amplitude, and hydrophone diameter [74]. In 2018, Keith A. Wear [64] developed a guide for the effect of sensitive element size on the distortion of nonlinear ultrasound signals from pressure measurements performed with needle and fiber-optic hydrophones. They also provided an inverse filter to correct this distortion.

The output of a hydrophone is generally related to the average pressure across its active area. If the acoustic field varies in amplitude (or phase) across this area the output of the hydrophone will differ from the case acting as a point-like receiver. This can cause errors in the measurement of the pressure in the focused and nonlinear acoustic fields [75,76]. The ratio of the spatial average to axial pressure applied to the hydrophone is termed the area-averaging factor [74]. This factor is another consideration for designing hydrophones.

2.3. Sensitivity

Sensitivity of a hydrophone reflects its ability to transform acoustic pressure to an output voltage for normally incident, quasi-planar acoustic pressure waves as a function of frequency [66]. Due to features such as weak and non-contact underwater acoustic sig-

nals, high sensitivity in hydrophones is essential. If the sensitivity over the frequency band is approximately uniform in the pressure spectrum, it simply requires multiplying a scale factor (S). For broadband signals (e.g. nonlinear signals containing multiple harmonics) the sensitivity may vary considerably over the frequency band in the pressure spectrum and the deconvolution can provide a significant improvement in the accuracy compared with scaling [49,77–84].

Usually, in underwater acoustics, it is a common practice to specify hydrophone sensitivity in term of dB (re: 1 V/Pa), instead of the simpler linear unit of mV/MPa used at higher frequencies. It can be easily shown that -240 dB (re: 1 V/μPa) is equivalent to 1 V/MPa. The equation describing sensitivity is shown below:

$$S = 20\log(\Delta U / \Delta P \sigma^{-1}) \quad (1)$$

Where ΔU is the changes of the output signal of the hydrophone, as a result of increased acoustic pressure ΔP . $\sigma = 1 \text{ V}/\mu\text{Pa}$ is considered as a reference sensitivity level. For multi-dimensional hydrophones, as sensitivity is defined in each dimension. A balanced multi-axis sensitivity largely promises ease of signal processing [85].

Another feature of the hydrophones is FFVS [86]. It is defined as the rms voltage measured from the open circuit output terminals of the hydrophone in response to $1\text{ }\mu\text{Pa}$ input pressure [51].

Today, to define hydrophone properties, measurement standards use only the amplitude response criterion. However, access to the phase information, not only completes the specifications but also enables the conversion of voltage to the pressure using full complex deconvolution [87]. Martin P. Cooling and Victor F. Humphrey [88] have demonstrated the feasibility of obtaining phase calibration for a membrane hydrophone.

The sensitivity of hydrophones depends on many factors such as the materials used, the dimensions of the structure, the transduction mechanism used, and even the electrical parameters of the structure. In general, piezo-based hydrophones should have a high value of RC (Where R is the DC resistance and C is the capacitance between the terminals of the hydrophone.) because if their resistance is low, the open-circuit nature of the hydrophones reduces their sensitivity [89]. Sensitivity can usually be characterized by various calibration methods, usually depending on the frequency response of the hydrophone.

2.4. Noise

2.4.1. Background acoustic noise

Studying the operation environment of hydrophones which can be as complex as the sea in terms of noise is essential for the engineering of practical devices. The sensitivity of hydrophones in the test condition in an ideal anechoic water tank is high but when signal source distance to the hydrophone is long, the signal is severely attenuated and may impair hydrophone performance. On the other hand in the maritime environment, there is plenty of background noise, which includes the sound of waves, ocean flows, eddy currents, and biological and artificial activities. These noises are often serious and powerful and depend entirely on the ambient conditions [90]. In this environment, the signal may be sunk into the noise and reduce the SNR which affects the performance of the hydrophone. Therefore, environmental noise limitations are important in the development and application of hydrophones [62]. In this regard, Zhili et al. [91] have studied and characterized marine ambient noises. Also, John A. Hildebrand [92] in 2009 have studied the ocean ambient noise that results from both anthropogenic and natural sources. According to this, different noise sources are dominant in 3 frequency bands: low-frequency band ($10\text{--}500\text{ Hz}$) that is dominated by anthropogenic sources such as shipping and seismic sources which has had an increasing trend in recent years, medium frequency band (500 Hz to 25 kHz) which includes some noises caused by natural and anthropogenic phenomena and high frequency band ($>25\text{ kHz}$) such as thermal noise that is dominated noise source above about 60 kHz .

In the absence of periodic and local effects, such as lack of anthropogenic sources and calm sea conditions, acoustic background noise reaches its minimum value, which can be used as a reference for hydrophone design. Fig. 3a shows the acoustic background noise (Wenz's minimum noise) [93] decreases with increasing acoustic frequency (dashed curve). Also, the ambient thermal noise increases proportionally with the acoustic frequency (dotted curve) due to the Brownian motion of the water particles [94]. Therefore, at around 30 kHz , the ocean noise is minimized (solid curve).

When using hydrophones in noisy seawater environments, undesirable interferences such as swing and vibration of suspended hydrophone cables or noise generated during the flow of water adjacent to the hydrophone must be eliminated or reduced [95]. Based on the experimental results measured by Lee et al. in the shallow sea, screening the hydrophone with 3-cm-thick foam reduced the ambient noise up to 24 dB below 50 Hz . It also seems that

the effect of foam to reduce noise at higher frequencies is greatly reduced [96].

On the other hand, although noise may be considered as a negative factor, in some applications noise is used to identify the type of the target only by analyzing its noise because the noise generated by each particular object has a unique signature. Many databases have been developed in the field of underwater sounds. ShipsEar is one of these databases that contains both natural and anthropogenic background noise with more than 90 recorded sounds from 11 different ships. It has been prepared for the use of researchers in different fields such as vessel detectors and classifiers or to monitor maritime traffic. The results of accuracy and usage of this database are available in [97].

2.4.2. Mechanical noise of platform

Hydrophones are usually attached to the case of a platform. Therefore, some kind of non-acoustic and mechanical noises due to acceleration and vibration of the platform are transmitted to them. As a result, Hydrophones should have low sensitivity to acceleration so that the output voltage imposed by the platform is less than water-borne noise [89,98].

Mechanical noise reduction in hydrophones can be realized using a variety of techniques such a rigid mounting and shock resistance, which are described in more detail later in this paper. Generally, the acceleration sensitivity plot of a hydrophone should not have peaks in the desired bandwidth [89]. Fig. 3b shows a sample hydrophone with a bandwidth not exceeding 80 kHz , but it has provided strong acceleration sensitivity at higher frequencies.

2.4.3. Electrical noise - minimum (noise equivalent) acoustic signal/pressure

All electrical systems have inherent noise. Hydrophones are no exception and their noise figure can be measured. The minimum measurable acoustic signal is related to the electrical noise due to acousto-electrical transduction in hydrophones. This is conveniently achieved by noise equivalent pressure (NEP), which is the acoustic pressure that triggers an SNR of unity. This quantity is insensitive to the details of the transduction method and implicitly includes any hydrophone gain or attenuation. It is also inherently related to the sensitivity of the hydrophone and the noise floor of the system used to record the output signal of the hydrophone which is called the data acquisition (DAQ) system. Consider an idealized hydrophone with a uniform sensitivity of 100 mV/MPa over the 100 MHz bandwidth and noise level of $50\text{ }\mu\text{V rms}$ over this bandwidth. NEP is as follows:

$$\frac{50\text{ }\mu\text{V}}{100\text{ mV/MPa}} = 0.5 \times 10^{-3} \text{ MPa} = 500 \text{ Pa rms} \quad (2)$$

This simple and initial example illustrates two complexities. First of all, the minimum quantifiable signal in the majority of current DAQ systems is about 0.5 mV . Therefore the practical NEP of the hydrophone connected to such a DAQ system is at least equal to the inherent noise floor of the hydrophone. As such, the theoretical and practical differences that can be obtained due to limitations of using the DAQ system should be considered. Secondly, contrary to the above assumption, the sensitivity of the hydrophone depends on the frequency and ideally a spectral method is needed to obtain the NEP. However, in many applications, in order to prevent complexity, the sensitivity of the nominal hydrophone is assumed to be uniform in the bandwidth [71].

Ideally, the hydrophone self-noise throughout the operation bandwidth should be on the same order of magnitude of the noise floor of the target environment, such as the ocean. Therefore, ambient noise is not collected and it will also not have to compromise dynamic range and non-sensitivity to hydrostatic pressure to achieve excess sensitivity [99].

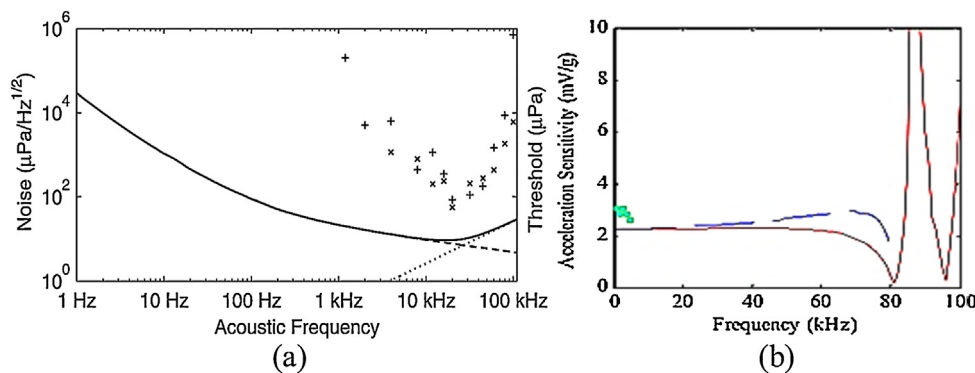


Fig. 3. a) Minimum acoustic noise in the sea (solid curve), with contributions from the acoustic background (dashed curve) and the thermal agitation of water molecules (dotted curve) [94]. b) The magnitude of the acceleration sensitivity of a hydrophone. Solid Line: Analytical Model, Dashed Line: finite element model, Dot: Measurement [89].

In addition, having a high NEP can limit the use of hydrophones in high acoustic pressure regions. Liu et al. [77] have described the effects of hydrophone choice in the high-intensity ultrasound pressure field.

Methods for noise characterization of various types of hydrophones and preamplifiers have been studied in [100,101].

2.5. Signal to noise ratio

Signal characteristics and the specifications of the ambient (such as ocean) are of fundamental parameters in the design of acoustic systems, including hydrophones which have a major impact on the quality of detection, classification, localization and tracking of the acoustic signals. The SNR is one of the critical performance parameters that should be estimated. Bosworth et al. [102] identified methods for determining SNR and have begun applying these techniques to test and evaluate marine engineering systems. Moreover, there are complexities in measuring SNR. There are various approaches to compute the SNR when the signal power relative to the noise power is high in one band and low in the other band. For example, integrating the power of signal divided by the integration of the power of noise over all frequencies, i.e., a total signal power to total noise power. Each method may have a different result in obtaining an average SNR.

Carey [103] suggests that the characterization of the acoustic signal source depends entirely on whether it is continuous or discrete, or whether the transient duration is short or long. Moreover, the results may be dynamic. Ross [104] also observed that the increase in world shipping has caused the low-frequency marine ambient noise to increase by an average rate of about 1/2 dB per year.

There are generally many things to do to control SNR in hydrophones, but as a general rule, hydrophones must have a high value of M^2C (where M is the FFVS and C is output capacitance of hydrophone) to minimize SNR-damage in the hydrophone-preamplifier combination [105]. Fig. 4a shows the spectral noise of a typical hydrophone/preamplifier compared to the ocean ambient noise level.

2.6. Maximum acoustic signal/pressure

Limitations of linearity are usually due to the overload conditions of the input stages of preamplifiers or sensitive elements of hydrophones. If the amplitude of the input signal corresponding to the acoustic pressure exceeds the supply voltage of the preamplifier, then a hard clipping in the waveform is created at the maximum and/or minimum voltage excursions. In contrast, the overloading of the sensitive element is often accompanied by a

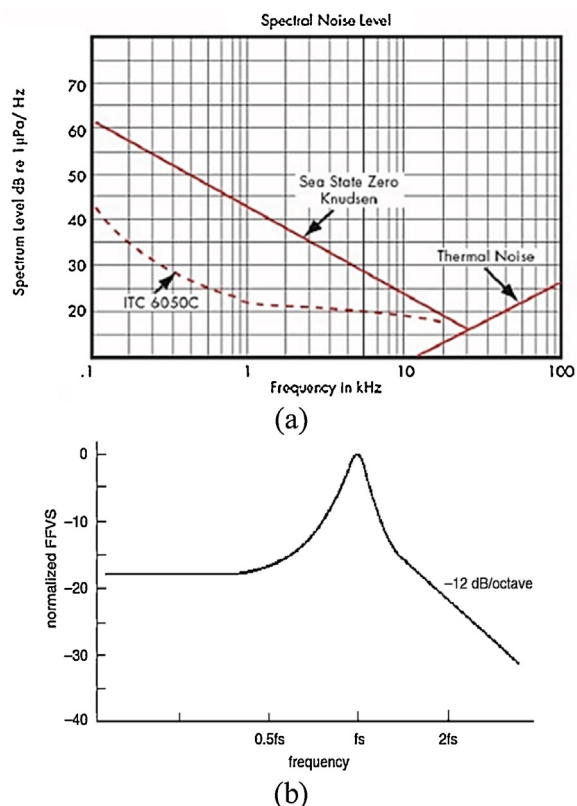


Fig. 4. a) Spectral noise level of a typical hydrophone and its preamplifier to be compared to the ocean ambient noise level [112]. b) An idealized FFVS of a piezoelectric hydrophone [51].

kind of soft clipping, which is usually accompanied by a progressive linear deviation between the output and input signals.

These limitations are often addressable by defining a suitable attenuator in the structure and usually do not result in damage to the hydrophone structure.

Damage thresholds are one of the serious considerations for the development of hydrophones because they may be subjected to temporary or even irreversible degradation in their performance. In some applications, such as therapeutic ultrasound where destructive acoustic fields are deliberately designed, or Lithotripsy, which uses high-amplitude and short-duration pressure pulses, waveforms have a long rarefaction phase that pulls the sensitive element of the hydrophone away from other parts of the device.

Additionally, gas emboli inside the liquid may cause the active element of the hydrophone to cavitate. Even the High Intensity Focused Ultrasound (HIFU) or High Intensity Therapeutic Ultrasound (HITU), which operate at lower pressures, may damage or deform the sensitive elements of hydrophones. These effects are caused by a thermal mechanism (for example, thermal depolarization of piezoelectric devices) due to the quasi-continuous nature of HIFU/HITU signals. As a result, an acoustic intensity threshold alongside the cavitation-induced degradation potential needs to be considered [71]. In the literature of hydrophones, pressures over 100 MPa are considered as high pressure.

2.7. Dynamic range (D/DNR)

Dynamic range (D) indicates the range of variations in the undistorted pressure measured by the hydrophone that determines the amount of hydrophone resolution and is usually calculated by the following equation [106]:

$$D = 20\log(P_{\max}/P_{\min}) \quad (3)$$

Where P_{\max} is the Maximum acoustic pressure that the hydrophone can tolerate or measure and P_{\min} is the Minimum acoustic pressure discussed previously.

2.8. Frequency response (Bandwidth)

A temporally localized acoustic signal contains a wide range of frequencies and one of the most important factors in hydrophones is their ability to measure different acoustic frequencies. In other words, the sensitivity of hydrophones generally depends on the frequency at which the description of this dependence is necessary.

The first conceivable refinement for the sensitivity equation is that its variables are considered as a function of frequency, f [71].

$$S(f) = \frac{\Delta U(f)}{\Delta P(f)} \quad (4)$$

Where ΔU is the output signal variation and ΔP is the change of the acoustic pressure. International Electro-technical Commission (IEC) (2007a) [107] recommends two possible approaches for conversion of voltage to pressure incorporating frequency-dependent sensitivity. If the bandwidth of an acoustic signal is narrow or the variations in the sensitivity of the hydrophone are minimal within the acoustic working frequency (AWF) range, it can be assumed that the sensitivity is constant and the approximation of a narrow band acoustic pressure can be considered as follows [71]:

$$P(t) = \frac{\Delta U(t)}{S(f_{awf})} \quad (5)$$

If this narrowband approximation is not appropriate, then a frequency domain deconvolution is used to express the voltage to pressure conversion [71]:

$$P(t) = \mathcal{I}^{-1} \left\{ \frac{\mathcal{I}\{\Delta U(t)\}}{S(f)} \right\} \quad (6)$$

Where \mathcal{I}^{-1} denote the Inverse Fourier transform.

Hydrophone bandwidth requirements are specified by the American Institute Of Ultrasound In Medicine/National Electrical Manufacturers Association (AIUM/NEMA) measurement standard [108]. In general, Hydrophones should have high bandwidth regardless of the direction in which the acoustic signal reaches. Bandwidth may be limited by factors such as a roll-off in the sensitivity at low frequencies, a resonance in the sensitivity at a high frequency, or even a change in the directivity of the hydrophone [109].

In the ultrasonic domain, the revised AIUM/NEMA measurement standard recommends that the ultrasound hydrophone probe

should be designed to work within a range of one-twentieth of the central frequency to more than eight times its operating frequency in order to accurately determine the acoustic signals. The upper frequency limit is usually considered for the nonlinear propagation phenomena, which leads to the generation of higher harmonics in the pressure-time waveform in liquid mediums. The lower frequency limit is also considered to minimize the overall error in determining the mechanical index, which is an important safety parameter [110]. These considerations are carefully documented in [111].

In some cases, the system bandwidth is intentionally filtered to a lesser extent than the hydrophone bandwidth to increase the SNR ratio. In other cases the bandwidth may also be increased by using compensating filters to neutralize the effect of resonance.

Among all the bandwidth limiting factors, the resonance frequency of the hydrophone is more important as an indicator of the performance of a hydrophone. It is generally preferable to use hydrophones under their resonance frequency so that the transfer function remains flat over a wide frequency range. As a result, hydrophones should be designed in such a way that their mechanical resonance frequency should be several times above the desired operating frequency band [51].

Fig. 4b shows an idealized FFVS of a piezoelectric hydrophone.

As a special case in piezoelectric hydrophones, the sensitivity (S) of a piezoelectric element is equal to the open-circuit voltage (V_i) it generates relative to the stress (σ_j) applied to it, or

$$S = \frac{V_i}{\sigma_j} = g_{ij} h \quad (7)$$

Where g_{ij} is the piezoelectric voltage coefficient and h is the element thickness [51].

Besides, fluid-structure interaction also affects the bandwidth of the hydrophone. Zhang et al. [113], based on a Fluid-Structure Interaction (FSI) mathematical model, examined the effect of this interaction on the resonance frequency and other factors of the hydrophone.

As a general consideration, 20 Hz–1 kHz range, is sufficient for underwater acoustic detection at low frequencies.

2.9. Directional response (Directivity)

Hydrophone sensitivity is also a function of the angle between the hydrophone's acoustic axis and the direction of propagation of the incident wave. To express this feature, directivity or beam pattern is defined. The directivity of a hydrophone indicates the voltage or the output corresponding to the quasi-planar acoustic pressure as a function of the angle relative to the hydrophone axis [114]. The characteristics of the beam include the main or the primary beam located at the acoustic axis and the direction in which the acoustic pressure has the maximum value, as well as the beam width. The beam width is defined as the angular width of the main beam in degrees. It is defined by the points on the main beam which are 3 dB less than the maximum points [51].

Therefore, to improve the sensitivity, in addition to the frequency, all variables can be considered as a function of the angle of direction, θ . In this case, the equation becomes

$$S(f, \theta) = \frac{\Delta U(f, \theta)}{\Delta P(f, \theta)} \quad (8)$$

Where θ is the angle of incidence. A 3D graphical representation of a hydrophone response as a surface in the frequency angle space is shown in **Fig. 5a**. This method was used in 1985 by Harris Shomber [115] to characterize the directional response of hydrophones.

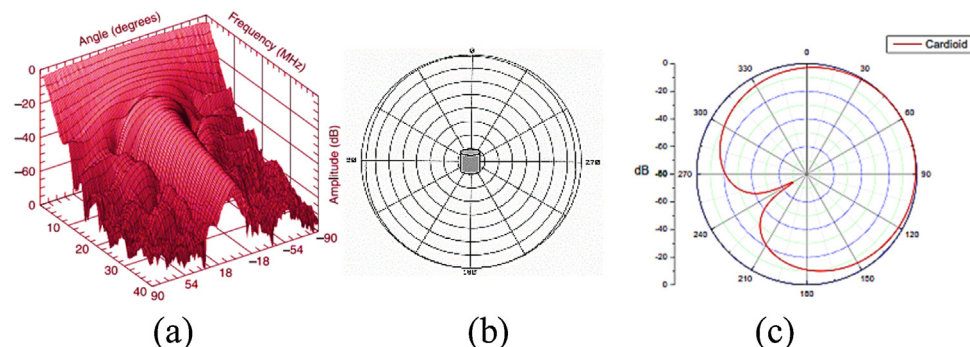


Fig. 5. a) 3D graphical representation of an ultrasonic hydrophone response surface [51]. At low frequencies (< 3 MHz), a hydrophone placed perpendicular to the incident waveform would experience at most a 6–8 dB reduction in signal relative to a perfectly aligned device. However, multiple, well-defined minima appear in the directional response as frequency increases. At 15 MHz a misalignment of only 15° coincides with a minimum and very little signal would be recorded by the hydrophone [89]. b) Omnidirectional beam pattern. c) Cardioid beam pattern [121].

The directivity of a hydrophone is defined as a function of the output voltage:

$$D(a, \theta) = \frac{|V(a, \theta)|}{|V(a_0, \theta_0)|} \quad (9)$$

Where $|V(a, \theta)|$ refers to the amplitude of the output voltage of the hydrophone when the incident acoustic wave is at the angle of (a, θ) , and $|V(a_0, \theta_0)|$ refers to the largest amplitude of the output voltage of the hydrophone when the incident acoustic wave is at the (a_0, θ_0) angle [116].

Sometimes the directivity is represented as a directivity factor/index (DI), which is a decibel display (Beranek) [117]. Ideally, the frequency-dependent directional response should be measured practically. In the absence of measurement data, an analytical statement can be an acceptable alternative. The formulation is based on a rigid baffle model performed in 1980 by Archer-Hall and Gee [118]. In 1982, Shomber et al. [114] have also obtained other analytical models based on the soft or unbaffled circular elements by measuring the directional response of several different hydrophones.

Directivity measurement of hydrophones has technical advantages, some of which are:

- 1) The effective size of the sensitive element of hydrophones depends directly on the directivity.
- 2) The accuracy of the measurement of the angle of the incoming pressure wave to the hydrophone is described by the directivity.
- 3) The potential of distortion in a highly focused beam with a wide range of the angular spectrum is explained by this factor.
- 4) The rate of rejection of non-axial waves by hydrophones, such as reflections inside the water tank, is described by directivity [66].

In terms of directivity, hydrophones are divided into two general categories: Omni-directional and unidirectional. Unlike directional hydrophones, Omni-type detects acoustic waves with the same sensitivity in all directions, while directional hydrophones are more sensitive in certain directions [9]. Directional hydrophones are sometimes made of a number of Omni-directional types or can even be created by an array of hydrophones. The acoustic wave reaches each of these arrays depending on the position of the source at a given time, and the time intervals between the arrivals of the waves to the arrays are used to calculate the direction of the acoustic wave. Such a structure allows for better detection than a single hydrophone, making it possible to remove noise from other directions, increase SNR, and so on.

Today's vector hydrophones usually create a dipole mode beam [119]. If the dipole mode beam pattern of these hydrophones is combined with the omnidirectional mode beam pattern of a

scalar hydrophone, a cardioid mode beam pattern (Fig. 5b and c) is generated. The sensitivity of generated cardioid beam pattern on receiving side is very different from the other. With this technique, the direction of the acoustic wave is easily detected. Various types of hydrophone structures that form a dipole beam pattern have been reported [120].

The directional response is a function of hydrophone dimensions, aperture area (and to a lesser extent its shape) and like all other hydrophone types, when the dimensions of the hydrophone become smaller than the wavelength of the received signal, the response becomes wider [71]. In other words, the larger the element size, the greater the directivity, and because the output is the result of the average pressure over a larger area, acoustic radiation with a larger angle is measured with greater errors such as underestimation. In addition, the directivity depends on the frequency as well as its mounting conditions. Ideally, the directional pattern must be in good "8" shape and the pit depth or concave point must be sufficiently reduced. Also, the pattern should be as smooth as possible. The small non-uniformity of the axial sensitivity is negligible and the orthogonality of pattern in the X and Y two-way should also be good. However, the directivity pattern may not be ideal due to reasons such as: low-pressure level in the standing test tube and subsequent reduction of signal to noise ratio, lack of complete elimination of interference in the tube, the close proximity of the projector and the test hydrophone in the calibration process (inaccurate assumption of-plane wave formation) and the asymmetry of the hydrophone structure during construction.

2.10. Cable effect

Many hydrophones, especially piezoelectric hydrophones, are good voltage sources but may be weak in the current. Accordingly, they relatively perform poorly in driving the transmission line (cable) between the hydrophone and the oscilloscope or any other DAQ device. For this reason, the total electrical impedance and the output load of the hydrophone change, especially in cases where the cable length is long, and the measurement results need to be corrected [122]. Any change in the condition of the transmission line, such as an additional cable or a change in the impedance of the terminals will also lead to an additional load on the cable. Therefore, in cases where the measuring devices are located at a distance from the hydrophone or the working frequency of the hydrophone is about a few kHz, the calibration of the hydrophones should be accompanied by consideration of the effects of the cable. Correction of additional cable effects is often done by measuring the capacitances of the hydrophone and cable at typical frequencies of about 1 kHz or lower. This method may even be used to correct the open circuit sensitivity of a hydrophone in integrated hydrophones and

cables [109]. Hayman et al. [123] described a method for correcting electrical impedance and hydrophone sensitivity due to the effects of additional cable.

Another alternative approach is to exploit the preamplifiers. If they are placed immediately next to the sensitive element, the cable effects are favorably reduced. Preamplifiers in addition to works such as the impedance buffer between the hydrophone output and other steps and providing a gain stage to amplify the signal can also be considered as transmission line drivers to preserve signal integrity. If the hydrophone output impedance is matched to the input impedance of the DAQ and intermediate cable, the cable effects can be minimized. Accordingly, preamplified hydrophones are preferred to unbuffered hydrophones that require cable loading correction [71]. As a general rule, the capacitance of hydrophones is designed to be as high as possible to reduce the effects of the cable on the acoustic sensitivity of the hydrophone [89]. Other techniques have also been proposed to reduce the effects of the cable, such as M. Abdillahi-Said and C. Park [124] who proposed multiplexing the signals of several hydrophones to an optical fiber and then transmitting it.

2.11. Consistency & durability against hydrostatic pressure

There are three main challenges in using a sensitive hydrophone at any depth of the ocean: 1) the hydrostatic pressure varies enormously with depth, and one atmospheric pressure increases almost every 10 m. Hydrostatic pressure in the hydrophone's operating environment may also reach several tens of mega-pascals. Therefore, a sensitive hydrophone for oceanic applications sometimes requires the detection of a very small pressure of about $10 \mu\text{Pa}$ in the background pressure of a few tens of mega-pascals [125]. 2) The properties of materials such as compressibility also naturally change over the large static pressure ranges. Therefore compressibility changes cause the sensitivity of the hydrophone to vary gradually as the hydrophone goes to lower depths. However, calculations show that this effect is negligible because water has linear mechanical properties and its compressibility changes with pressure in the range of 0 to 100 MPa, only about 21 %. The effect of hydrostatic pressure on the elastic properties of solids such as silicon can also be neglected [126]. 3) The water compressibility is also very low, about $5 \times 10^{-10} \text{ 1/Pa}^{-1}$. This small amount makes it difficult to move the sensitive element of the hydrophone against the water when it is full of water and it will be difficult to detect a weak acoustic signal.

One of the most effective solutions to keep hydrophones from being sensitive to hydrostatic pressure is to connect them both inside and outside water through a pressure equalization channel. In other words, at least part of the hydrophone space needs to be filled with water. Also, a method for improving the deflection of the sensitive element of hydrophones such as the diaphragm, is to apply a volumetric displacement into a limited area of it [99].

The most important criterions that are proposed for the design of deep-sea hydrophones include: the open circuit receiving response (OCRR), receiving voltage sensitivity (RVS) at the desired frequency, and roughness of frequency response as a function of sensitivity. Some researchers have carefully studied the consistency and durability of hydrophones to hydrostatic pressures at depths of more than 200 m [127–129].

2.12. Acoustic impedance matching

An important figure of merit in designing hydrophones is the acoustic impedance (Z) which describes the coupling efficiency of the acoustic waves between the material of the active element and the adjacent media. In other words, acoustic impedance describes the resistance to propagation of sound waves within a tissue and is

a unique quantity for each tissue. The acoustic impedance can be calculated by [130]:

$$Z = \rho V \quad (10)$$

Where ρ is the density and V is the speed of sound in the tissue. The acoustic impedance of a hydrophone is written as the product of radiation area \times density \times sound speed. Matching good acoustic impedance to the adjacent media means that more incident energy is transferred to the hydrophone active element and its loss or reflection from the interface between the active element and the medium is minimized. This way, more energy is propagated into the active element, resulting in a better response. Due to the fact that the acoustic impedance of water is 1.5 Mrayl [131], the acoustic impedance of piezoelectric materials that have a reasonable match to water are attractive for underwater applications. The material used to encapsulate the hydrophones must also be transparent in terms of acoustic impedance at operating frequencies, or in other words, have acoustic impedance close to the water. Accordingly, in packaging, materials such as epoxy resin [17], a mixture of epoxy resin and glass beads [132], polyurethane [133] and nitrile butadiene rubber (NBR) [134] are used as a cap (shell). Silicone oil which has low viscosity is also commonly used as a filler due to the acoustic impedance matching.

2.13. Influence of water electrical conductivity/dielectric constant

Water, which is usually one of the main mediums for hydrophones, has two major effects on hydrophones. First, due to the low dielectric constant of piezoelectric materials relative to water ($\epsilon=80$), the effect of parasitic loading capacitance may appear. Second, due to the electrical conductivity of the water, the sensitivity of the hydrophone may be reduced, especially at low frequencies. Sapozhnikov et al. [135] have studied the role of water conductivity in the calibration of a low-cost PVDF hydrophone to detect a wide range of signals and frequencies.

2.14. Fragility

Hydrophones are usually fragile due to the transition of pressure waves, especially near the sensitive element that is very important in the use of hydrophones.

2.15. Immersion

Water is a relatively corrosive and aggressive solvent. It can even pass through plastic. Therefore, when the hydrophone are not actively used, it must be taken out of the tank.

2.16. Cost

Membrane hydrophones are usually more expensive than needle hydrophones. These hydrophones are less compact and followed by capsule. In general, the smaller the hydrophone dimensions, the more difficult it is to fabricate and the higher the cost.

As the last point in this section, it should be noted that hydrophone calibration can be achieved using various techniques: reciprocity, planar scanning, time delay spectrometry (TDS), optical interferometry, etc. [136,137]. Each method has specific properties such as precision, direct/indirect determination, rapidity, frequency range, using a free-field environment or laboratory tank, etc. This paper does not address this issue because there are many sources available.

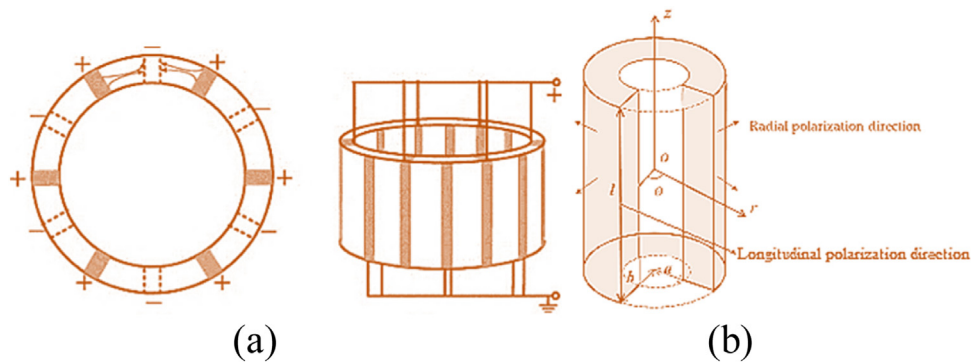


Fig. 6. a) Multi-segment piezoceramic with tangential poling. b) Piezoceramic with radial and longitudinal poling.

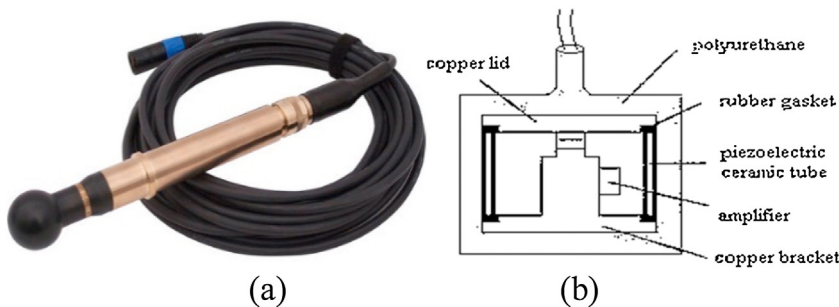


Fig. 7. a) Ambient recording TC4042 low-noise spherical hydrophone. b) Structure of a cylindrical hydrophone with built-in amplifier [139].

3. Piezo material for hydrophones

At the end of the twentieth century, lead zirconate titanate (PZT) compounds were widely used in underwater acoustic transducers [138]. The main constituents of early hydrophones were piezo materials. Gradually mechanical elements were integrated with piezo material to improve the sensitivity. The development of suitable piezo material for underwater applications is still a research trend. Today, most piezoelectric hydrophones are still based on piezoceramic or piezopolymer. Single crystal and piezocomposite devices are also available but are less common in hydrophones. Following sections explain the acoustic properties of the piezo materials and the hydrophones developed on the basis of these materials.

3.1. Piezo-ceramics

The piezoelectric ceramic hydrophone is currently widely used for the excellent ceramic performance, which it is easy to fabricate, has a wide linear output, it is highly consistent and can be made into different shapes and sizes such as cylinder, column, annular and block, etc. [139–141]. Piezoelectric ceramics have a high piezoelectric strain coefficients (*d*-coefficients) due to the limited internal loss mechanisms and are very efficient for generating acoustic signals from electrical signals. Instead, piezoelectric ceramics have a low piezoelectric voltage coefficients (*g*-coefficients) and are less common in receive-only devices [71]. Piezoelectric ceramic is used more in measurement of high-intensity acoustic fields due to its hardness and high sensitivity [142]. These materials have high acoustic impedances (typically > 17 MRayl and often > 30 MRayl). The use of porosity in the passive phase, which is associated with a decrease in density, is a solution to this problem [143–145].

One of the advantages of piezoceramic devices are the ability to define resonant modes based on their geometry. Thickness mode, radial mode, length expander, and width expander modes are typical examples. In resonance, piezoceramic-based devices exhibit

high sensitivity and often have high mechanical Q and therefore provide a much smaller off-resonance response.

Based on geometry, these types of piezoceramic-based hydrophones are widely used in rectangular, spherical, and cylindrical shapes.

The simplest configuration is a rectangular block of piezoceramic, on the top and bottom of which are placed electrodes and poled in the thickness direction.

The cylindrical shape is commonly used in audio and low ultrasonic frequency range applications. This configuration usually has a uniform directivity and in addition to simple structure, it is more sensitive than others. The direction of piezoceramic poling in this geometry also has a significant effect on the hydrophone performance. There are three poling configurations for this type of hydrophone. They can be poled either radially, longitudinally, or divided into several segments by electrodes and tangential poling. Fig. 6 shows the types of poling in cylindrical geometry.

Radial poling generally has the lowest sensitivity and tangential poling has the highest receiving sensitivity [146]. Instead, radially poled cylinders are often preferred in applications that require a long cable drive due to higher capacitance [147].

The cylindrical PZT-5 tangentially poled hydrophone designed by Zhang et al. [148] in 2012 had an average acoustic pressure sensitivity of about -182 dB within 30 Hz–10 kHz.

Thin shell spherical hydrophones, in addition to simple structure, have advantages such as flat response, high sensitivity, and omnidirectional beam pattern [149]. This configuration can also be developed in two poling designs, the radial, and tangential poling [150]. The radial poling exhibits one of the highest sensitivities. In this configuration, sensitivity and bandwidth are functions of the ratio of the wall thickness to the outer diameter [61,151]. Reliable mechanical strength in the design of this should be considered [151]. At higher frequencies, the sensitivity of this configuration decreases, and the directivity beam patterns deviate [152]. Fig. 7 shows the cylindrical and spherical configurations. When the acoustic wave hits the structure and passes through the transparent

acoustic region, it reaches to the piezo material and by generating mechanical stress in it, the distribution of electric charges changes and these variations are pre-amplified and finally read out.

One of the improved designs in the field of structure is the cymbal which consists of a piezoelectric disk sandwiched between two metal cymbal-shaped end-caps (Fig. 8) which was originally developed by Newnham et al. in 1990s [153–158]. The cymbal is named for the crescent cavity shape created by the endcaps. Metal endcaps act as converter and amplifier and convert the axially applied force into both axial and radial stressed inside the ceramic disk [159]. Therefore, higher coefficients of piezoceramic participate in the generation of charge, and higher sensitivity is produced. The performance of the cymbal transducers depends on several factors such as properties of the active elements, mechanical properties of end cap materials, mechanical properties of gluing material, cavity depth, the thickness of metal cap, and gluing techniques, etc. On the other hand, due to some manufacturing limitations, the performance of the cymbal hydrophone is not stable enough and the received bandwidth is narrow [155,160]. In 2006, Li et al. [161] designed and fabricated a small hydrophone combining the cymbal-type transducer and material of PMN-0.33 PT with a sensitivity of higher than -190 dB and a bandwidth below 8 kHz. Chen Sheng and Lin Guan-Cheng [162] also improved the cymbal hydrophone structure in 2009.

3.2. Piezo-polymers

Piezo polymers are more flexible than piezo ceramics and have lower acoustic impedance (typically 3–4 MRayl). These materials are inherently low Q and consequently have a wide bandwidth. The compliant nature of these substances makes them easy to compress and show a high g-coefficient but low d-coefficient. Therefore, piezo polymers are excellent materials for the development of high-sensitive and broadband hydrophones [71,165–167]. Another major advantage of piezopolymer or copolymer hydrophones for use in two-dimensional arrays is the relative lack of lateral mode resonances. In small quasi-rod ceramic elements with lateral dimensions less than half a wavelength, the lateral vibration modes are generated near the desired thickness mode frequency, and there is an inherent coupling between the modes [168]. The ceramic materials allow hydrophones to be constructed with smaller sensitive elements compared to polymer ones. However, when the area of the sensitive element of piezo polymers is small, their sensitivity will be insufficient and they cannot obtain a satisfying SNR and therefore they are not desirable in applications such as ultrasonic. This is due to their lower piezoelectric coefficients and dielectric constants, especially compared to piezo ceramics. This is because the low dielectric constants reduce the output signal because of stray capacitances. Several groups have developed different types of hydrophones to try to solve this problem by using piezo ceramics [169–173], and some researchers tried to improve the capacitance by lamination [174]. Piezo polymers often need a preamplifier because of their low dielectric constant [175].

3.3. PVDF polymer

Since the discovery of its piezoelectric nature in 1969, PVDF is one of the most common materials used in underwater devices and for the detection of ultrasonic fields and calibration of ultrasound devices at frequencies of several MHz [140,141,176–180]. They have a very high bandwidth compared to ceramics. Today, the PVDF films in different thicknesses, surface electrodes and protection layers, etc. are commercially available. PVDF films have a fast response and in addition to their high mechanical strength that causes them to be used in measuring high-pressure acoustic waves which may cause traditional piezoceramic to fail [181], they are also

mechanically very flexible and can be shaped into a variety of configurations and can have applications at curved surfaces [85,182]. Accordingly, they can be seen in various structures such as needle type hydrophones [165,166], the membrane type hydrophones [167,183], and one-dimensional arrays of hydrophones.

For a needle-type hydrophone, one side of the PVDF film is firmly attached to the end surface of a solid needle as the backing material and the other side is exposed to the acoustic pressure waves. For the membrane type hydrophone, the PVDF film acts as a membrane or diaphragm that is fixed on a frame and can be exposed to acoustic pressure from both sides. Some researchers have also developed acoustic and ultrasonic hydrophones based on Piezo electret layer or fluorinated ethylene propylene (FEP) piezoelectric layers, which are porous and cellular polymer films with an electric charge that have a large d_{33} piezoelectric coefficient and low acoustic impedance [184,185].

3.4. Piezo-composites

Piezoelectric ceramic-polymer composites or piezocomposites have long been developed for underwater applications. The inclusion of the second phase of polymer in a piezoelectric ceramic provides advantages such as reduced permittivity, reduced density, improved impedance matching, high-pressure tolerance, and lower fabrication costs.

Traditionally, researches on piezoelectric materials have concentrated on producing high-density samples to be used at low frequencies. It has been shown that low-density piezo electrics which can result from a high degree of porosity, have a high hydrostatic figure of merit [186] and high sensitivity [144,187]. For dense materials, the hydrostatic figure of merit, d_h ($d_{33}+2^*d_{31}$), is low because both d_{33} and d_{31} coefficients are large but marked with the opposite sign. The porous structure increases the value of d_h by retaining d_{33} and decreasing the absolute value of d_{31} [188].

Further, by changing the ceramic/polymer volume fractions, it is possible to adjust the piezocomposite parameters for specific requirements [189]. Although piezocomposites of various connectivities do exist, only composites with 1-3 and 3-3 connectivities are found to be more useful for transducer applications. Piezocomposite hydrophones are predominantly of 1-3-type connectivity. Also, literature is relatively available on 0-3-type composites.

In 2001 Lau et al. [190] showed that a needle-type hydrophone made of PT/P (VDF-TrFE) 0-3 nanocomposite thin film is more sensitive than the hydrophone with P (VDF-TrFE) as the sensing element. Also, a shear-polarized hydrophone fabricated from 0 to 3 PZT/P(VDF-TFE) piezoelectric composites was introduced by Zhu JL et al. [191] in 2005, which had a sensitivity about -190 dB.

Many studies have been performed in the field of 1-3 type piezo electrics. After a period of finite element modeling (FEM) phase on 1-3 piezocomposite for use in transducers, the practical use of 1-3-type piezocomposites in acoustic transducers effectively began at frequencies spanning from Hz to MHz. Piezoelectric-polymer composites with 1-3 connectivity consist of piezoelectric ceramic (generally PZT) rods embedded in a host matrix of polymers. If these materials are solely used for hydrophones, the volume fraction of piezoelectric ceramic in the composite is generally between 15 % and 25 %. Also, the optimal percentage has been studied and reported for single transmitting or dual modes In [147].

These composites have high hydrostatic sensitivity and higher thickness mode coupling coefficient and lower radial and lateral mode coupling coefficients from bulk PZT materials. Excellent mechanical toughness [192], high bandwidth, and low weight are other advantages of these materials. On the other hand, the production of these materials is tedious and expensive [193]. However, there have been many reports of the use of 1-3 type piezoelectric composite materials for a variety of hydrophones [194–197].

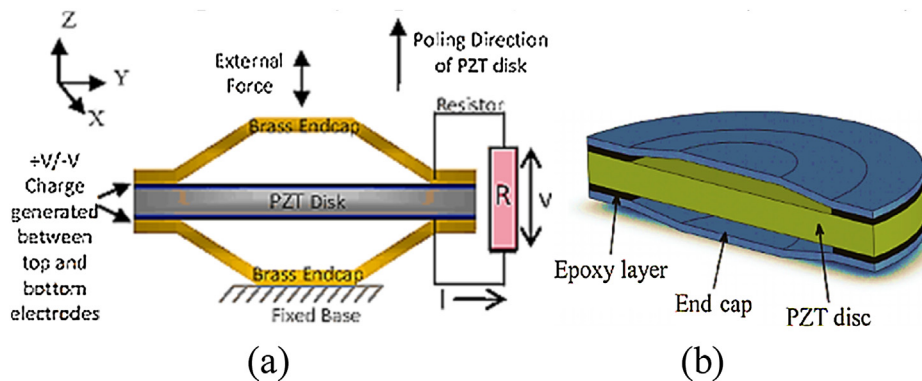


Fig. 8. a) Schematic of piezoelectric cymbal traducer. [163] b) Cut-away diagram of a cymbal transducer [164].

3-3 piezocomposites were introduced as a proven alternative to 1-3 type with comparable material properties and a relatively simpler synthesis method [186]. The porous form of the 3-3 piezocomposites features a significant considerable improvement in the characteristics of acoustic transducers. Perryl et al. [188] optimized the properties of 3-3 piezocomposites in 2002 and studied the effect of the size of the porosity on the figures of merit of hydrophones. In 2005 Ramesh et al. [193] have compared the features of the 3-3 types with the dense and porous piezoceramic disc hydrophones and suggested that these materials are suitable for use with broadband hydrophones.

3.5. Single-crystal

Since the first successful growth of single-crystal Lead Magnesium Niobate-Lead Titanate (PMN-PT) in 1990, it has piqued considerable interest in being replaced by conventional piezoelectric materials. These crystals have a high electromechanical coupling up to close to the theoretical maximum ($k_{33} > 0.92$) and piezoelectric coefficients up to more than five times that traditional PZT ceramics, [198,199] which can show the inherent potential of using these materials to increase the sensitivity of hydrophones [200]. However, these crystals are highly anisotropic and only cause a lot of sensitivity if they are oriented in a specific direction. These materials are widely used in ultrasonic and underwater hydrophones [201,202]. In 2006, Li et al. [161] designed and fabricated a small hydrophone with a combination of a cymbal-type transducer and the PMN-0.33 PT single-crystal. In 2013 Brown et al. [203] directly compared the sensitivity of a composite PMN-PT single-crystal cylindrical hydrophone to a similarly sized PZT hydrophone. They conclude that because of highly anisotropic nature of PMN-PT, simply replacing it with PZT is not the optimal solution. Therefore with by using a single cut $<110>$ and designing a novel structure, the sensitivity was well improved.

3.6. Piezoelectric metamaterial

Numerous studies have demonstrated that porosity configuration and its connectivity are responsible for increasing the electromechanical properties of piezoelectric materials. Smith has also shown that a polymer matrix with the negative Poisson's ratio enhances the performance of the piezocomposite materials [204]. Piezoelectric metamaterials and piezoelectric architected materials [205–209] have the potential to tailor the microstructure for any porosity configuration (such as 0-3, 1-3 and 3-3) and achieve a negative Poisson's ratio to produce new innovative materials with optimal multi-functionality for specific applications [210]. Using a topology optimization method, Sigmund et al. [211] designed a three-dimensional anisotropic porous matrix piezocomposite

microstructure with a negative Poisson's ratios in certain directions similar to re-entrant honeycomb network with optimal properties in hydrophone applications. Silva et al. [212] tried to find the optimal distribution of material and void phases in a periodic unit cell to achieve higher piezocomposite electromechanical efficiency by using an optimization technique. Several porous 2D and 3D piezocomposite microstructures were proposed with negative Poisson's ratio behavior for hydrophone applications [213].

4. MEMS hydrophones

MEMS technology has improved many sensors and actuators such as switches [214], energy harvesters [215–218], pressure sensors [219], and hydrophones [220,221]. MEMS vector hydrophones have been developed in recent years that have the superiorities of small size, high sensitivity, desired low-frequency response, good consistency, light weight, low power consumption, high reliability, proper robust, mass produced and bargain price enabling them to be a viable alternative to today's diverse hydrophones [57,86,99,222–225]. Also, combining MEMS with hydrophone will help us to have a better SNR [226] and makes it easy to carry out low-frequency detection [227].

So far, the study of MEMS hydrophones has been increasingly mature [30,228]. In 1994, Draper Labs reported the design and fabrication of fluid-filled variable-capacitor hydrophones on a 3-mm silicon chip based on MEMS technology [229]. This hydrophone had a relatively large oil-filled package. In 1996, based on the U.S. Navy's need for smaller size hydrophone, Howard K. et al. invented an 8-cm³ acoustic vibration speed hydrophone using MEMS technology. This was probably the first report of the use of MEMS vector hydrophone as a directional underwater acoustic sensor [230]. In 2000, a MEMS hydrophone on a silicon wafer using n-type metal-oxide-semiconductor (NMOS) technology and PVDF piezoelectric was fabricated [168]. Meanwhile, the report of bionic technology opened a new gate on the design and manufacture of hydrophones. In 2002, Fan et al. [231] introduced the artificial lateral line flow sensors by imitating the lateral line organ of fish. In 2004, Zhang W. et al. [232] successfully developed a cilium MEMS bionic vector hydrophone for low-frequency applications after several years of development, the sensitivity of this type of hydrophone reached -189 dB. In 2006, Li Y. et al. [233] developed a piezoresistive MEMS hydrophones fabricated by Silicon-On-Insulator (SOI) technology that had a high resonant frequency of about a few kHz. (See Fig. 9)

In 2006, Shi-E et al. [234] devised a MEMS vector hydrophone based on piezoresistive principle and in 2007, Uma. G et al. [235] proposed a scheme for integrating PVDF thin film and metal-oxide-semiconductor field effect transistor (MOSFET) pre-amplifier for MEMS hydrophone development. In 2008, Shang et al. [133] designed a cilia-type MEMS vector hydrophone as a four-beam

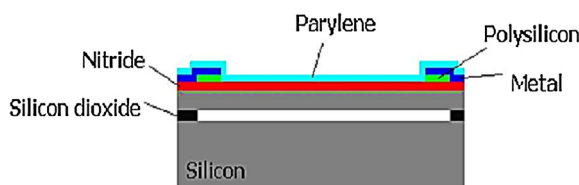


Fig. 9. Design of piezo-resist underwater acoustic sensor [233].

micro-structure based on bionic theory and the principles of acoustics vibration. The rubber cap was filled with silicone oil to vibrate the fiber and the particle at the same time. This design had a small size, high consistency, and good directivity. A micro machined hydrophone based on piezoelectric effect with hydrostatically balanced air backing was developed in 2010 [236]. Guan et al. [237] in 2012 designed and fabricated a T-shape vector hydrophone based on MEMS technology inspired by the fish lateral line. A multilayer hydrophone was made in 2014 using 1-3 piezocomposite [238]. Another attempt was made in 2014 to achieve greater sensitivity by optimizing the cilium-type MEMS bionic vector hydrophone [239]. In 2015, Linxian et al. [37] have studied a double-T-shape MEMS bionic hydrophone to get smaller size and higher sensitivity. Mengran et al. [240] in 2016 developed a four-unit array microstructure on a chip to address the need for more bandwidth. A sound-transparent cap with the ability to increase sensitivity has been designed and fabricated in 2015 [134]. A whisker-inspired MEMS vector hydrophone encapsulated with parylene has been fabricated in 2016 so that the frequency response lacked a flat region [222]. In 2017, Bai et al. [1] have proposed a high g shock resistance MEMS vector hydrophone with cross-supported plate structure. Zhang et al. [241] developed a stress centralized MEMS vector hydrophone (SCVH) based on piezoresistive effect to improve sensitivity by placing piezo resistors in the areas of stress concentration on four-beams.

Based on the transduction mechanism, there are three main types of MEMS vector hydrophones including capacitive, [242,243] piezoresistive [42,86,237,244], and piezoelectric [231,245]. Strain-gauge based items have already been presented [246].

The micro-capacitive vector hydrophones are usually highly sensitive. However, capacitive hydrophones use large external circuits and amplifiers due to the need for bias voltage and DC-DC convertor. Also, small air gaps that exist have made these hydrophones vulnerable to the impact of underwater pressure. Besides, a narrow gap between capacitance in the sticky liquid causes viscous damping, which limits the sensitivity [59]. An example of a capacitive vector hydrophone is the work of Li et al. [247] in which a low noise vector hydrophone was studied based on the principle of differential capacitance with a sensitivity of -179.9 dB over the $20\text{--}2000 \text{ Hz}$ frequency range.

MEMS piezoresistive hydrophones have advantages such as simple structure and easy fabrication [59]. These hydrophones can

be used to detect low-frequency signals even at zero Hz. In contrast, piezoresistive hydrophones have low sensitivities due to the low energy transfer efficiency of piezoresistive materials. Also, thermal noise is unavoidable in them [44].

MEMS piezoelectric vector hydrophones are not only theoretically more sensitive than piezoresistive vector hydrophones, but also, according to reports by Tabib-Azar et al. [248] minimum detectable signals of piezoelectric hydrophones have lower values. However, some believe that the sensitivity of piezoelectric vector hydrophones is not high enough to be used in practical applications [227]. These hydrophones have a relatively simpler structure without a small air gap and due to the structural strength of the piezoelectric material compared to piezoresistive material, they can sustain the water pressure from the outside [233]. Also, in piezoelectric materials, SNR is higher than that of piezo resistors. Compared to capacitive and piezoresistive hydrophones, piezoelectric hydrophones usually have higher bandwidth, better linearity, more temperature stability, lower power consumption, and a simpler readout circuit [59].

Today, in accordance with the principles of bionics and the combination of MEMS technology with it, desirable results such as improved low-frequency sensitivity as well as miniaturization have been achieved [9,31,42,121,133,249]. Maybe one of the most famous designs developed by some researchers based on MEMS technology in recent years is the nature-inspired cilium-type MEMS bionic vector hydrophone, shown in Figs. 10 and 11. It is shown how this is inspired by nature for the development of MEMS bionic vector hydrophone. It consists of a four-beam microstructure and a rigid cylinder fixed in the center of the microstructure. There is also one or more piezo resistors on each beam. Corresponding to the acoustic signals caused by acoustic waves, vibration waves or water flow velocity, the cilium begins to vibrate and the square mass in the bottom of the cilium is deformed. Beams will be subjected to deformation and the piezo resistors located on the beams transform the acoustic signal into a strain and finally, through the Wheatstone bridge circuit, a differential output voltage signal is produced [250].

Compared to the traditional piezoelectric hydrophones, such a hydrophone have advantages of being a single sensor with directional functions and location finding ability which means that a single hydrophone can acquire the target location [86,252,253].

Acceleration-based vector hydrophone is another category of MEMS hydrophones. It usually consists of a mass block and a piezoelectric composite cantilever beam composed of a piezoelectric layer and an elastic layer like silicon. When an inertia force is applied to a hydrophone in an underwater acoustic domain, the relative motion of the mass block causes the beam to deform and generate a charge at the upper and lower surfaces of the piezoelectric, which is read after the amplification. Typically, these hydrophones are made by joining and packaging multiple accelerometers, which leads to an increase in their volume. Also, the sensitivity of the hydrophone is usually constrained by the characteristics of the accelerometer. Compared with piezoelectric

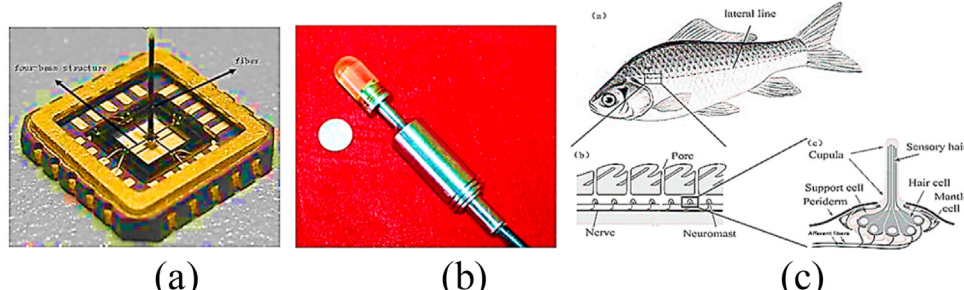


Fig. 10. a) Chip with four-beam structure [251] b) Photo of the MEMS hydrophone's packaging [251] c) fish lateral line [226].

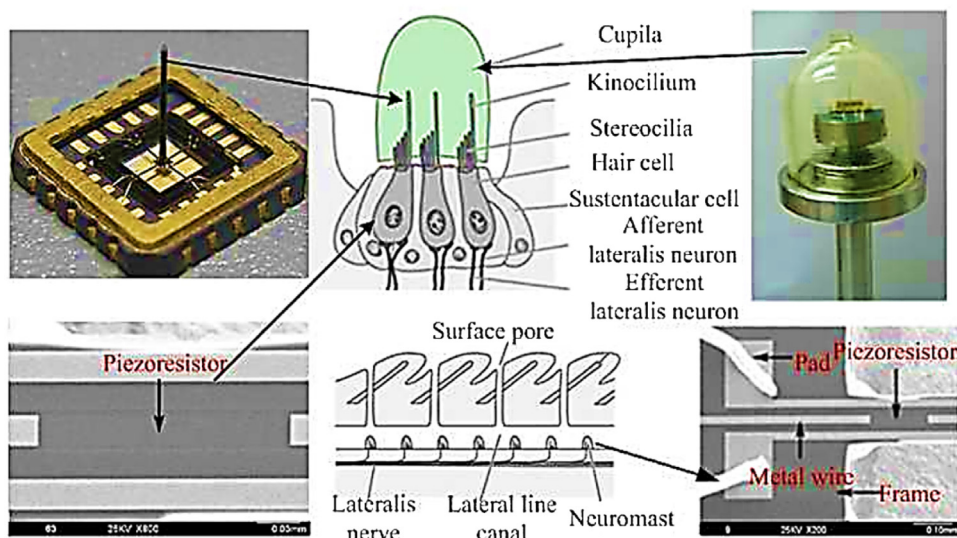


Fig. 11. Package of the MEMS bionic vector hydrophone [251].

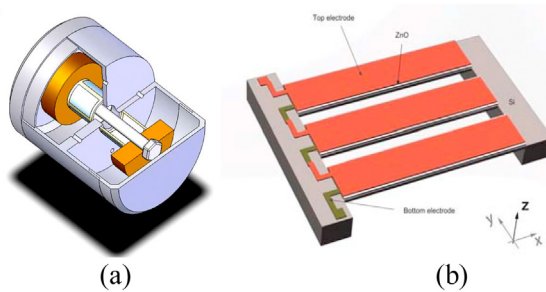


Fig. 12. a) Cutaway view of the 2D vector hydrophone [256] b) The schematic of piezoelectric accelerometer with double U grooves [257].

hydrophones, these hydrophones can also respond to zero frequency [39,230,254,255].

In 2012, Qiqi Ge [256] designed a mini-type 2D piezoelectric ceramic accelerometer by selecting cantilever beam mode with a sensitivity of about -193 dB in water. According to Fig. 12a, inside the cylindrical shell, two piezoceramic tubes act as sensitive elements and are located symmetrically on both sides of the center plate. The mass blocks are also located in the direction of the cylinder and connected to the center plate, which vary the charges produced in the piezoceramic by applying inertial force and creating stress in the center plate. To improve the sensitivity, in 2019, a novel MEMS piezoelectric accelerometer consisting of a piezoelectric composite cantilever beam and a series of U grooves and electrodes was presented by Li et al. [257]. The average stress in the ZnO film of each cantilever beam was about 50 % higher than that of a regular cantilever beam. (See Fig. 12b)

MEMS hydrophones making use of a membrane or a diaphragm have also been developed. Membrane hydrophones convert the acoustic pressure into voltage using a diaphragm stretched taut within a frame. One or more layers of piezo material are patched in areas of maximum stress [258]. The choice of materials, location and direction of placement of these materials is quite effective on sensitivity and performance [259]. However, optical mechanisms are also combined with these diaphragms. For example, in 2006, Rebello et al. [45] introduced a chip-scale optical MEMS membrane hydrophone based on SOS FP (Silicon On Sapphire Fabry-Perot) using ultra-thin PIN (positive-intrinsic-negative) photodiodes as shown in Fig. 13a, which measured the pressure based on interference with static waves generated by diaphragm displacement

and it had advantages such as low power consumption, unique wavelength and easy package capability.

In 2005, the frequency response of the membrane hydrophone was modeled by Gélat et al. [260] using the membrane resonance peak. Li Y. et al. [233] developed a piezoresistive MEMS membrane hydrophone in 2006 using an SOI wafer. In 2013, Chang et al. [261] optimized the structural parameters of a miniaturized PZT based hydrophone with perforated membrane as shown in Fig. 13b and c using genetic algorithm.

In 2016, a piezoelectric aluminum nitride (AlN) based MEMS hydrophone with ultra-narrow bandwidth, very high noise resolution and sensitivity of -182.5 dB was reported by Xu et al. [262].

MEMS hydrophones are structurally different. Some structures, such as the bionic structure, are designed to satisfy the vector properties which have been described in later sections. In this section, the types of Field Effect Transistor (FET) Based hydrophones are discussed.

4.1. FET based hydrophone

On the one hand, the development of MOSFETs, and on the other hand, the idea of placing the amplifier or buffer adjacent to the sensitive element of the hydrophone led to the merging of the two concepts in the 1980s. The idea was to help the reduction in size, avoid the sensitivity losses and solve the interconnect capacitance issues. A prototype of such a concept was developed by bonding a PVDF film to an extended gate of a MOSFET in 1979 and was named piezoelectric oxide semiconductor field effect transistor (POSFET) [263]. By applying an acoustic signal, the charge is redistributed on the surfaces of the piezoelectric film, which in turn changes the charge on the MOSFET gate and modulates the drain-source current. This structure has been used extensively [264–268]. Such a structure is compatible with integrated circuit (IC) fabrication processes [269]. However, the silicon dioxide layer is usually thinner than piezoelectric film and the dielectric constants of the two materials closely match, so the extended gate capacitance is larger than the piezoelectric capacitance, where a large part of the signal generated in the piezoelectric film is shunted and the sensitivity is degraded. This problem has been addressed by developing various fabrication techniques [270–272]. In 1992, Kühnel and Hess [273] designed and fabricated a transistor with a movable gate for acoustic applications that suffered from noise despite its acceptable sensitivity. In 2000, Zhu et al. [168] designed and fabricate

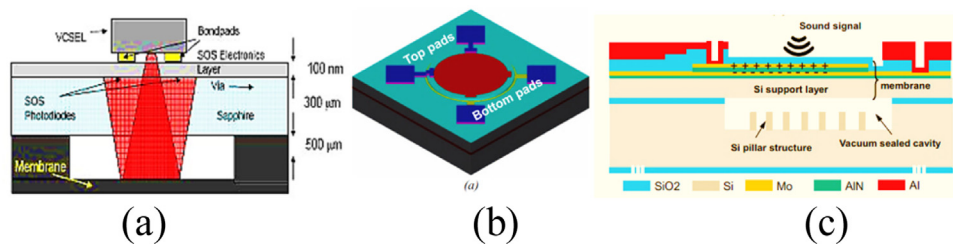


Fig. 13. a) Cross-section schematic of the SOS-MEMS hydrophone [45] b) Miniaturized PZT based hydrophone with holes (a) perspective view, (b) cross-sectional view [262].

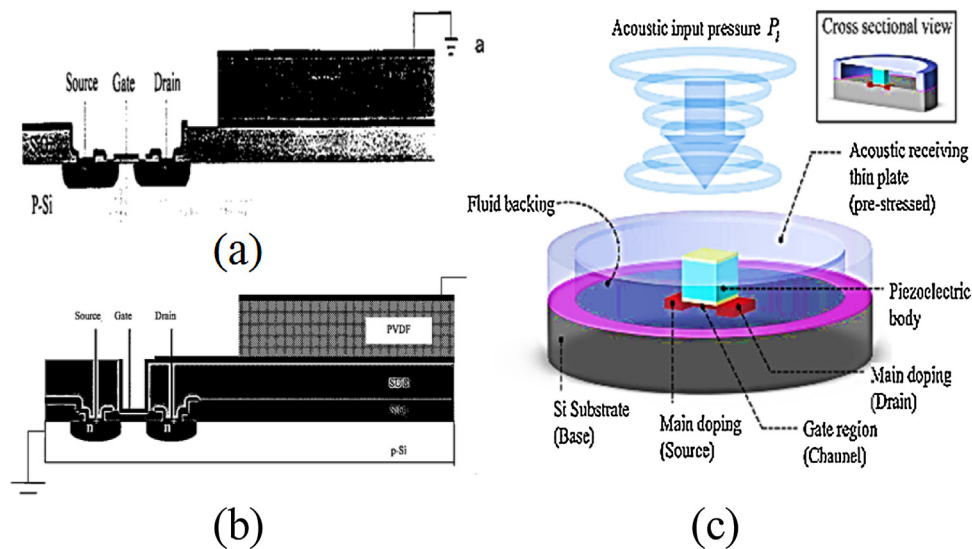


Fig. 14. a) PVDF-MOSFET Hydrophone structure [168] b) Basic piezoelectric-MOSFET structure [272] c) Schematic diagram of the PiGoFET hydrophone [274].

an integrated PVDF-MOSFET hydrophone as shown in Fig. 14a, the technology of which was also integrable with MEMS devices. This improved the sensitivity, but the parasitic noise of the gate capacitor was high. Again, in 2002, Zhu et al. [272] used a thick layer of photoresist as a dielectric under the gate electrode to minimize the parasitic capacitance as shown in Fig. 14b. To improve the reliability, a silicon nitride passivation was used and an improvement in SNR was obtained by using a differential amplifier. Uma et al. [235] proposed a MOSFET hydrophone with W/L = 100 in 2007. In 2015, Sung et al. [274] introduced a new transduction mechanism that used the piezo-body in combination with the gate of a FET, termed the piezoelectric gate on a field effect transistor (PiGoFET). A schematic of this structure is shown in Fig. 14c. As a result of the deformation of the piezo-body and the variation of the electric field of the gate surface, the FET current changed. Unlike POSFETs, where the acoustic signal was coupled indirectly to the gate, in PiGoFETs, the electric field directly modulated the FET current, and therefore the sensitivity was decoupled from the dimensions of the piezo-body. Sung's structure achieved a sensitivity of -175.5 dB and a bandwidth in the range of 50–500 Hz. In 2016, a miniaturized hydrophone was designed using conventional MEMS and CMOS (Complementary Metal-Oxide-Semiconductor) fabricating process [275]. Amiri et al. [221] in 2018 enhanced the sensitivity of this structure by using thinner piezo layers on the top of the diaphragm.

5. Piezoelectric/piezoresistive and fiber-optic hydrophones

Many methods have been used to convert the pressure signal into an output signal. These mechanisms include moving coil, [16,38] piezoresistive, piezoelectric [276], resistive heating [277], and magnetostrictive [278]. Piezoelectric hydrophones have been

available for many decades due to their optimum performance, while fiber optic hydrophones have only been widely developed in the last decade. Piezoelectric hydrophones have advantages of high manufacturability, low cost, excellent piezoelectric coefficient and availability of piezoelectric materials [180,183]. Thin layers of metal are usually placed on either side of the piezoelectric material to convert the stress-proportional electrical charge variations into a processing electrical signal. Therefore, the electric charge generated is directly related to the dimensions of the sensitive element. Achieving a higher sensitivity limits the miniaturization of conventional piezoelectric hydrophones. The improvement of sensitivity depends on the careful selection of materials, dimensions, transduction mechanisms, and correct design. Electrical signals are also used to store, analyze, calculate, record and display in the measurement system [279]. It is also common to use a preamplifier that is typically matched with the piezo-body. The capacitor formed due to the charge generated in the piezoelectric also leads to a low frequency cut-off, which is usually difficult to increase the first order resonant frequency without loss of sensitivity [274]. So that it is difficult to obtain adequate acoustic sensitivity with small size (below 100 μm) and the frequencies up to about a few MHz are required. In addition, the sensitivity of piezoelectric hydrophones to electromagnetic interference (EMI) makes continuous wave field measurement difficult. Piezoresistive hydrophones have also been developed and studied extensively. Yang [280] manufactured a micro-silicon-piezoresistive vector hydrophone. A piezoresistive bionic vector hydrophone was also developed by north university of China based on MEMS technology that had features such as low-cost and fine consistency [1,281]. The conventional electrical hydrophones especially the piezoelectric types have exhibited several drawbacks such as large size, sensitivity to electromagnetic

interference, the possibility of corrosion in aggressive medias, the need for special protective coating that reduces efficiency at high hydrostatic pressures, circuit malfunction especially underwater, fragility and the possibility of breaking at high pressures, limited cable length due to high electrical impedance, narrow frequency bandwidth, sensitivity dependence on resonant frequency, poor multiplexing capabilities and unsuitable for hostile conditions such as high temperature, high voltage, strong electromagnetic fields and conditions likely to explode [282–285].

The search for the optical version of hydrophones has also been vigorously pursued for decades until it was realized with the maturity of fiber optic technology and low-cost optical elements. The idea of using an optical hydrophone was first proposed by Bucaro [286]. The first approach based on fiber optic hydrophones (FOHs) was published by Eisenmenger and Staudenraus in 1988 [287]. Since then, fiber optic based hydrophones have been extensively developed in a range of applications and its performance is comparable to the best electric hydrophones [288–293].

FOHs have many advantages such as simple structure, easy to use, light weight, low cost, mechanical flexibility, much less fragile, chemically inert, intrinsic robustness, adhesion of silica-glass end-face to water, less susceptible to mechanical and thermal damage, durability against high acoustic pressure, non-sensitive to hydrostatic pressure, insensitive to ocean noise level, high reliability, immunity to electromagnetic interference, suitable for the hostile environment, high multiplexing capacity with negligible crosstalk, high discrimination to noise, and compact structure that has a high potential for use in small spaces and allows it to be used in some fields such as ultrasonic and minimally invasive surgery, however they have difficulties in characterizing CW (Continues Wave) or quasi-CW fields [286,294–297]. This compactness also allows a large number of them to be arrayed [298,299]. The wet end of FOH usually does not include the electronic parts and allows long distance remote interrogation for these hydrophones [300–302].

Although it is difficult to generalize the operation principle of FOHs due to the diversity of transduction mechanisms, [71] it can be noted that almost all extrinsic FOHs due to the potential for smaller element size development, have less directional response than the piezoelectric hydrophones. The core diameter of an optical fiber is as small as a few microns, while fabricating piezoelectric elements on these scales with sufficient sensitivity is complex and problematic. The sensitivity of piezoelectric hydrophones also reduces with decreasing the area of the sensitive element. This inevitably implies that FOHs are more sensitive than equivalently sized piezoelectric hydrophones. For example, the minimum detectable acceleration for practical FOH is about 25 ng/Hz at 100 Hz [303], which is one order of magnitude larger than its piezoelectric counterpart [17]. By contrast, intrinsic FOHs usually offer much lower sensitivity and generally do not have the advantage of sensitive element size over piezoelectric hydrophones. However, they have other benefits, such as a high upper detection range and robustness, which make them susceptible to high-pressure applications.

Furthermore, FOHs especially the extrinsic type are comparable in bandwidth to piezoelectric hydrophones so that many well-known FOHs have been developed that measure low-frequency sound waves (<20 kHz) and the ultrasonic waves [304,305].

However, the disadvantages of the fiber optic hydrophones are the damageable fiber, which tends to break during the measurement process while its re-cutting is complicated and necessitating its repositioning [297]. The measurement accuracy of FOHs is also limited by the difficulty of controlling the fiber cut relative to the wave front, the finite width and the possibility of inaccurate determination of the frequency response by the manufacturer [304]. Due to the high level of noise (2–3 MPa), it is almost impossible to measure a small amplitude linear field by FOHs. Also, many of the reported FOHs are highly acoustic sensitive, but their normal-

ized sensitivity is very low, which is why long fibers are used to increase sensitivity [306]. FOHs demand an expensive setup and the minimum measurable pressure typically about 100 kPa [307,308].

The similarities between the two types of hydrophones ensure that the measurement methods developed for piezoelectric hydrophones can be generalized for FOHs. At the initial level, these two types of hydrophones are entirely interchangeable, but it is the measurement scenario, complexity, practicality, and availability that determines the choice [275]. Research tools on the performance of some FOHs are complex and confined to the optics laboratory and require specialized knowledge and professional personnel, while others can be constructed by practitioners with basic knowledge of commercial optical instruments such as piezoelectric hydrophones [71]. The FOHs that are currently in use have become less widespread and their behavior is not well known or even misunderstood. Therefore, regardless of their benefits, users are rarely persuaded to use FOHs instead of piezoelectric hydrophones.

In terms of the sensing mechanism, FOHs have two general types. In the first type, which is rarely used, optical fiber acts as a conduit to deliver a light beam to the tip of the fiber. The pressure acoustic wave by applying mechanical effects such as micro bending or deflection at the tip of the fiber modulates the optical refractive index and the mass density of the fluid. In the simplest case, Fresnel reflection coefficient of the light beam from the fiber tip changes and the absolute acoustic pressure information is provided quantitatively [285,290,309,310]. This method, which is also a kind of intensity modulation, is termed the extrinsic FOH. These FOHs are usually small in size and low in cost but suffer from low sensitivity because they are made of glass material that is high in Young's modulus and difficult to compress [310]. Also, since the change in length relative to the fiber strain has a negative sign and the refractive index changes with the fiber strain, the normalized responsivity (NR) is compromised [311]. In addition to single-mode optical fiber, this method is also implemented using photonic crystal (PC) mirror deflection, which has advantages for deep-sea applications due to high hydrostatic pressure tolerance [312,313].

In the second type, acoustic pressure changes the properties of the light beam guided within the optical fiber. Due to the fiber elongation caused by acoustic pressure, the wavelength or phase or polarization of the light beam is modulated. In this case, the fiber itself is known as a sensitive element [314]. This method is termed an intrinsic FOH. Optical fibers can be attached or wrapped to a mechanical structure such as flattened mandrel [315], rigid mandrel [316], air-backed mandrel [317], and flexural disk (diaphragm) [318] to increase the sensitivity by amplifying the strain and minimizing the averaging effect on flow noise due to the limited size of the structure along its axis [319–321]. (See Fig. 23) For example, Yang et al. [314] developed a high-resolution fiber laser hydrophone using a corrugated diaphragm.

There are several techniques for FOHs. The interferometric approach usually employs a pre-tensioned single mode fiber inside a shell or cavity. This technique, which is based on wavelength or phase modulation, is able to measure extremely weak hydro-acoustic pressure perturbations less than 1 Pa in the wide band and less than 0.1 Pa in the narrow band, so it is one of the techniques that has the highest sensitivity [295,322,323].

Along with traditional interferometric schemes based on Mach-Zehnder interferometer (MZI) and Michelson interferometer configurations, [324] FOHs utilize diaphragm based structures [325], distributed feedback fiber laser (DFBFL) [326–331], fiber Bragg grating (FBG) [332,333], distributed Bragg reflector (DBR) fiber laser [334–341], dynamic holographic Grating and FP cavities [342,343] as sensitive elements.

MZIs are based on phase demodulation and provide high-resolution, [344,345] but among all interferometers, the Michelson interferometers is more widely used [346].

In the 1990s, a variety of interferometric FOHs were proposed using a number of FBGs [347,348]. This acts as a reflector with the ability to select the wavelength and does not require extra accessories such as couplers, joints or other interconnects other than the optical fiber core. Therefore it can be made or arrayed with less complication and more reliability than other types of FOHs [349–351]. FBG-based FOHs are made to measure the frequency range from a few Hz to a few kHz [352] and due to their inverse proportion of the frequency response to the length, an extremely short FBG must be developed to increase bandwidth. However, due to their low reflectivity, their sensitivity is low. In contrast, they provide a high SNR [353].

Hydrophones based on MZI, FBG and DFBFL are relatively sensitive and large in size [354].

Fabry-Perot interferometer (FPI) hydrophones are often operate on the principle that acoustic pressure induces changes in the optical thickness of a solidified polymer FP cavity constructed at the tip of an optical fiber [285,305,342,343,355,356].

This technique is part of the intrinsic FOH mechanism and helps to achieve higher sensitivity and spatial resolution with smaller size, higher compactness and more flexible structure but at the cost of a greater fragility. Sensitivity can also be increased simply by selecting a soft material as the FPI gap material or using multilayer reflectors with improved finesse [99,285,355–357]. Multilayer reflectors also ensure the robustness of the sensing head by using deposition method [355,356,358].

It was demonstrated that this structures have a relatively high bandwidth of up to 50 MHz, especially compared to Mach-Zehnder based FOHs that require several meters of optical fiber windings, which makes them bulky and expensive and provides bandwidth above several hundred Hz. These FOHs usually have small SNR due to low reflectivity and small Young's modulus [352]. In addition they have high stability, lower large-scale manufacturing cost [359,360].

FPI based hydrophones are generally susceptible to external noise such as accidental mechanical stresses, temperature deviation and static pressure variations because the length of cavity may be affected by these factors [180].

Drifting in the working point of the FOHs can significantly reduce the sensitivity or even lead to failure of the measurement process. One of the proposed approach to address the working point drift is to use a tunable laser as a light source to adjust the wavelength of the laser for deviation in the working point. However, this approach increase the cost [354]. Many approaches have been developed to stabilize the operating point today [361].

Photonic crystal fibers (PCFs) have also been tested for better performance in the field of FOHs. Experiments have shown that solid-core PCF (SC-PCF) has the same performance as SMF [362] and hollow-core photonic band gap fiber (HC-PBF) can have advantages such as better sensitivity [363]. Using the ray tracing model, Abdallah et al. [364] has conducted comprehensive studies on the propagation of acoustic waves in deep water to predict the dynamic behavior of HC-PBF in underwater environment.

FOHs use other techniques, such as polarimetry [365,366]. Laser adaptive holographic hydrophone (LAHH) have also been developed [361]. The combination of nanotechnology and fiber optics has led to the development of optical fiber micro-knots that have exhibited good response to acoustic waves from low frequency up to several MHz [367,368]. MakSYM & Greentree [369] theoretically showed that an ultra-small plasmonic nano-antenna can be employ as an optical ultrasonic hydrophone using higher-order plasmon mode. This can develop a variety of modalities including intravascular imaging of small blood vessels.

Hydrophones can be divided into broad categories. Below we describe each type in detail.

- i Measurement type: vector and scalar hydrophones
- ii Frequency range: infrasonic, low frequency and ultrasonic hydrophones
- iii Working principles (mechanisms): inertia type and etc.
- iv Structure and geometry: needle and membrane hydrophones etc.

6. Vector hydrophones

In addition to scalar information such as the pressure, there is some information such as acoustic pressure gradient, acceleration, particle vibration velocity, acoustic energy flux, etc. that determine the vector information at a certain point of the acoustic field [370]. Vector hydrophone was developed by combining pressure and particle velocity hydrophones based on the view of Leslise [13,371–373]. They were fixed on two orthogonal axes and had disadvantages such as channels' incomplete orthogonality, phase variance, low bandwidth, and large size. Kendan developed a sound pressure gradient vector hydrophone in 1941, and the vector hydrophone was successfully used in 1970 to find direction and range in the sonobuoy system [374]. US Wilcoxon research company developed a 3D resonance vector hydrophone for the US Navy, and vector hydrophones were applied to the underwater acoustic warning system [276,375]. Later, vector hydrophones consisted of an array of scalar hydrophones due to the advantage of easy target detection and localization. The direction of the acoustic targets could be measured with a beam forming technique. The most common approach for underwater source detection and localization was to use time delays in the array to define curves of constant time difference [376,377]. However this structure had disadvantages such as large volume and poor consistency, as well as many challenges in detecting very low-frequency signals [378–380]. Aperture enlargement also required more hydrophones, more complex fabrication, a greater quantity of data, complicated signal processing, and increased cost for locating the acoustic sources properly. With the use of MEMS technology and ICs and development towards integration and miniaturization, vector hydrophones have found many advantages and a single hydrophone can act as a vector hydrophone [381]. From the perspective of energy detection, a vector hydrophone is able to resist isotropic noise from each direction and perform a far-field target recognition [234]. It can effectively reduce the intensity received from isotropic hindrances and work with relatively small dimensions at low frequencies. Furthermore, ideally, a single vector hydrophone has an intrinsic 2-D directivity in terms of azimuth and elevation and has a constant 8-shaped pattern independent of received signal bandwidth and source location [382,383]. Vector hydrophone can also solve the problem of the direction of arrival (DOA) removing ambiguousness in the left or right side of the array which has been a trouble for a long time [384].

Positioning using a single vector hydrophone requires less hardware and is easier to carry and place but less accurate [385]. The same small size and good directivity of vector hydrophones make it possible to array them as well. Such an array has no limitation of the half-wavelength and offers advantages such as improved DOA estimation performance without array aperture size increase, positioning coherent sources, higher accuracy, flexible beam control, higher signal gain, strong anti-interference capabilities, and high spectral resolution and this method has met the requirements of some applications such as small aperture and long-range exploration such as sonar and has made improvements in the field of detection, identification, positioning and communica-

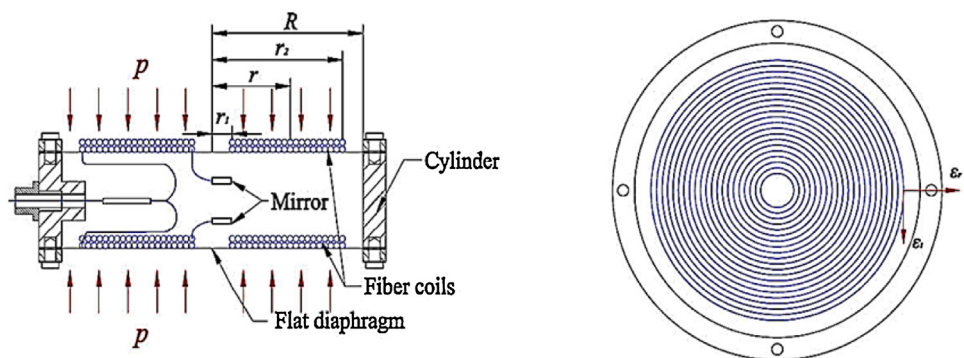


Fig. 15. The diagram of the FOH based on a flat diaphragm. [306].

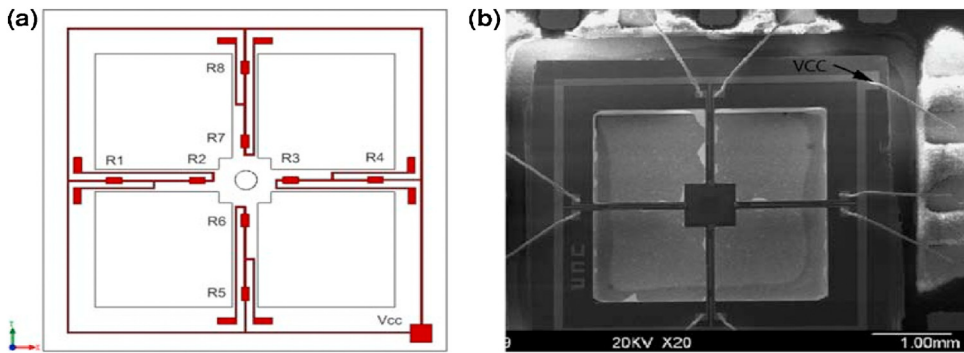


Fig. 16. a) The schematic arrangement layout of piezo resistors on the microstructure of the hydrophone. b) SEM (Scanning Electron Microscope) of the fabricated microstructure [409].

cation of underwater targets [179,386–394]. On the other hand, this structure has low mobility and requires a complex system. As the frequency increases, the resolution of detection improves, but the dimensions of each hydrophone element reduces so that at a frequency of several hundred kHz, the distribution of array elements becomes so dense that fabrication accuracy cannot be easily achieved using traditional materials and methods [85]. The use of multiple hydrophones leads to the degradation of performance in ocean environments due to multi-path without prior environmental information. Also, in some cases, space constraints make installation difficult. In 2017, Han et al. [395] proposed a method that transferred the measurement results from a single hydrophone to the results of a virtual array and achieved high positioning accuracy using virtual spectral distribution. Estimation of the range and the direction of the acoustic source may be based on coherent signals from multiple sources or asynchronous signals from one or more sources each has a different algorithm. In the field of the vector hydrophone signal processing, in recent decades, many subspace based techniques such as the multiple signal classification (MUSIC) method, [396] equation-error (EE) method [397], estimation of signal parameters via rotational invariance technique (ESPRIT) [398], focused beam forming approach [399], bearings-only cross [400], matched field processing (MFP) [401], subspace-base method for direction-of-arrival estimation without eigendecomposition (SUMWE) [402], the average acoustic power approach, and line-spectra estimation or the bar graph approach have been combined with single or array vector hydrophones to estimate 2D/3D directions of underwater narrowband signals. These algorithms have their special weak and strong points and they can be compared in estimation accuracy, computational complexity and simultaneous estimation of multiple separate bearings [384,403–408].

6.1. Cilia-type four-beam vector hydrophone

With the broad development of MEMS vector hydrophones, a bionic conventional two-dimensional micro-silicon four-beam vector hydrophone (CFVH) was first presented in 2007 by Xue et al. [86], which integrated a bionic high aspect ratio hair onto a four beam structure and had a sensitivity of -197.7 dB (with 10 dB pre-amplifier) and a bandwidth of 1 kHz as shown in Fig. 15. In 2008, the same team focused on the modeling and primary characterization of their hydrophone as well as its sensing principles [409]. This structure has two main parts: a hair cell, which according to the acoustic theory of cylinder should be much smaller than the wavelength of the acoustic wave, and second, the mechanoreceptors where the generated stress-dependent signal due to the deformation of the beams is measured [410]. The advantages of CFVH were the miniaturization of a single hydrophone, rigid mounting, low-cost, good low frequency, and vector characteristics. But this design also had its drawbacks, such as low sensitivity, low bandwidth, off-center cilia, being two dimensional, left-right ambiguity, etc. Also, the need for the secondary integration of cilia and four beams did not guarantee the consistency. Therefore, various approaches have been adopted by researchers to address these disadvantages.

6.1.1. Sensitivity enhancement approach

The sensitivity of the cilia structure was not suitable for conventional hydrophone applications. So, in 2008, Chenyang Xue et al. [249] designed a CFVH that integrated the resonant tunneling diode (RTD) as its sensitive element. This structure is shown in Fig. 16a and b. This design converts a weak mechanical signal into a strong tunneling current signal, thus increasing the sensitivity to -184.6 dB at 1 kHz. Xue et al. [42] proposed four aspects in 2011 to improve the performance of their CFVH. First, fiber was chosen as a sub-

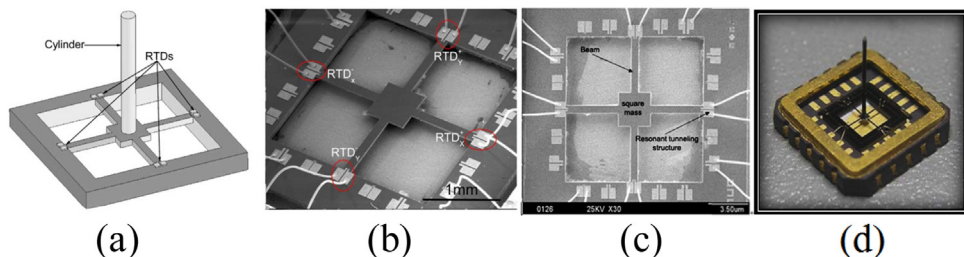


Fig. 17. a) Illustration of the structure model of four-beam structure, b) SEM photograph of the four-beam structure [249]. c) SEM images of the NEMS CFVH [232] d) Microstructure of the four beams-cilia [414].

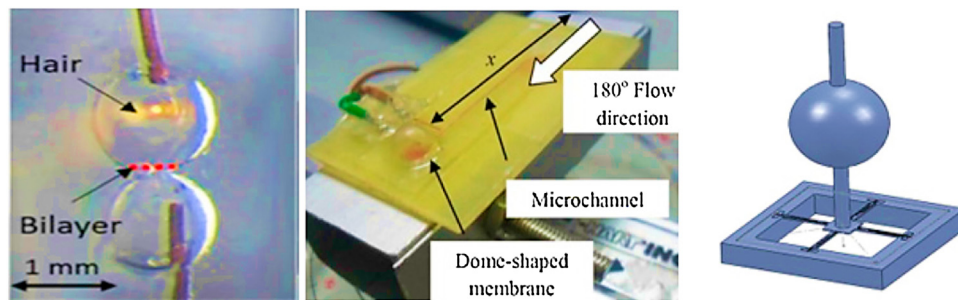


Fig. 18. “lollipop-shaped” MEMS vector hydrophone (LVH).

stitute for plastic rod; second, a mature diffusion technology was used to improve the consistency of piezo resistance; third, a novel package was proposed; fourth, polychloroprene whose density is more matched with water was used. With this improvements, the sensitivity was increased to about 12 dB and frequency response curve was greatly improved. In 2011, Guan et al. [232] developed a nano-electromechanical system (NEMS) CFVH based on meso-piezo resistance effect using a resonant tunneling thin layer a shown in Fig. 16c. This quantum effect, which is commonly found in super-lattices and quantum wells, causes the tunneling current of the structure to change under mechanical stress and increases the sensitivity to -170 dB [411,412]. In 2012, Zhang et al. [413] chose glass optical fiber with greater stiffness instead of plastic cylinder because of its more impedance matching with water. They implanted it with 502 glue and optimized the sheet resistance and could reached a sensitivity of -165 dB (20 dB pre-amplifier) and a bandwidth of 20 Hz to 2 kHz. In the same year, Liu et al. [414] have designed a resonant-column type MEMS CFVH as shown in Fig. 16d, based on the relationship between vibration velocity, density and dimensions, with an X-channel sensitivity of -177.9 dB (2 kHz) and Y-channel sensitivity of -175.4 dB. One of the main hindrance to further improvement of MEMS hydrophones is that the sensitivity and bandwidth of the hydrophone restrain each other. Guan and Zhang [237] tried to solve the problem by devising a T-shape vector hydrophone, nevertheless, the shortcoming if this design was that the detecting space of hydrophone was reduced from 2D to 1D.

Later, the method of multiple stress concentration regions (MSCRs) was introduced to increase the sensitivity, which referred to the areas of stress localization on the microstructure. Many researchers have studied this idea but the sensitivity did not improve effectively [415–419]. Guojun et al. [420] improved the sensitivity of the ordinary structure by 1.5 times by proposing a structure as shown in Fig. 18a in which grooves were formed using etching. However, the bandwidth was limited to 500 Hz. In 2015, Han et al. [421] changed the vector hydrophone mechanoreceptors to piezoelectric transduction by using the PMN-PZT ceramics. In the same year, by splicing a low-density sphere and CFVH, Liu et al. [422] proposed a “lollipop-shaped” MEMS vector hydrophone

(LVH) by extending the sensing area as shown in Fig. 17, which improved the sensitivity by 10 dB compared with CVH.

In 2015, COMSOL Multiphysics was used by Smitha et al. [423] to study the piezoresistive effect of p-type silicon on a range of pressure variations as shown in Fig. 18b. In 2016, Mengran et al. [240] proposed a monolithic cilia type 2×2 array hydrophone integrated on a chip as shown in Fig. 18c and studied different cilia lengths. This microstructure exhibited a high sensitivity of -189 dB (without pre-amplifier) and a higher bandwidth of 20–5000 Hz. In the same year, Kumar et al. [9] presented a modified design of crab-meander like beams as shown in Fig. 18d, which increased the sensitivity by increasing the effective length of the beams.

In 2016, with an idea of increasing the sensing area, Xu et al. [424] integrated a low-density cup-shaped with the cilium structure as shown in Fig. 19a and obtained a sensitivity of -188.5 dB and a bandwidth of 20 Hz – 1 kHz, which was more stable than LVH. Focusing on stress concentration areas, Zhang et al. [241] developed a SCVH based on piezoresistive effect in 2018 as shown in Fig. 19b. This structure increased the sensitivity to LVH and CFVH by 7.6 dB and 17.2 dB respectively. In the same year, Zhang et al. [425] introduced a multi-unit (4-unit) vector hydrophone as shown in Fig. 19c, which was integrated on a chip. This structure increased the sensitivity and SNR to the 1-unit hydrophone by an average of 11.8 dB and 1.9 dB, respectively. The fabrication of the cilia of LVH and cup-shaped structures were complex and the success rate was difficult. The load on the cross-beams also increased. Accordingly, in 2018, Xu et al. [426] developed a two-component cilia cylinder structure (TCVH) shown in Fig. 19d, using a simple manufacture method that optimally reached a sensitivity of -188.1 dB and a bandwidth in the range of 20 Hz to 1 kHz.

In 2019, CFVH was improved by Singh et al. [427] by optimizing various structural parameters. In this year, also L. Zhang et al. [428] designed a cilia cluster MEMS vector hydrophone (CCVH) in optimal size according to Fig. 20a. This configuration improved the sensitivity of hydrophones up to -183.3 dB without adding appendants to cilia or reducing the bandwidth.

Contrary to the perceived contradictory relationship between sensitivity and bandwidth in MEMS hydrophones, in 2019 Qingda Xu et al. [429] developed a two-degree of freedom mathematical

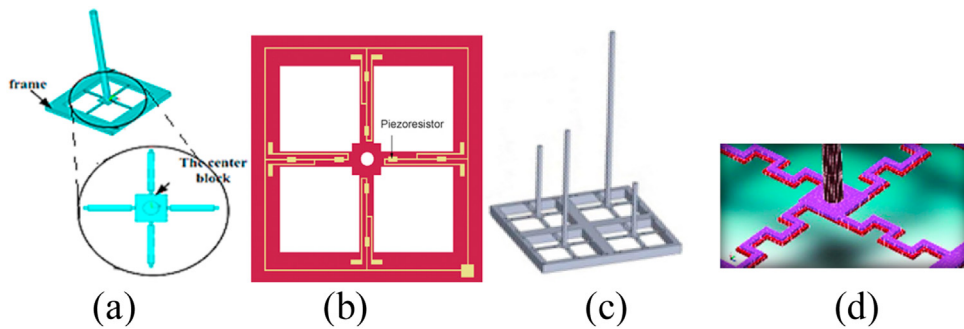


Fig. 19. a) The model of cilium microstructure with MSCR [420] b) 4 Beam Microstructure [423] c) a 3D view of the 2×2 array microstructure [240]. d) 3-D model showing crab-meander and reduced cross-section CFVH.

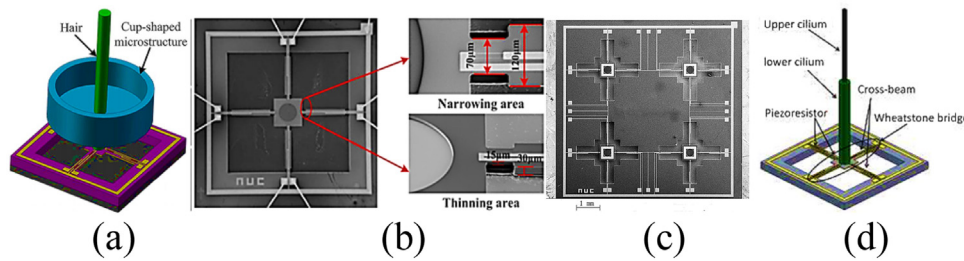


Fig. 20. a) cup-shaped structure. b) The SEM image of SFVH chip [241]. c) top view SEM image of multi-unit vector hydrophone [425] d) TCVH [426].

vibration model (which accounts for the effect of cilium bend on the vibration). Conventional single-degree of freedom models are weak in conditions such as being too small cilia diameter. They discovered that increasing the diameter of the cilia increases the sensitivity and bandwidth simultaneously. Other reported MEMS hydrophones typically had limitations such a low noise resolution and variable in depth operation.

6.1.2. Technology improvement approach

The structure proposed by Xue et al. [44] in 2007 was fabricated separately by a plastic molding step and a manual artificial hair cell (AHC) attachment to the structure. The lack of cilia in the center of the structure had a direct effect on the inaccuracy of the hydrophone measurement. There were problems with microscale matching. Also, due to use of bonding materials, the signals were damped. To overcome these drawbacks, Han et al. [421] used the near-net-shape manufacturing process, and powder injection molding (PIM) technique to manufacture AHC. The steps are shown in Fig. 20b.

6.1.3. 3-D redesigning approach

The design presented by Xue et al. [44] was a 2D MEMS vector hydrophone (2DVH) with all its innovations. Due to requirements for the 3D detection of acoustic signals, in 2014, a 3D median-low frequency MEMS vector hydrophone was developed by Hang et al. [31] as shown in Fig. 20c. This hydrophone was based on CFVH in X and Y channels and had long cantilever beams in Z channel. This configuration achieved a sensitivity of more than -180 dB and a bandwidth in the range of 25 Hz–1500 Hz. In 2015, Zhang et al. [430] presented a 3D T-structure-combined vector hydrophone (TSVH) by integrating a CFVH with a T-shaped cantilever as Z channel, as shown in Fig. 20d. This structure had a nonlinear relationship between output and input due to isolation of the Z channel from other channels. However, this configuration suffered from the impossibility of monolithic integration of channels and low bandwidth (under 1 kHz). A fitness-wheel-shaped MEMS vector hydrophone (FWVH) was developed by Wang et al. [431] in 2017 to achieve a 3D configuration via appropriate construc-

tional design, as shown in Fig. 20e. In addition to linear relationship between output and input of the channels, it also had a sensitivity of -174 dB. This configuration had a low bandwidth of about 300 Hz and was not suitable for mass production. J. Song et al. [432] proposed a monolithic integrated 3D configuration according to Fig. 20f in which acoustic pressure gradients in the Z channel was measured by the supporting block and beams. It had also a simple structure and the possibility of mass production. It also had a higher sensitivity and a wider bandwidth.

6.1.4. Left-right ambiguity resolving approach

Although much progress has been made in the field of hydrophones after years of optimization, the problem of left-right ambiguity has rarely been addressed. That is, the exact direction cannot be identified. Traditionally, left-right ambiguity has been eliminated by integrating vector and scalar into a shell to simultaneously measure sound pressure and its gradient and use combined algorithm of acoustic energy flux [17,276,433]. In 2010, Li et al. [281] have solved this problem by proposing a composite MEMS hydrophone as shown in Fig. 21a by adding and integrating a capacitor microstructure near the cilium-four-beam. The accuracy of distinguishing the direction of signal arrival in this structure was 1 degree. The drawbacks of this design were the lower pressure part (capacitor) sensitivity to the vector part (cilium-four-beam), process complexity and the high cost. In 2019, Li et al. [434] also proposed an array MEMS hydrophone with four-cilium-four-beam microstructures oriented at different direction angles as shown in Fig. 21b. Simultaneous measurement of the direction by the arrays would determine the exact direction and position of sound source and eliminate the ambiguity.

6.1.5. Vibration/acceleration suppressing approach

Various experiments have shown that the MEMS vector hydrophones interfered greatly with noise sources such as structural vibration in the host hull, acceleration and even acoustic cavitation accruing around the surface of the hydrophone [435,436]. This interference with noise has degraded the performance of the hydrophones. Therefore, it is very interested

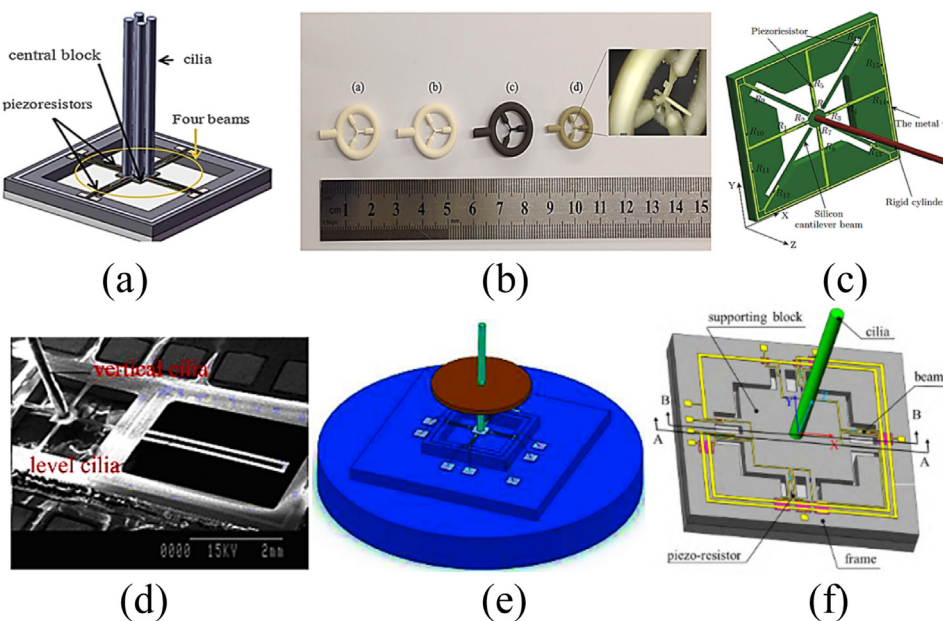


Fig. 21. a) cilia cluster MEMS vector hydrophone (CCVH) [429] b) AHC structure fabricated through each process of PIM: (a) injection, molding, (b) solvent debinding, (c) thermal debinding, (d) sintering [421] c) Schematic of bionic 3D MEMS hydrophone [31] d) The SEM image of the TSVH [430] e) FWVH [431]. f) Monolithic integrated bio-inspired three-dimensional MEMS vector hydrophone [432].

to develop the noise suppressing hydrophones. Several types of hydrophones have been proposed to solve this problem [437–442]. Generally, the first method for designing a noise insensitive hydrophone is an electrical method that refers to filtering noise in the follow-up circuit that is usually difficult and increases the complexity of the system. Another method is mechanical, which isolates the transducer from the noise propagation path using resiliently-mounted or flexible installation techniques, which is usually more practical and easier. However it is difficult to miniaturize the external soft connection, which lead to scattering in the acoustic field. Strengthening or stabilizing are also a challenges, especially when the system is composed of an array [17]. In 2000, Im et al. [443] developed an effective noise suppression mechanism by means of the acoustic walls including air pockets and compliant layers, without sacrificing the performance of the hydrophone. In 2011, using two pairs of springs shown in Fig. 21c, a novel damping structure was proposed at the chip-level [62]. Guo et al. [251] tried to isolate the hydrophone from noise by using a type of elastic damping element in 2015 as shown in Fig. 21d. However, elastic elements often have weak effects on the isolation of low-frequency vibration acceleration signal [444]. They are also susceptible to fatigue aging due to micro-cracks or expansion [445]. A sponge covering with a proportional pore size and thickness was used by Tao et al. [446] in 2014 to eliminate the noise. Despite the effective filtering of the pressure interferences, the construction of such a structure was to some extent complex. In 2017, According to the operational principle of the differential amplifier, Zhang et al. [2] proposed a differential-type MEMS vector hydrophone as shown in Fig. 21e. The design consisted of two sensitive elements that was encapsulated in two acoustic packages, one with good acoustical transmission properties to properly receive acoustic signals and the other with poor acoustical transmission properties to block the noise. This structure reduced the sensitivity to acceleration by about 17 dB while remaining the hydrophone sensitivity. However, assembling such a structure was complex and required two symmetrical and identical cilia. In order to improve the high g shock resistance in airdropped application, Bai et al. [1] in 2017 developed a cross-supported planar MEMS vector hydrophone with a larger elastic coefficient as shown in

Fig. 21f. In 2018, Song et al. [447] proposed a crafty piezoresistive 8-beams vector hydrophone with thick mass block as shown in Fig. 21g to solve the problem. Conventional solutions for suspending the hydrophone elastically, although they may reduce the effect of high-frequency vibrations, have little effect on reducing low-frequency vibrations. Mathematical models and experimental results by Song et al. [447] in 2019 showed that the actions of the supporting block and cilium on the piezo-resistors counteract each other. Therefore, by increasing the volume of the supporting block as much as possible (instead of increasing the cilium), the vibration is largely suppressed. The hydrophone provided by them is shown in Fig. 21h.

6.2. T-shape vector hydrophone

Based on fish lateral line, in 2004 Guan et al. proposed a T-shape hydrophone with a sensitivity of about -180 dB and a resonant frequency of 2 KHz [449]. Based on this idea, Guan et al. in 2011 and Liu Linxian et al. in 2015 [37,450] proposed a novel double T-shape piezoresistive MEMS vector hydrophone using MEMS technology and a SOI wafer (Fig. 22a) that had a flat frequency response curve. In 2017, a T-Shape PZT vector hydrophone was analyzed by Naik et al. [226] to increase the bandwidth and the sensitivity by minimizing the damping effect.

In 2018, Ganji et al. [451] also increased the bandwidth to 10.4 k Hz with a sensitivity of -191 dB by designing a novel MEMS T-shape piezoelectric hydrophone as shown in Fig. 22b consisting of a power transmission beam that is connected to the piezoelectric section by four anchors.

6.3. Co-vibrating vector hydrophone

Another idea used to develop vector hydrophones was to exploit the free vibration theory of underwater object that describes the conditions under which a sphere or cylinder moves freely. In this case, a rigid structure is defined as a structure which is not influenced under the action of radiation of an acoustic wave, for example, the wave cannot move the spherical or cylindrical elements of a rigid structure [452]. In classic applications,

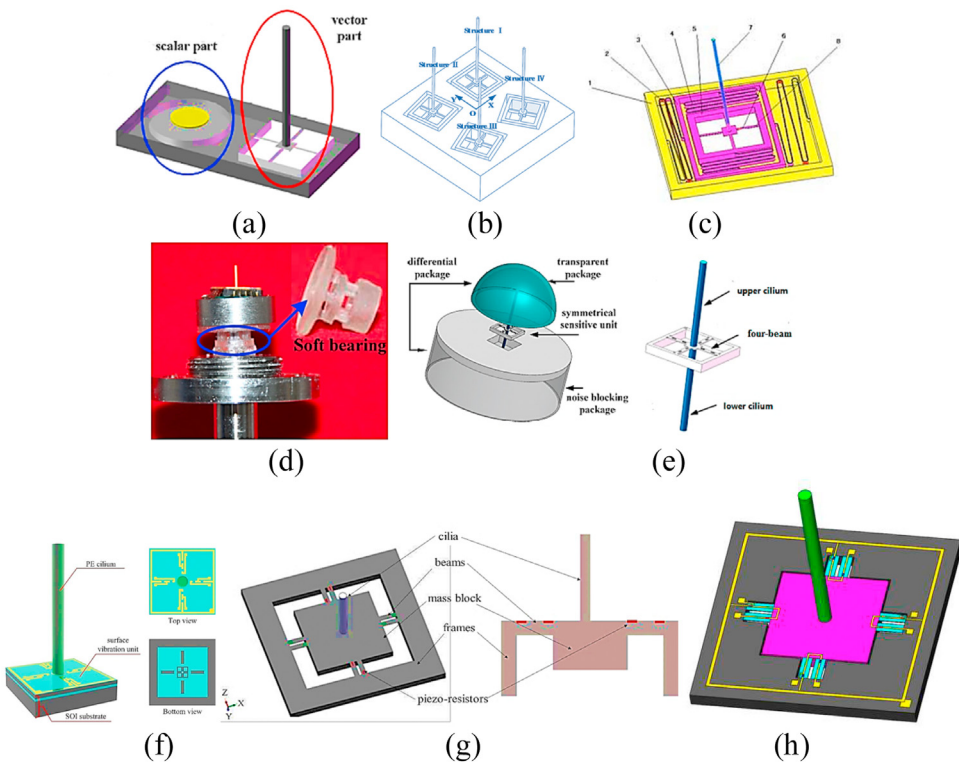


Fig. 22. a) Overall design of the composite MEMS hydrophone. [281] b) Overall design of the array hydrophone [434] c) Vibration sensor chip schematic. d) vibration-isolation packaging structure [251] e) Structure diagram of the differential MEMS vector hydrophone [2] f) The new structure of cross-supported planar MEMS vector hydrophone [1] g) Structure of designed 8-beams vector hydrophone with a thick mass block [447] h) proposed hydrophone in [448] for suppressing vibration.

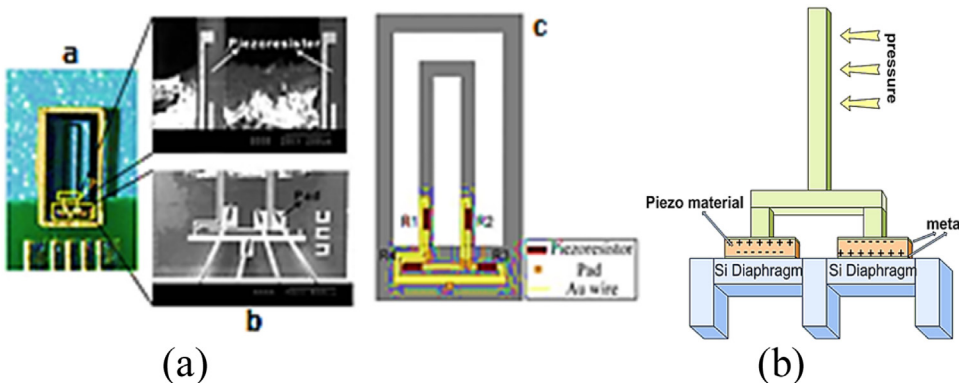


Fig. 23. a) (a) Schematic of the double T-shape hydrophone's package and (b) photo of the packaged double T-shape bionic vector hydrophone (c)The layout and connection of piezo resistors [37] b) The new structure of a novel MEMS T-shape piezoelectric hydrophone [451].

the hydrophones was considered a rigid object in water, but at present, due to the reduced effect of the platform, the hydrophone is placed inside a shell and filled with a acoustically transparent material such as synthetic resin or syntactic form [453]. In order to achieve an approximate free state in the water, the vibrating mass is connected to the fixed framework by elastic elements such as springs, which have effects on the motion measurement and increase the overall size of the hydrophone. Recently, American researchers designed a small vector hydrophone with a central mounted structure that could be easily installed on various platforms [454]. In 2004, Shi et al. [455] theoretically derived the effect of elastic element parameters on the measurement values. Zhao et al. [456] analyzed the fluid-solid coupling in 2013 to consider effect of the water medium on the structure. In 2012, Wang et al. [457] analyzed a centrally fixed structure co-vibrating (co-oscillating) vector hydrophone based on cymbal transducer. The

characteristics of a spherical co-oscillating vector hydrophone in an acoustic field consisting of plane waves analyzed by Zhao et al. in 2014 [458]. In the same year, a combined co-vibrating vector hydrophones prototype with three orthogonal accelerometers as velocity channels and a piezoceramic as pressure channel in a cylinder with irregular shape was designed by Qin et al. [459] which had a sensitivity of -185.3 dB and a bandwidth in the range of 20–5000 Hz.

2D or 3D design of co-vibrating vector hydrophones using the combination and packaging several accelerometers or other sensitive elements require considerations such as accuracy in selecting base level, symmetry and structural balance [39,254]. These hydrophones usually have low resonant, high cost and large volume which may limit their practical applications.

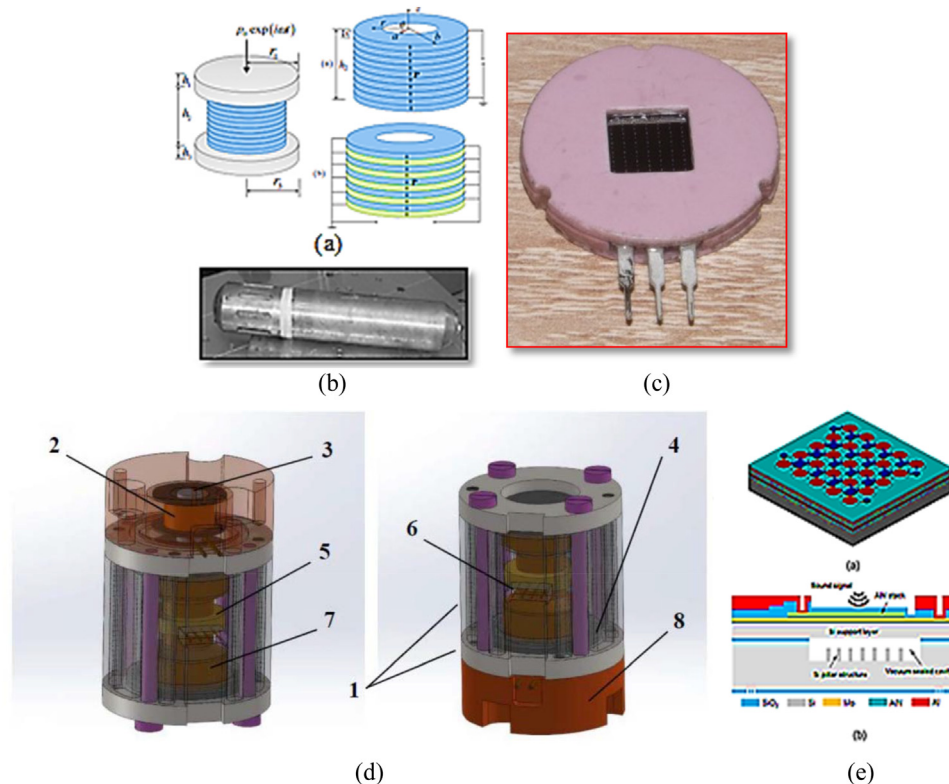


Fig. 24. a) Models of IPH, (a) series, (b) parallel [469] b) General view of the pyroelectric hydrophone module [465]. c) New prototype of a high-precision ultra-low-frequency hydrophone based on a planar type electrochemical transducer (ECT) [471]. d) Constructional parts of the MET hydrophone. 1 – external body; 2 – coil; 3 – magnet; 4 – membranes; 5 – electrical package; 6 – electrical terminals of anodes and cathodes; 7 – electrolyte; 8 – cover with air bubble under it [472]. e) MEMS hydrophone, (a) perspective view of a 5-5 arrayed design, (b) cross-sectional view of a single-element [183].

7. Hydrophones for different frequency ranges

The frequency spectrum for hydrophone applications ranges from below 10 Hz to several MHz [460,461]. Hydrophones can be divided into three general categories based on the operating frequency range and applications required. Hydrophones developed for infrasonic applications and capable of measuring tens and hundreds of Hz, Hydrophones for ultrasonic applications capable of measuring up to several MHz, and low frequency hydrophones that can sense from a few tens of Hz to several kHz. This classification is basically an application-based division. The need for specific applications has usually led to fundamental changes in structures.

7.1. Hydrophones for infrasonic applications

The operation frequency of infrasound hydrophones is always below 20 Hz. This frequency range has some applications such as very long underwater acoustic communication range, because as the frequency increases, acoustic waves are absorbed immediately [221]. In some cases, such as studying the noises of the earth and the ocean, earthquakes, tsunami phenomena, studies of natural and techno-genic seismicity, the interaction between the lithosphere and the hydrosphere, and even intercept ship propellers, the operating frequency range is substantially reduced to below 0.1 Hz [462–464]. Up to now, although hydrophones have been widely used in underwater studies, there has been no tendency to use them in the infrasonic frequency band due to their frequency characteristics. In recent years, the interest in studying this frequency range especially frequencies below 0.01 Hz has increased [465]. Improving sensitivity in this area has many advantages such as finer resolution about mapping the depth structure of the earth [466–468].

Extremely weak signals by current technologies are not effective enough, so many physical principles are being developed due to the growing trend in this field. Chen et al. [469] proposed two models of infrasound piezoelectric hydrophones (IPH) with certain geometric parameters using the fluid-solid coupling effect and underwater acoustic wave propagation with the ability to measure frequencies about 0.01 Hz and lower. (Fig. 24a) Zheng et al. [470] proposed an infrasound hydrophone model in 2016 using a radially polarized piezoelectric cylindrical tube. In 2016, an infrasonic hydrophone was reported by Xu et al. [183] which was fabricated using piezoelectric AlN on a cavity SOI substrate and was compatible with CMOS as shown in Fig. 24b. The structure reached a sensitivity of -182.5 dB and a bandwidth of 10 Hz–100 Hz. In 2018, a new prototype of a high-precision ultra-low-frequency hydrophone based on a planar type electrochemical transducer (ECT) was demonstrated by T. V. Krishtop et al. [471]. Their microchip with a mechanical system could detect the alternating pressure at low frequencies up to 0.01 Hz. The main advantage of this type of electrochemical hydrophone was high sensitivity in the infrasound range (Fig. 24c). In this year, Zaitsev et al. [472] presented an electrochemical hydrophone based on the principles of molecular electronic transfer (MET). Their work showed that their device could reach a sensitivity of 0.75 mVPa⁻¹ in the 0.02–200 Hz frequency band. Also, the theoretical self-noise floor of MET hydrophone in the low-frequency range has shown that it has the potential to achieve values much lower than the Wenz model. (Fig. 24d) In 2019, E. V. Romanenko [465] presented a high sensitive infrasound hydrophone based on the pyroelectric effect with a limit in depth and operating frequency range in the order of 0.001 to 0.01 Hz. Schematic of this hydrophone is shown in Fig. 24e.

7.2. Hydrophones for ultrasonic applications

Ultrasound is generally referred to as having a center frequency greater than 15 MHz. The range of 1 MHz–10 MHz is extensively developed in biological tissue imaging. Frequencies over 20 MHz, referred to here as micro-ultrasound, have been developed for pre-clinical and clinical research [108]. Interest in hydrophones with the operation frequency in 100 MHz has also recently grown for diagnostic applications. Although calibration of ultrasonic hydrophones at the frequency beyond 20 MHz is extremely time-consuming and difficult, nowadays many calibration methods have been developed to calibrate ultrasonic hydrophones at several hundred MHz [50,473–475]. In this regard, international standards (IEC 2007a, 2007b, 2007c) [107,476,477] have been established to define the properties, calibration, and measurement of hydrophones.

In addition to fulfilling fundamental specifications, there are many limitations to the development of ultrasonic hydrophones. An excellent overview of the challenges of high-frequency measurement with numerous examples can be found in Nagle et al. [478]. Most commercial hydrophones have a sensitive element with a nominal diameter on the order of 500 μm. such aperture is too large to measure acoustic fields beyond 3 MHz due to disturbance, reflection, or diffraction of ultrasound waves that occur at the tip of the hydrophone. It also increases the spatial averaging effect and makes it difficult to achieve adequate sensitivity. Generally, sensitive elements dimensions below 0.1 μm are required for obtaining the desired measurement [479]. The effect of the hydrophone dimensions on the acoustic field at high frequencies has mostly been studied by theoretical analyses [480–482] or numerical simulations [483,484]. Many groups have developed different types of hydrophones to reduce the aperture of hydrophones [169–172]. As long as the operating frequency of the hydrophone increases, the requirements become harder to meet [61]. Also, due to the nonlinear propagation of sound waves, for measuring the nonlinearly distorted ultrasonic pulses, international guidelines recommend that the bandwidth of the hydrophone should be varied from less than ±6 dB or ±3 dB in the frequency range up to more than eight times the acoustic working frequency [108,485]. Other considerations in the field of ultrasonic hydrophones include the desirability of phase response and the stability of the responses of temporal and environmental conditions.

Several designs are offered for ultrasonic hydrophones such as rod-guided waves, [486] thermoacoustic [487], fiber optic [290], piezoelectric and piezoresistive [249] and other structures such as membrane and needle.

Piezoceramic hydrophones have a broad frequency response and have time stability properties [488,489]. They have a pronounced directivity, even when their dimensions are below the wavelength. But they have a low sensitivity [141,490,491]. Piezo polymers, especially PVDF, are easily prepared in small dimensions and the required shape. They have sufficiently large bandwidth and are used commercially in ultrasonic hydrophones with higher sensitivity and lower cost [492]. However, due to their fragility, poor wettability, high pass filtering [111], cavitation formation [308], etc. they are not preferred to be constructed for measuring high-pressure fields and shockwaves. However, some researchers recently believe that due to their lower price, flat response, and very broad bandwidth of up to a few MHz, with some modifications, they can be used in shockwave measurement [135,492]. But in general, for frequencies below 1 MHz for low-intensity acoustic waves, their use is limited due to low sensitivity [61].

Piezoelectric needle and membrane hydrophones are used in various branches of ultrasound metrology, including medical application, characterization of ultrasonic induced cavitation, under-

and post-graduate academic training, as well as for many wide research purposes.

FOHs with a fiber diameter of about 125 μm are suitable for use in ultrasound frequencies [332]. However, these expensive devices have poor sensitivities and are limited to the measurement of temporally stable signals that can be averaged over a long period of time. Some techniques including tapering have been developed to improve the sensitivity [290,308,309,335,474,493,494]. FBG based FOHs are more sensitive to ultrasonic fields but the spatial resolution in the direction of the fiber axis is not sufficient and they usually have to be long enough to improve [305,334,495,496]. But FPI based hydrophones improve the spatial resolution but suffer from the complex fabrication process and fragile structure [497–500]. Also, unlike piezoelectric hydrophones, some FOHs are sensitive to temperature, which is usually previsioned in ultrasound measurements [71].

Despite their ubiquity, piezoelectric hydrophones are not suitable for achieving small size and sufficient sensitivity in the tens of MHz regime, which is a challenge in some applications such as medical imaging as part of quality assurance. They are also unsuitable for measuring very high amplitude and power ultrasound fields due to their fragility. Sensitivity to EMI is another limitation that often accompanies high power CW fields. FOHs are a serious emerging competitor [501,502].

In general, conventional hydrophones cannot meet the requirements of HIFU measurement due to the very high intensity levels, lateral dimensions of the focal area, thermal effects, cavitation caused by it in the focal area, generation of higher harmonics in the wave spectrum, and even the shock front formation [503–505]. These effects usually lead to the erosion and damage of the hydrophones. Although the use of hydrophones is not the only method for this purpose, several attempts have been made to develop hydrophones with adequate robustness and temporal and spatial resolution for measuring HIFU fields [69,506,507].

One strategy is to modify conventional hydrophones, for example, a needle hydrophone with a metal coating on top of the sensitive element based on the multi-element phased array has been presented [508,509]. Also, a novel membrane hydrophone with spot-poled has been developed comprising a thin stainless steel foil as a protection layer [510]. In addition, efforts have been made to reduce the effects of cavitation, for example, some researchers have fabricated a thick film of PZT on a titanium membrane as shown in Fig. 25a [3,511–514] Another strategy is to use FOHs, which have advantages such as the greater robustness, lower unit cost and ability to measure temperature and pressure simultaneously.

In 2012, Haller et al. [515] evaluated a comparison of hydrophones and a numerical model in HIFU fields and showed that there is a need for further improvement in the characterization of HIFU field. Olga V. bessonova and Volker Wilkens [5] also developed a numerical model based on KZK equation for HIFU field in linear to nonlinear regimes in 2013.

Another issue that is especially important in the case of ultrasonic hydrophones which is rooted in non-uniformity of the hydrophone frequency response is the study of the effect of calibration methods on the uncertainties of calibration data. Correction of the measured frequency data is made by using techniques such as deconvolution, enhancing the calibration frequency, and determining complex-valued calibration data instead of amplitude-only data [83,84]. Many studies have been done in this regard [49,78,304,515]. Factors related to the properties of the hydrophone or associated with the source, acoustic field, and measurement set-up such as fluctuations in electrical impedance and drive voltage, changes in water temperature especially during long scans, non-orthogonality of the tank axes, inaccuracies in motor positions, reflections from the equipment, poor water qual-

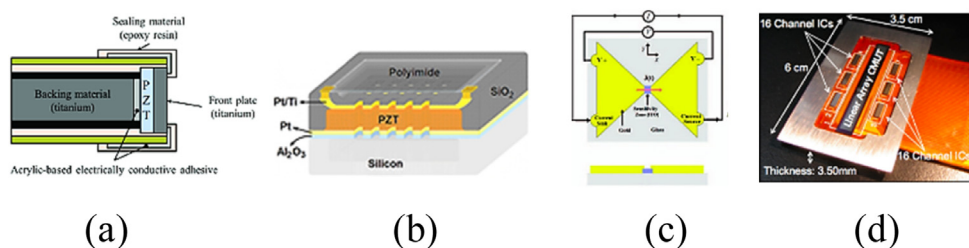


Fig. 25. a) Structure of conventional anti-cavitation hydrophone [531]. b) 3D view of PMUT hydrophone [261]. c) Top of the bowtie AE hydrophone [378]. d) Integration of CMUT and ICs on flexible PCB (Printed Circuit Board) [529].

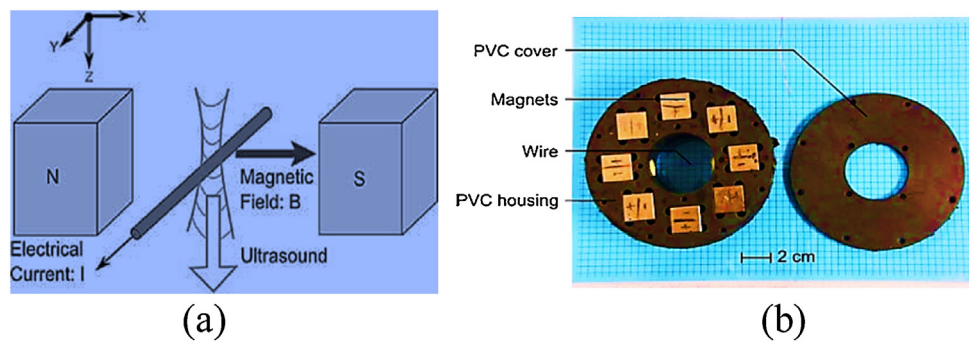


Fig. 26. (a) Principle of the electromagnetic hydrophone (b) Picture of the electromagnetic hydrophone [536].

ity, electrical and mechanical noises can affect the calibration data [516–518]. Much research has been devoted by many authors on studying the effect of these factors on the repeatability, stability, and accuracy of measurements made by different hydrophones, especially in the ultrasonic regime [73,77,79,515,517].

Ultrasonic hydrophones have been developed using various mechanisms or structures, some of the most important of which are discussed below.

Piezoelectric micro-machined ultrasonic transducer (PMUTs) have been intensively studied due to their high efficiency and accomplished fabrication technology. In PMUTs, the sensitive element is a micro-machined multi-layered membrane with a piezoactive layer, typically a thin PZT layer [149,173,519]. (See Fig. 25b). Such a film can be made using batch mode fabrication technologies to integrate bulk piezoelectric materials into MEMS devices [519]. In 2014, Shevtsov et al. [129] presented a multi-objective Pareto-based optimization for a PMUT hydrophone based on a miniaturized perforated piezoceramic membrane.

Acousto-electric (AE) based ultrasonic hydrophones are another type of ultrasonic hydrophones which have a different measurement mechanism from piezo-resistive ones. Piezo resistivity generally describes a linear change in the resistivity ($\Delta\rho/\rho_0$) of a material as a function of stress (σ) with equation $\Delta\rho/\rho_0 = \Pi_1^\sigma \sigma$, [520] which is the result of a geometric change in a solid under pressure and redistribution of its electrical charge [378]. Π_1^σ is defined as longitudinal piezoresistive coefficient. There is a more general effect, AE that determines the change of resistivity with pressure with equation $\Delta\rho/\rho_0 = -K_1 \Delta P$ [521] where K_1 is constant of interaction. This effect is not limited to solids and also is applied to liquids. This coupling of electrical and mechanical energy has been considered to detect the propagation of an ultrasonic wave in a conductive medium [522–525]. Witte et al. [526] described a disposable bowtie-graphite hydrophone based on the AE effect. Wang et al. [378,527] examined an inexpensive type of AE hydrophone that used a combination of a rectangular dumbbell configuration and a resistive element of indium tin oxide (ITO) based on MEMS technology. (See Fig. 25c)

These hydrophones are dependent on piezoelectric materials embedded between two semiconductors, although they are not limited and can be used with any other conductive materials. They have simple structures, low cost, high sensitivity, are robust against high-intensity ultrasound fields, potentially wide bandwidth, capable of achieving high resolution at low frequencies, and accurate [526].

With the development of CMUTs (Capacitive Micro-machined Ultrasonic Transducers), advantages such as wide bandwidth, simple integration with electronics, the ability to construct large arrays on a small scale, and low cost, this technology was used to design ultrasonic hydrophones [528,529]. In 2009, P. Cristian et al. [530] tried to solve some problems like long scan time and multiple source pulses using a 2D array. CMUT is also inherently capable of tuning its sensitivity by changing DC bias. (See Fig. 25d)

Lorentz force was first applied to ultrasound in 1969, by which an electromagnetic hydrophone was introduced by Filipczynski [532] using a thin wire attached to an insulator. According to Fig. 26a, under the influence of a magnetic field caused by an ultrasound pulse, the wire vibrates and an electrical signal is induced by the Lorentz force which is proportional to the amplitude of the pulse.

A 5 mm Lorentz force hydrophone has been introduced by Etienne et al. [533] in 1997 and was too wide for ultrasound measurement with high resolution. This design improved by Sharf et al. [534] by transmitting the electrical signal to a pick-up coil, which provided better resolution but reduced the sensitivity. In addition to providing a hydrodynamic model, Grasland et al. [535,536] also proposed a Lorentz force hydrophone with a suitable spectral resolution as shown in Fig. 26b. However, they did not take into account the potential for tension in the wire in their model. A compact Lorentz force hydrophone with a wire diameter between 70 and 400 μm with features such as high resistant, linear performance in the pressure range of 50 kPa to 10 MPa, low cost, and 1 MHz bandwidth was presented and characterized by Mongrain et al. [537].

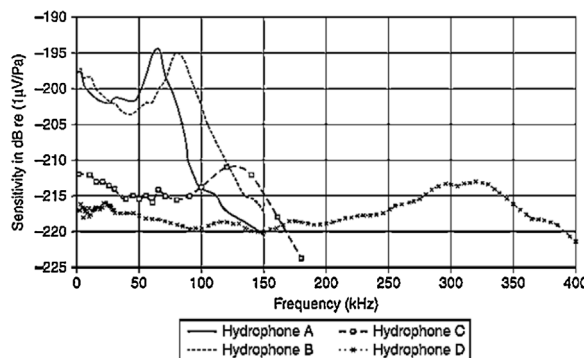


Fig. 27. Frequency response of various low frequency cylindrical and spherical hydrophones [71].

In general, these hydrophones have a high sensitivity and resistance in high-pressure regime, especially to cavitation, but usually do not have a suitable spatial resolution.

7.3. Hydrophones for low-frequency applications

The low-frequency acoustic wave with a frequency of less than 10 kHz for underwater applications have suitable properties such as relatively long propagation, low interference, and strong penetrating power [236]. Accordingly, they are used in a wide range of applications such as disaster early warning like earthquakes and volcanic eruptions, detection, and underwater target positioning and military purposes [538]. The majority of underwater low-frequency hydrophones also operate at frequencies below 500 kHz [71]. Interest in the development of low-frequency hydrophones also appears in the number of reported devices due to the lack of reduction in acoustic resolution by decreasing the frequency of the acoustic field [539].

As a general rule in low-frequency non-optical hydrophones, the larger size improves the sensitivity, [540] weights more, increases output impedance, which in turn reduces the cut-off frequency and SNR, improves directivity, makes it more sensitive to acceleration [183], and more difficult to control the depth and hydrostatic pressures. Fig. 27 shows that the sensitivities of -220 dB and -200 dB will be easily achievable by low-frequency hydrophones. Encapsulating the structure with polyurethane rubber generally causes a kind of attenuation that increases with frequency, and the fall-off in sensitivity may decrease more rapidly above the resonant frequency. Also, because low-frequency hydrophones do not usually use a preamplifier or impedance buffer to introduce noise, NEP is usually limited only by the combination of the sensitivity of the hydrophone and the noise floor of the DAQ. Similarly, the maximum pressure that can be measured by hydrophone is not limited by preamplifier dynamic range and is limited only by the values that are derived from the hydrophone sensitivity and the maximum measurable signal of the DAQ. In the ocean medium, the possibility of encountering acoustic signals greater than 1 MPa and less than 100 kPa is highly unlikely.

Common commercial low frequency hydrophones can be needle or membrane type [71].

The size of the sensitive element of low frequency membrane hydrophones varies from 0.2 to 0.6 mm and larger. They typically have a uniform frequency response and a wide bandwidth [174,541]. The two sub-types of these hydrophones that are identified by configuration of their electrodes include co-planar shielded and bi-laminar shielded. Co-planar hydrophones have a single layer film and therefore have twice the thickness resonance compared to bi-laminar hydrophones of similar thickness. As a result, it has twice the bandwidth. In bi-laminar hydrophones, unlike co-planar

hydrophones, the electrode is not exposed to water, which reduces EMI.

Needle hydrophones are available in a wide range of sensitive element sizes from 40 μm to several millimeters. This type is more economical and more compact and has a lower cost than membrane hydrophones of similar size. Needle hydrophones are usually more sensitive than membrane hydrophones with comparable size. This is because they usually have a rigid termination to the piezoelectric element. As a result, the reflectance is passed back through the piezoelectric element and re-measured. Whereas in membrane hydrophones, which are designed to be acoustically transparent so as not to perturb the acoustic field, the sensitive element does not experience such reflection [71].

In needle hydrophones, NEP is strongly related to sensitivity, which also depends on sensitive element size. Also, the maximum linear pressure range and the damage threshold depend entirely on the hydrophone sensitivity and the linear input range of the preamplifier. The upper limit of the dynamic range also depends on the area of sensitive element in addition to the linear range of preamplifier. However, with a switchable gain or an attenuator before the preamplifier, the upper linear range can be extended.

At high frequencies, the directional response of needle hydrophones is generally conformed to that of the 'circular plane piston in a rigid baffle', while at low frequencies the efficiency of this type is severely impaired.

Table 1 compares the sensitivity and bandwidth of the most important low frequency vector hydrophone structures.

8. Hydrophones geometries

8.1. Needle hydrophones

Piezoelectric needle hydrophones are usually cost effective measurement solutions and preferred for use in high-frequency acoustic fields because they are simple, they have a high bandwidth of about several MHz and have a smooth frequency response. However, the frequency response of these hydrophones is deeply influenced by the wave modes generated due to the interference of the incident waves with the needle tip, which itself depends on the structural parameters and the acoustic field wavelength. The directional responses of these hydrophones are also highly frequency dependent in ultrasonic regime. Fig. 28 shows the data of a 0.5 mm diameter needle hydrophone [71]. Such structures are suitable for measurements where space is limited such as in vitro measurements where the sensitive element should be inserted into tissue. They are also suitable for measuring CW fields due to their low back reflection [542]. Needle hydrophones generally have a damage threshold in the range of 15–20 MPa. At these pressure levels, non-linear acoustics are certainly present and asymmetric shock waves are formed. As an example, Boechat et al. [543] have developed a PVDF-based needle hydrophone for use in measuring ultrasonic fields.

8.2. Membrane hydrophone

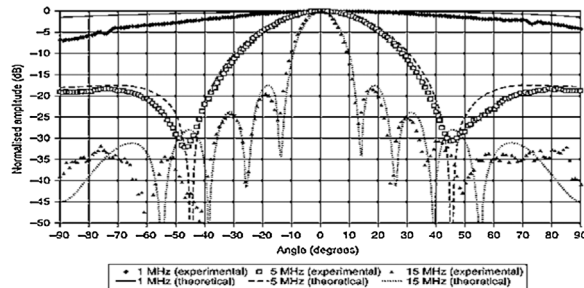
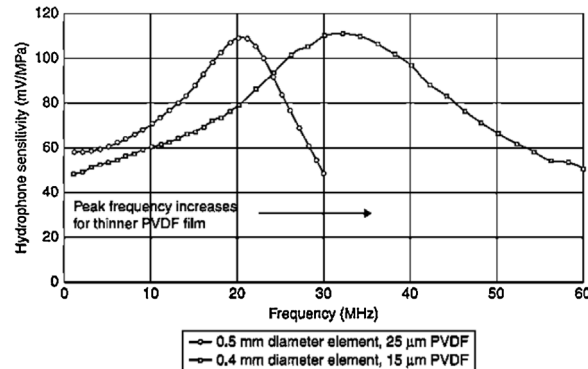
Piezoelectric membrane hydrophones are excellent devices for characterizing broadband, short pulse, ultrasonic signals that are commonly required in diagnostic applications. While membrane hydrophones are less suitable for measuring long-pulse or CW signals because there is a possibility of forming flexural standing wave modes on the membrane, which may interfere with the measurements [66]. This hydrophones usually have a smooth frequency response. The experimental frequency response of two configurations of membrane hydrophones are shown in Fig. 29. These hydrophones do not suffer from the planar modes of vibration if

Table 1

Comparison of sensitivity and bandwidth of the most important low frequency vector hydrophone structures.

Hydrophone	Sensitivity	Linear bandwidth	Scalar/Vector	Ref.
Conventional Two-Dimensional Micro-Silicon Four-Beam Vector Hydrophone (CFVH)	-197.7 dB (with 10 dB pre-amplifier)	<1 kHz	2D vector	[86]
Micro Machined Artificial Hair Cell Vector Hydrophone	-197.2 dB	40–400 Hz	2D vector	[409]
Integrated Resonant Tunneling Diode (RTD) CFVH	-184.6 dB	1 kHz	2D vector	[249]
Improved CFVH	-165 dB (with 20 dB pre-amplifier)	20 Hz to 2 kHz	2D vector	[42].
NEMS CFVH	-170 dB	40 Hz to 4 kHz,	2D vector	[411,412]
Optical Fiber CFVH	-165 dB (with 20 dB pre-amplifier)	20 Hz to 2 kHz	2D vector	[413]
Resonant-Column Type MEMS CFVH	X-channel : -177.9 dB (2KHz) Y-channel : -175.4 dB (2KHz)	0–2 kHz	2D vec-	[414]
MSCR Bionic Vector Hydrophone	-	0–500 Hz	2D vector	[420]
Lollipop-Shaped Vector Hydrophone (LVH)	-183 dB	20 Hz–500 Hz	2D vector	[422]
Monolithic Integrated Cilia Type 2 × 2 Array Hydrophone	-189 dB	20 Hz–5000 Hz	2D vector	[240]
Cup-Shaped Vector Hydrophone	-188.5 dB	20 Hz–1 kHz	2D vector	[424]
Stress Centralized MEMS Vector Hydrophone (SCVH)	-183 dB	20 Hz–500 Hz	2D vector	[241]
Multiple Sensor Units (4-Unit) Vector Hydrophone	-188.5 dB	0 Hz–1000 Hz	2D vector	[425]
Two-Component Cilia Cylinder Structure (TCVH)	-188.1 dB	2 Hz 0 Hz to 1 kHz	2D vector	[426]
Cilia Cluster MEMS Vector Hydrophone (CCVH)	-183.3 dB	20 Hz–1085Hz	2D vector	[428]
Monolithic Integration 3D MEMS Vector Hydrophone	X-channel : -187 dB Z-channel : -163 dB	X/Y-channel: 20 Hz–400 Hz Z-channel: 20 Hz–500 Hz	3D vector	[432]
3D Median-Low Frequency 3D MEMS Vector Hydrophone	-180 dB	25 Hz to 1500 Hz	3D vector	[31]
3D T-Structure-Combined Vector Hydrophone (TSVH)	X/Y-channel : -185 dB (2KHz) Z-channel : -181 dB (2KHz)	< 1 kHz	3D vector	[430]
Fitness-Wheel-Shaped MEMS Vector Hydrophone (FWVH)	-174 dB	300 Hz	3D vector	[431]
T-Shape Vector Hydrophone	-180 dB	-	2D vector	[237]
Double T-Shape Piezoresistive MEMS Vector Hydrophone	-180 dB	20 Hz to 2 kHz	2D vector	[37,450]
MEMS T-Shape Piezoelectric Hydrophone	-191 dB	10.4 kHz	2D vector	[451]
Piezoelectric Gate On A Field Effect Transistor (PIGOFET)	-175.5 dB	50 Hz–500 Hz	2D vector	[274]
MEMS Diaphragm Hydrophones	-155.6 dB	40 kHz <	2D vector	[221]

1

**Fig. 28.** Comparison of experimental and theoretical directivity patterns for a 0.5 mm diameter needle hydrophone. [71].**Fig. 29.** Frequency response of two types of bi-laminar membrane hydrophones.

large diameter membranes are used. Also, due to their relatively fragile construction, their measuring range is limited to low acoustic amplitudes of less than 10 MPa.

Thin films of piezo material with a typical thickness of 10–30 μm usually work as receptors in the regions of stress concentration [175,541]. PVDF membrane hydrophones have become very popular in the early 1980s [165,175,542,544] and were used in a wide range of applications, including ultrasonic exposimetry [70,108,494,545,546], materials characterization [547–549], and even as a reference hydrophone in laboratories. Although ultrasonic fiber optical detectors are increasingly being used [78,356,550,551], piezoelectric membrane hydrophones are still not dispensable for portable and easy use.

A membrane hydrophone using PVDF trifluoroethylene copolymer and electrode with thicknesses of 4 μm and 8 μm , respectively, was designed by Lum et al. [552] in 1996 with a bandwidth of about 150 MHz. In 2007, a PVDF spot-poled membrane hydrophone was designed by Volker et al. [541] with a PVDF foil thickness of 9 μm and an electrode diameter of 210 μm . It was also integrated with a differential preamplifier to increase SNR and was useable up to 140 MHz. A miniature membrane hydrophone array was also proposed by Okada et al. [173] using a thin film of epitaxial PZT

grown on an epitaxial γ -Al₂O₃/Si substrate based on the MEMS fabrication process as shown in Fig. 30a in 2008. It was suitable for frequencies over 20 MHz. In 2016, a membrane hydrophone was designed by Chaggares et al. [473]. By creating aligned electrodes on opposite sides of a polymer membrane with an active area of 10 μm as shown in Fig. 30b. The device had a very low fringing field effects, with a bandwidth of up to 110 MHz. A disposable membrane hydrophones was fabricated using pre-poled PVDF films and PET (Poly-Ethylene Terephthalate)-coated aluminum foils with active element of 2 \times 2 mm as shown in Fig. 30c, which showed sensitivity of -270 dB and bandwidth in the range of 1–10 MHz [518].

In general, the study of a variety of diaphragm structures and mechanisms for converting deflection to electrical signals is a mature topic. As recent examples, structure "Piston Coupled Diaphragm" (Fig. 30d) has been introduced by Mahlouji et al. [553] and its advantages have been enumerated. A MEMS capacitive microphone has been designed based on a similar structure in [554]. These innovations can also be generalized in the field of membrane hydrophones.

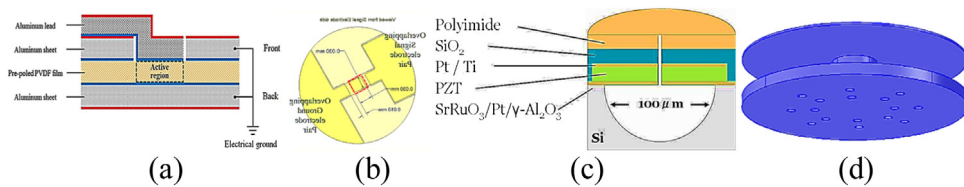


Fig. 30. a) Ultrasound diaphragm hydrophone [173] b) Double electrodes designed to suppress electric fields apart from the intended active area [473] c) Principle of construction of a disposable membrane hydrophone: exploded view [518] d) The schematic diagram of the Piston Coupled Diaphragm (PCD) [553].

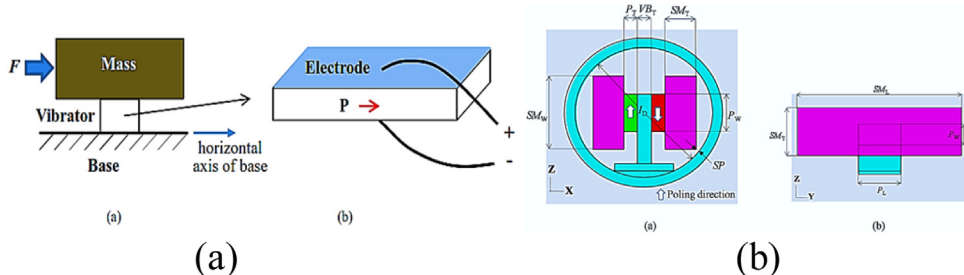


Fig. 31. a) Concept of the accelerometer and thickness-shear mode vibrator: (a) Accelerometer and (b) Vibrator [580] b) Structural parameters of the shear type accelerometer vector hydrophone: (a) XZ plane view, (b) YZ plane view [584].

9. Hydrophone operation mechanism

9.1. Operating at the resonance frequency

Currently, nearly all piezoelectric hydrophones operate in a wide frequency range below their resonant frequency to provide a flat frequency response [149]. Recent studies have shown that if hydrophones operate at around their resonant frequency, they have great potential to improve the sensitivity in applications such as weak signal diagnosis, study of nonlinear emission from gas-filled bubbles, and so on [555]. For example, latest study has shown that a hydrophone operated around the resonant frequency could be used for vibro-acoustography, which is an alternative ultrasonic image technique in medical diagnosis [556]. Among the models developed for analyzing the piezoelectric hydrophones including hydrostatic model [186,196,557–564], FEM [238,558], and electrical loading correction method [123,565,566], the hydrostatic model is very popular and has been successfully used in describing the behavior and optimization of hydrophones in off-resonant frequency [559,562,558–564]. However, due to the independence from frequency it is not able to analyze the performance of hydrophones around the resonant frequencies, where dynamic behavior prevails and the electromechanical response changes sharply with frequency. Recently, a dynamic fluid-structure interaction model for characterizing the piezoelectric hydrophones over a wider frequency range has been developed by some researchers [192,567].

9.2. Multimode hydrophone

The multimode vector hydrophone is a more traditional approach that combines several pieces with omnidirectional beam pattern to produce a high sensitivity dipole beam pattern in a specific direction. The cardioid beam can be also generated by combining the omnidirectional and dipole beam patterns. These types of hydrophones are available in spherical and cylindrical configurations [568–572]. In 1974, Ko et al. [571] acquired a dipole beam pattern by dividing a spherical piezoceramic into eight pieces and Gordon et al. [573] did the same with a cylindrical two-piece piezoceramic ring in 1975. Butler et al. developed a directional structure by stacking several divided cylindrical piezo ceramics with improved sensitivity [568,574,575]. McConnell et al. [119] also

analyzed the first- and second-order dipole beam patterns of a four and eight piece cylindrical hydrophone. In recent years, the study of multimode hydrophones has been pursued in Korea [121,576]. For example, a new hydrophone with the head mass division of a conventional tonpilz transducer was proposed by Roh et al. [577,578].

Multimode vector hydrophones are relatively easy to use and have a relatively low sensitivity and use the phase difference between the incident acoustic waves to each divided piece to detect the direction of the acoustic signal. Their size is inversely proportional to their bandwidth and they usually have many limitations in detecting low frequency bands at several hundred Hz or less [149]. However, many studies have been done to overcome this shortcoming with and without signal processing techniques [16,29,579].

9.3. Inertia type hydrophone

In the 2000s, research on inertia-type vector hydrophones was led to form a cardioid beam pattern by combining the dipole beam pattern from accelerometers with the omnidirectional beam patterns. These studies have continued over the past several years [23,276,580,581]. These types of hydrophones usually have an inertial element that due to the application of inertial force as a result of acoustic pressure, stresses the structure and stimulates the piezo elements located in the structure.

Silvia et al. [23] examined the acoustic wave reception characteristics of a piezoceramic accelerometer in the frequency range of 50–2000 Hz. Wlodkowsky et al. [582] developed a flexural accelerometer using a single crystal oscillator to reduce the electric noise level and increase sensitivity. In addition to describing an inertia-type vector hydrophone for line array application, Shipps et al. [276] also evaluated the performance of a PMN-PT single crystal accelerometer. McConnell et al. [178] mathematically modeled an inertia-type vector hydrophone encapsulated in a spherical hydrophone and examined the effects of environmental parameters on the performance of the hydrophone. Kim et al. [17] also evaluated the characteristics of an accelerometer mounted on a cylindrical hydrophone as an inertia-type vector hydrophone. Deng et al. [583] also proposed a shear type accelerometer using PMN-PT single crystals in 2006. In 2017, Kim et al. [580] by analyzing a shear type vector hydrophone made of PMN-PT single crystals as shown

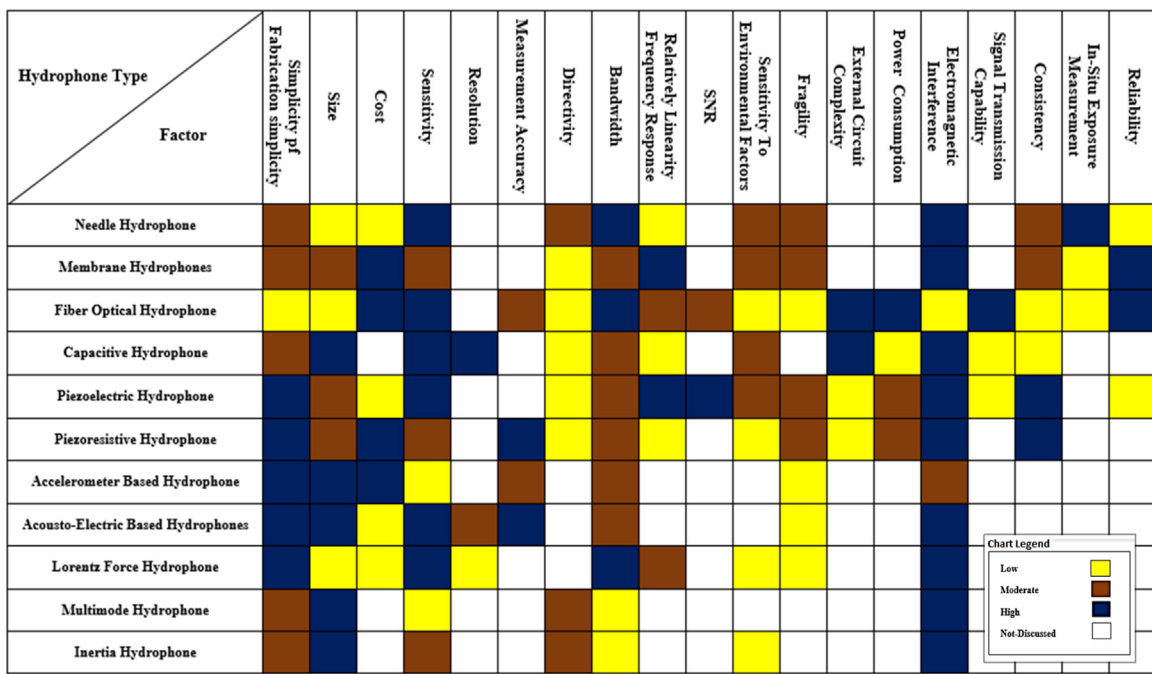


Chart 1. Different factors of various hydrophone structure.

in Fig. 31a. In 2018, an optimal sensitivity was achieved based on a shear type accelerometer according to Fig. 31b [584].

In general, inertia type vector hydrophones are more sensitive than multimode types, but they are less sensitive to conventional piezoceramic hydrophones, and it is possible to measure low frequencies with them. The piezoelectric accelerometers for the hydrophone can usually be divided into two types: compressive and shear. The compressive type accelerometer, which uses the longitudinal vibration mode of a piezoelectric element, and the direction of poling of the piezoelectric element is parallel to the output voltage. In the shear type accelerometer the shear vibration mode of a piezoelectric element is used and the direction of poling of the piezoelectric element is perpendicular to the direction of output voltage. The sensitivity of the shear type is generally higher than the compressive type. It is also more stable toward environmental factors and although it has been extensively studied, it has been less practical.

Chart 1 is a first-time comprehensive comparison in this case. This chart helps the readers to select the desired hydrophone structure depending on the required features. Chart 1 shows different factors of hydrophone structures.

10. Applications

Generally, hydrophones have a variety of applications as listed below:

- 1) Characterization of transcranial [585–589],
- 2) High-intensity therapeutic [77,515,590],
- 3) Gene-delivery systems [591],
- 4) High-frequency transducer characterization [592],
- 5) Cavitation studying and Passive cavitation detection [593],
- 6) Medical applications (ophthalmology, dermatology, intravascular imaging) [594,595],
- 7) HITU/HIFU [304,308,502,596–598],
- 8) SWL [599,600],
- 9) Exposimetry experiments [69],
- 10) Biomedical/Biological tissue

- 11) imaging and therapy,
- 12) Focused ultrasound surgery,
- 13) Ultrasonic Device Tracking (UDT) [601],
- 14) Pipeline ground markers [602],
- 15) Underwater acoustic/noise monitoring,
- 16) Underwater telecommunication [603],
- 17) Underwater or target detection, recognition and classification,
- 18) underwater search and rescue [604,605],
- 19) SONAR [606],
- 20) Towed Array Sonar System (TASS) [607],
- 21) Underwater obstacle avoidance [37], Underwater objects localization,
- 22) Submarine or surface vessels detection,
- 23) Icebergs detection,
- 24) Ship noise signature recognition [608],
- 25) Ocean topography and profiling,
- 26) Seabed mapping and imaging [609],
- 27) Measuring reflection coefficient of underwater acoustic materials [610],
- 28) Acoustic holography,
- 29) Seismic measurement and exploration and survey,
- 30) Natural phenomena such as earthquakes, underwater volcanic eruptions and tsunami detection,
- 31) Active and passive geo-acoustic inversion exploration [611],
- 32) Long-range underwater explosions detection [612],
- 33) Ultra-high energy neutrino acoustic detection [613],
- 34) Oilfield Services [614],
- 35) Offshore/Deep water oil and gas exploration,
- 36) Ambient or biological noise measurements,
- 37) Ocean hydrological detection,
- 38) Marine mammal vocalization [615],
- 39) Ocean mammal and ecosystem study,
- 40) Small weapon platform,
- 41) Sonobuoys [616],
- 42) Fishing [617],
- 43) Unmanned underwater vehicle [618],
- 44) Harbor surveillance tasks [346],
- 45) Underwater salvage,

- 46) Permanent reservoir monitoring [619],
 47) Subsea gas leakage detection

11. Summary and conclusion

In this paper, first, the hydrophone design considerations and analogies of the performance factors was studied. The research efforts in the field of development and design of various hydrophone structures over the past two decades were listed with a historical and thematic approach. Most of the published works in this field in the last decade have been related to the development of MEMS hydrophones. In Table 1 and Chart 1, these topics are highlighted for comparison. Research trends in this field are slowly changing toward smaller hydrophones with greater sensitivity and bandwidth, and the presentation and study of new transduction mechanisms has progressed. Theoretical work has received less attention recently.

The works presented in this field were classified in terms of MEMS, vector hydrophone, different frequency ranges, different geometries, operation mechanism with a great effort to avoid overlap so that the reader has a general overview of the progresses happened in this field. Based on the presented information in this paper, the reader can select the appropriate hydrophone for a determined application scenario or measurement considerations. Based on the comprehensive literature review made in this paper the following conclusions can be deduced in the field of hydrophone development:

- i How to better balance the bandwidth and the sensitivity remains an open question. Even multi-objective optimizations in this area are rare.
- ii The development of serious piezo materials with suitable coefficients and high durability is still considered for MEMS applications.
- iii Integration between the measurement section and the preamplifier section to reduce the unwanted effects.
- iv In the field of infrasonic hydrophones, few publications are available, so due to the widespread use of this field, the development of hydrophones in this area is a basic need.
- v Simultaneous attention to the structural parts and processing of output signals can distribute the complexities of each part to the other, which is less common in papers.
- vi Hydrophone calibration methods still have serious challenges in terms of accuracy and timing.
- vii Introducing new mechanisms and biological modeling of nature are two strategies for developing higher quality hydrophones.

Declaration of Competing Interest

The authors report no declarations of interest.

Acknowledgments

The authors state that they had no known financial competition, personal interests, or personal relationships that could influence the work reported in this paper.

References

- [1] B. Bai, et al., Cross-supported planar MEMS vector hydrophone for high impact resistance, *Sens. Actuators A Phys.* 263 (2017) 563–570.
- [2] G. Zhang, et al., The development of the differential MEMS vector hydrophone, *Sensors* 17 (6) (2017) 1332.
- [3] N. Okada, S. Takeuchi, Effect on high-intensity fields of a tough hydrophone with hydrothermal PZT thick-film vibrator and titanium front layer, *IEEE Trans. Ultrason. Ferroelectr. Freq. Control* 64 (7) (2017) 1120–1126.
- [4] K.A. Wear, et al., Improved measurement of acoustic output using complex deconvolution of hydrophone sensitivity, *IEEE Trans. Ultrason. Ferroelectr. Freq. Control* 61 (1) (2014) 62–75.
- [5] O.V. Bessonova, V. Wilkens, Membrane hydrophone measurement and numerical simulation of HIFU fields up to developed shock regimes, *IEEE Trans. Ultrason. Ferroelectr. Freq. Control* 60 (2) (2013) 290–300.
- [6] R. Carpenter, M. Silvia, B. Cray, The design of a broadband ocean acoustic laboratory: detailed examination of vector sensor performance Unattended Ground, Sea, and Air Sensor Technologies and Applications VIII, vol. 6231, SPIE, Orlando (Kissimmee), Florida, United States, 2006.
- [7] J.F. McEachern, et al., ARAP - deep ocean vector sensor research array, in: *OCEANS 2006*, Boston, MA, USA IEEE, 2006.
- [8] M. Hawkes, A. Nehorai, Acoustic vector-sensor beamforming and Capon direction estimation, *Ieee Trans. Signal Process.* 46 (9) (1998) 2291–2304.
- [9] M. Kumar, et al., Design and simulation of MEMS vector hydrophone with reduced cross section based meander beams, in: *AIP Conf. Proc. (ETMN 2015)*, Manipal University, Rajasthan, India: AIP Publishing LLC, 2016.
- [10] J.-l. Song, et al., Modeling and simulation of MEMS vector hydrophone for suppressing vibration output, *DEStech Transactions on Computer Science and Engineering* (2019).
- [11] M. Kumar, et al., Design and simulation of MEMS vector hydrophone with reduced cross section based meander beams, in: *AIP Conf. Proc. (ETMN 2015)*, Manipal University, Rajasthan, India, 2016.
- [12] R. White, L. Cheng, K. Grosh, Capacitively sensed micromachined hydrophone with viscous fluid-structure coupling, in: *MOEMS-MEMS Micro and Nanofabrication*, SPIE, 2005, Vol. 5718.
- [13] C. Leslie, J. Kendall, J. Jones, Hydrophone for measuring particle velocity, *J. Acoust. Soc. Am.* 28 (4) (1956) 711–715.
- [14] G.L. D'Spain, W. Hodgkiss, G. Edmonds, The simultaneous measurement of infrasonic acoustic particle velocity and acoustic pressure in the ocean by freely drifting swallow floats, *IEEE J. Ocean. Eng.* 16 (2) (1991) 195–207.
- [15] N.K. Naluai, *Acoustic Intensity Methods and Their Applications to Vector Sensor Use and Design (Ph.D.)*, The Pennsylvania State University, 2006, p. 242.
- [16] T.B. Gabrielson, D.L. Gardner, S.L. Garrett, A simple neutrally buoyant sensor for direct measurement of particle velocity and intensity in water, *J. Acoust. Soc. Am.* 97 (4) (1995) 2227–2237.
- [17] K. Kim, T.B. Gabrielson, G.C. Lauchle, Development of an accelerometer-based underwater acoustic intensity sensor, *J. Acoust. Soc. Am.* 116 (6) (2004) 3384–3392.
- [18] F. Jacobsen, A note on finite difference estimation of acoustic particle velocity, *J. Sound Vib.* 256 (5) (2002) 849–859.
- [19] I.I.I. Mann, J.A. J. Tichy, Acoustic intensity analysis: distinguishing energy propagation and wave-front propagation, *J. Acoust. Soc. Am.* 90 (1) (1991) 20–25.
- [20] T.J. Schultz, Acoustic wattmeter, *J. Acoust. Soc. Am.* 28 (4) (1956) 693–699.
- [21] F.J. Fahy, Measurement of acoustic intensity using the cross-spectral density of two microphone signals, *J. Acoust. Soc. Am.* 62 (4) (1977) 1057–1059.
- [22] S. Pauzin, D. Biron, Hydrophonic probe for underwater intensity measurements, *J. Acoust. Soc. Am.* 81 (S1) (1987) S89.
- [23] M.T. Silvia, R.T. Richards, A theoretical and experimental investigation of low-frequency acoustic vector sensors, in: *OCEANS'02 MTS/IEEE*, Biloxi, MI, USA IEEE, 2002.
- [24] R.S. Woollett, Diffraction constants for pressure gradient transducers, *J. Acoust. Soc. Am.* 72 (4) (1982) 1105–1113.
- [25] D. Scheiber, Directional pressure gradient hydrophone, 27th Navy Symposium on Underwater Acoustic (1969).
- [26] M. Mongiovi, Low-frequency pressure-gradient sensor, *J. Acoust. Soc. Am.* 59 (S1) (1976) S62.
- [27] M.B. Moffett, et al., A piezoelectric, flexural-disk, neutrally buoyant, underwater accelerometer, *IEEE Trans. Ultrason. Ferroelectr. Freq. Control* 45 (5) (1998) 1341–1346.
- [28] T.G. Bifano, et al., A novel microelectromechanical system (MEMS) design for an underwater acoustic field sensor, *J. Acoust. Soc. Am.* 105 (2) (1999) 998.
- [29] K.J. Basty, G.C. Lauchle, J.A. McConnell, Development of a velocity gradient underwater acoustic intensity sensor, *J. Acoust. Soc. Am.* 106 (6) (1999) 3178–3188.
- [30] L.-j. Chen, et al., Overview of vector hydrophone, *Transd. Microsyst. Technol.* 25 (6) (2006) 5–8.
- [31] G.-j. Hang, et al., A bionic fish cilia median-low frequency three-dimensional piezoresistive MEMS vector hydrophone, *Nano-Micro Lett.* 6 (2) (2014) 136–142.
- [32] R.J. Urick, *Principles of Underwater Sound for Engineers*, McGraw-Hill Book Company, 1967.
- [33] M. Wahlberg, B. Møhl, P. Teglberg Madsen, Estimating source position accuracy of a large-aperture hydrophone array for bioacoustics, *J. Acoust. Soc. Am.* 109 (1) (2001) 397–406.
- [34] H. Chen, J. Zhao, On locating low altitude moving targets using a planar acoustic sensor array, *Appl. Acoust.* 64 (11) (2003) 1087–1101.
- [35] J.C. Nickles, et al., A vertical array of directional acoustic sensors, in: *OCEANS 92 Proceedings@ m.Mastering the Oceans Through Technology*, Newport, RI, USA: IEEE, 1992.
- [36] G. D'Spain, et al., Initial analysis of the data from the vertical DIFAR array, in: *OCEANS 92 Proceedings@ m.Mastering the Oceans Through Technology*, IEEE, 1992.

- [37] L. Linxian, et al., Research on double T-shape MEMS bionic vector hydrophone and its application in obstacle avoidance sonar, *Sens. Rev.* 35 (1) (2015) 76–84.
- [38] B.M. Abraham, Low-cost dipole hydrophone for use in towed arrays, *AIP Conference Proceedings* (1996).
- [39] P. Palanisamy, N. Kalyanasundaram, P. Swetha, Two-dimensional DOA estimation of coherent signals using acoustic vector sensor array, *Signal Process.* 92 (1) (2012) 19–28.
- [40] Y. Yu, et al., Research on target depth classification in low frequency acoustic field of shallow water, *Acta Phys. Sin.* 58 (9) (2009) 6335–6343.
- [41] I.F. Akyildiz, D. Pompili, T. Melodia, Underwater acoustic sensor networks: research challenges, *Ad hoc Netw.* 3 (3) (2005) 257–279.
- [42] Z. Guojun, et al., Improvement of the MEMS bionic vector hydrophone, *Microelectron. J.* 42 (5) (2011) 815–819.
- [43] J.-w. Zhao, H.-w. Chen, J.-m. Li, Research on passive acoustics-guidance system based on vector hydrophones, *J. Harbin Eng. Univ.* (2004), 1.
- [44] S. Chen, et al., A novel MEMS based piezoresistive vector hydrophone for low frequency detection, in: *2007 International Conference on Mechatronics and Automation*, IEEE, 2007, pp. 1839–1844.
- [45] K.J. Rebello, et al., Low cost MEMS hydrophones, in: *Optics and Photonics in Global Homeland Security III*, International Society for Optics and Photonics, 2007, pp. 65400W.
- [46] M.S. Pearle, et al., Urologic diseases in America project: urolithiasis, *J. Urol.* 173 (3) (2005) 848–857.
- [47] J.A. Kettlerling, J.M. Kracht, R.O. Cleveland, Hydrophone arrays for instantaneous measurement of high-pressure acoustic fields, *AIP Conference Proceedings* (2010) 319–322.
- [48] M. Liu, et al., Design of array MEMS vector vibration sensor in the location of pipeline internal inspector, *Telkomnika Indones. J. Electr. Eng.* (2014) 6651–6657.
- [49] K.A. Wear, et al., Improved measurement of acoustic output using complex deconvolution of hydrophone sensitivity, *IEEE Trans. Ultrason. Ferroelectr. Freq. Control* 61 (1) (2014) 62–75.
- [50] P.E. Bloomfield, G. Gandhi, P.A. Lewin, Membrane hydrophone phase characteristics through nonlinear acoustics measurements, *IEEE Trans. Ultrason. Ferroelectr. Freq. Control* 58 (11) (2011) 2418–2437.
- [51] J.F. Tressler, Piezoelectric transducer designs for sonar applications, in: *Piezoelectric and Acoustic Materials for Transducer Applications*, Springer, 2008, pp. 217–239.
- [52] R.J. Bobber, *Underwater Electroacoustic Measurements*, Peninsula Publishing, 1988.
- [53] D. Stansfield, *Underwater Electroacoustic Transducers: A Handbook for Users and Designers*, University Press, Bath, 1991.
- [54] O.B. Wilson, U.S.N.S.S. Command, U.S.N.E.S. Command, *An Introduction to the Theory and Design of Sonar Transducers*, Naval Sea Systems Command, 1985.
- [55] S. Shevtsov, et al., Modeling and optimization of MEMS-based acoustic sensor for underwater applications, in: *Proc. 3rd International Conference on Theoretical and Applied Mechanics TAM-12*, Vouliagmeny, Greece, 2012, pp. 88–93.
- [56] M.I.H. Yaacob, M.R. Arshad, A.A. Manaf, Response estimation of micro-acoustic transducer for underwater applications using finite element method, *Indian J. Geo-Mar. Sci. (IJMS)* 40 (2) (2011) 176–180.
- [57] Z. Wang, et al., Simulation-based optimization of the acoustoelectric hydrophone for mapping an ultrasound beam, *Medical Imaging 2010: Ultrasonic Imaging, Tomography, and Therapy* (2010) 76290Q.
- [58] J.-W. Lee, W.-S. Ohm, Y.-T. Kim, Development of disposable membrane hydrophones for a frequency range from 1 MHz to 10 MHz, *Ultrasonics* 81 (2017) 50–58.
- [59] N. Lu, et al., Design of MEMS piezoelectric vector hydrophone, *Key Eng. Mater.* 562–565 (2013) 1143–1148.
- [60] A. Bharath, D. Groulx, S. Campbell, Hydrophone acoustic receiver modeling: turbulent flow modeling and acoustic analysis, in: *Proceedings of the 2014 COMSOL Conference*, Boston, MA, 2015, pp. 1–7.
- [61] S. Alkoy, et al., Design, performance and modeling of piezoceramic hollow-sphere microprobe hydrophones, *Meas. Sci. Technol.* 20 (9) (2009) 095204.
- [62] X. Liu, et al., The design of a vector hydrophone's chip-level damping structure, in: *2011 3rd International Conference on Computer Research and Development*, IEEE, 2011, pp. 358–360.
- [63] A. Khimunin, The maximum possible hydrophone size in the studies of the ultrasonic field structure, *Acoust. Phys.* 54 (2) (2008) 279–287.
- [64] K.A. Wear, Considerations for choosing sensitive element size for needle and fiber-optic hydrophones—part I: spatiotemporal transfer function and graphical guide, *IEEE Trans. Ultrason. Ferroelectr. Freq. Control* 66 (2) (2018) 318–339.
- [65] K.A. Wear, Y. Liu, Considerations for choosing sensitive element size for needle and fiber-optic hydrophones—part II: experimental validation of spatial averaging model, *IEEE Trans. Ultrason. Ferroelectr. Freq. Control* 66 (2) (2018) 340–347.
- [66] K.A. Wear, C. Baker, P. Miloro, Directivity and frequency-dependent effective sensitive element size of needle hydrophones: predictions from four theoretical forms compared with measurements, *IEEE Trans. Ultrason. Ferroelectr. Freq. Control* 65 (10) (2018) 1781–1788.
- [67] K.A. Wear, C. Baker, P. Miloro, Directivity and frequency-dependent effective sensitive element size of membrane hydrophones: theory versus experiment, *IEEE Trans. Ultrason. Ferroelectr. Freq. Control* 66 (11) (2019) 1723–1730.
- [68] K.A. Wear, S.M. Howard, Directivity and frequency-dependent effective sensitive element size of a reflectance-based fiber-optic hydrophone: predictions from theoretical models compared with measurements, *IEEE Trans. Ultrason. Ferroelectr. Freq. Control* 65 (12) (2018) 2343–2348.
- [69] G.R. Harris, Progress in medical ultrasound exposimetry, *IEEE Trans. Ultrason. Ferroelectr. Freq. Control* 52 (5) (2005) 717–736.
- [70] T.L. Szabo, *Diagnostic Ultrasound Imaging: Inside Out*, Academic Press, 2014.
- [71] A. Hurrell, P. Beard, *Piezoelectric and fibre-optic hydrophones*, in: *Ultrasonic Transducers*, Elsevier, 2012, pp. 619–676.
- [72] E.G. Radulescu, et al., The influence of finite aperture and frequency response of ultrasonic hydrophone probes on the determination of acoustic output, *Ultrasonics* 42 (1) (2004) 367–372.
- [73] E. Martin, B. Treeby, Investigation of the repeatability and reproducibility of hydrophone measurements of medical ultrasound fields, *J. Acoust. Soc. Am.* 145 (3) (2019) 1270–1282.
- [74] M. Cooling, V. Humphrey, V. Wilkens, Hydrophone area-averaging correction factors in nonlinearly generated ultrasonic beams, *J. Phys.-Conf. Ser.* (2011) 012002.
- [75] B. Zeqiri, A.D. Bond, The influence of waveform distortion on hydrophone spatial-averaging corrections—theory and measurement, *J. Acoust. Soc. Am.* 92 (4) (1992) 1809–1821.
- [76] M.A. Ghanem, et al., Field characterization and compensation of vibrational nonuniformity for a 256-element focused ultrasound phased array, *IEEE Trans. Ultrason. Ferroelectr. Freq. Control* 65 (9) (2018) 1618–1630.
- [77] Y. Liu, K.A. Wear, G.R. Harris, Variation of high-intensity therapeutic ultrasound (HITU) pressure field characterization: effects of hydrophone choice, nonlinearity, spatial averaging and complex deconvolution, *Ultrasonogr. Med. Biol.* 43 (10) (2017) 2329–2342.
- [78] V. Wilkens, C. Koch, Amplitude and phase calibration of hydrophones up to 70 MHz using broadband pulse excitation and an optical reference hydrophone, *J. Acoust. Soc. Am.* 115 (6) (2004) 2892–2903.
- [79] A. Hurrell, Voltage to pressure conversion: are you getting phased' by the problem? *J. Phys. Conf. Ser.* 1 (2004) 57–62, IOP Publishing.
- [80] K.A. Wear, et al., Correction for frequency-dependent hydrophone response to nonlinear pressure waves using complex deconvolution and rarefactional filtering: application with fiber optic hydrophones, *IEEE Trans. Ultrason. Ferroelectr. Freq. Control* 62 (1) (2015) 152–164.
- [81] S. Eichstädt, V. Wilkens, GUM2DFT—a software tool for uncertainty evaluation of transient signals in the frequency domain, *Meas. Sci. Technol.* 27 (5) (2016) 055001.
- [82] S. Eichstädt, et al., On challenges in the uncertainty evaluation for time-dependent measurements, *Metrologia* 53 (4) (2016) S125.
- [83] S. Eichstädt, V. Wilkens, Evaluation of uncertainty for regularized deconvolution: a case study in hydrophone measurements, *J. Acoust. Soc. Am.* 141 (6) (2017) 4155–4167.
- [84] A.M. Hurrell, S. Rajagopal, The practicalities of obtaining and using hydrophone calibration data to derive pressure waveforms, *IEEE Trans. Ultrason. Ferroelectr. Freq. Control* 64 (1) (2016) 126–140.
- [85] X.-R. Xu, Z.-y. Zheng, L.-l. Bai, Theoretical modeling and optimization design of high frequency piezoelectric polymer film hydrophone array, in: *Proceedings of the 2014 Symposium on Piezoelectricity, Acoustic Waves, and Device Applications*, Beijing, China: IEEE, 2014.
- [86] C. Xue, et al., Design, fabrication, and preliminary characterization of a novel MEMS bionic vector hydrophone, *Microelectron. J.* 38 (10–11) (2007) 1021–1026.
- [87] V.F. Humphrey, et al., P2C-1 The Peak Rarefactional Pressure Generated by Medical Ultrasound Systems in Water and Tissue: A Numerical Study, in: *2006 IEEE Ultrasonics Symposium*, IEEE: Vancouver, BC, Canada, 2006, pp. 1604–1607.
- [88] M.P. Cooling, V.F. Humphrey, A nonlinear propagation model-based phase calibration technique for membrane hydrophones, *IEEE Trans. Ultrason. Ferroelectr. Freq. Control* 55 (1) (2008) 84–93.
- [89] D. Ebenezer, et al., Design and development of a broadband hydrophone, in: *2011 International Symposium on Ocean Electronics*, IEEE: Kochi, India, 2011, pp. 121–128.
- [90] Committee on Potential Impacts of Ambient Noise in the Ocean on Marine Mammals, O.S.B., Division on Earth and Life Studies, National research council of the national academies, *Ocean Noise and Marine Mammals*, National Academic Press, 2003.
- [91] Z.L. Hu, L. Li, Z.H. Zhou, Offshore marine ambient noise measurement study based on laser interferometer hydrophone, in: *Advanced Materials Research*, Trans Tech Publ., 2014, pp. 746–749.
- [92] J.A. Hildebrand, Anthropogenic and natural sources of ambient noise in the ocean, *Mar. Ecol. Progress Ser.* 395 (2009) 5–20.
- [93] G.M. Wenz, Acoustic ambient noise in the ocean: spectra and sources, *J. Acoust. Soc. Am.* 34 (12) (1962) 1936–1956.
- [94] R.H. Mellen, The thermal-noise limit in the detection of underwater acoustic signals, *J. Acoust. Soc. Am.* 24 (5) (1952) 478–480.
- [95] M. Strasberg, Nonacoustic noise interference in measurements of infrasonic ambient noise, *J. Acoust. Soc. Am.* 66 (5) (1979) 1487–1493.
- [96] S. Lee, et al., Experiment on effect of screening hydrophone for reduction of flow-induced ambient noise in ocean, *J. Appl. Phys.* 50 (2011) 07HG02.
- [97] D. Santos, et al., ShipsEar: an underwater vessel noise database, *Appl. Acoust.* 113 (2016) 64–69.

- [98] D. Ebenezer, Acceleration sensitivity of radially polarized piezoceramic cylinders, Proceedings of the 3rd International Congress on Air and Structure Borne Sound and Vibration (1994).
- [99] O. Kilic, et al., Miniature photonic-crystal hydrophone optimized for ocean acoustics, *J. Acoust. Soc. Am.* 129 (4) (2011) 1837–1850.
- [100] T. Straw, Noise Prediction for hydrophone/preamplifier Systems, Naval undersea warfare center DIV newport RI, 1993, p. 39.
- [101] F. Coutard, E. Tisserand, P. Schweitzer, Optimal low noise amplifier for ultrasonic receptor, *Техническая акустика* 7 (2007) 157–163.
- [102] B.T. Bosworth, et al., Estimating signal-to-noise ratio (SNR), *IEEE J. Ocean. Eng.* 33 (4) (2008) 414–418.
- [103] W.M. Carey, Sound sources and levels in the ocean, *IEEE J. Ocean. Eng.* 31 (1) (2006) 61–75.
- [104] D. Ross, Ship sources of ambient noise, *IEEE J. Ocean. Eng.* 30 (2) (2005) 257–261.
- [105] J.W. Young, Optimization of acoustic receiver noise performance, *J. Acoust. Soc. Am.* 61 (6) (1977) 1471–1476.
- [106] G.M. Ballou, *Handbook for Sound Engineers*, Focal Press, Boston, 2008, 1778.
- [107] IEC, IEC (2007 A) 62127-1 – Part 1-Measurement and Characterisation of Medical Ultrasonic fields up to 40 MHz, International Electro-technical Commission, Geneva, 2007.
- [108] Paul L. Carson, C.H. John G. Aggott, Kurt Sandstrom, Douglas Worth, Gerald R. Harris, Peter A. Lewin, *Acoustic Output Measurement Standard for Diagnostic Ultrasound Equipment*, American Institute of Ultrasound in Medicine, 1998, 120.
- [109] H. Rijnja, Small sensitive hydrophones, *Acta Acust. United Acust.* 27 (4) (1972) 182–188.
- [110] Association, N.E.M. Standard for Real-time Display of Thermal and Mechanical Acoustic Output Indices on Diagnostic Ultrasound Equipment, National Electrical Manufacturers Association, 2004.
- [111] G.R. Harris, Pressure pulse distortion by hydrophones due to diminished low frequency response, *IEEE Trans. Ultrason. Ferroelectr. Freq. Control* 42 (6) (1995) 989–992.
- [112] W.A. Kuperman, P. Roux, *Underwater Acoustics*, Springer, New York, 2007, pp. 149–204.
- [113] G. Zhang, P. Zhao, W. Zhang, Resonant frequency of the silicon micro-structure of MEMS vector hydrophone in fluid-structure interaction, *AIP Adv.* 5 (4) (2015) 041316.
- [114] D.G. Shomber, S.W. Smith, G.R. Harris, Angular response of miniature ultrasonic hydrophones, *Med. Phys.* 9 (4) (1982) 484–492.
- [115] G. Harris, D.G. Shomber, A pulsed near-field technique for measuring the directional characteristics of acoustic receivers, *IEEE Trans. Sonics Ultrason.* 32 (6) (1985) 802–808.
- [116] D. Li, et al., Cymbal piezoelectric composite underwater acoustic transducer, *Ultrasonics* 44 (2006) e685–e687.
- [117] L.L. Beranek, A.S.O. America, *Acoustics*, Acoustical Society of America through the American Institute of Physics, New York, N.Y., 1993.
- [118] J.A. Archer-Hall, D. Gee, A single integral computer method for axisymmetric transducers with various boundary conditions, *NDT Int.* 13 (3) (1980) 95–101.
- [119] J.A. McConnell, S.C. Jensen, J.P. Rudzinsky, Forming first-and second-order cardioids with multimode hydrophones, in: *OCEANS 2006*, IEEE: Boston, MA, USA, 2006, pp. 1–6.
- [120] Y. Lim, et al., Design of a multimode piezoelectric spherical vector sensor for a cardioid beam pattern, *J. Acoust. Soc. Korea* 32 (1) (2013) 32–42.
- [121] Y. Lim, et al., Design and fabrication of a multimode ring vector hydrophone, *Jpn. J. Appl. Phys.* 53 (7S) (2014) 07KD07.
- [122] IEC, IEC 60565 Underwater Acoustics - Hydrophones - Calibration of Hydrophones - Part 1: Procedures for Free-Field Calibration of Hydrophones, International Electro-technical Commission, Geneva, 2006, p. 163.
- [123] G. Hayman, et al., A method for correcting the complex electrical impedance and open-circuit sensitivity of a hydrophone for the effect of added extension cable, *Meas. Sci. Technol.* 18 (7) (2007) N47.
- [124] M. Abdillahi-Said, C. Park, Designing and implementing a system of multiplexing and demultiplexing on fpga using matlab/simulink for the detection of acoustic signals, in: *OCEANS 2008*, Quebec City, QC, Canada: IEEE, 2008.
- [125] M.D. Szymanski, et al., Killer whale (*Orcinus orca*) hearing: auditory brainstem response and behavioral audiograms, *J. Acoust. Soc. Am.* 106 (2) (1999) 1134–1141.
- [126] H. McSkimin, P. Andreatch Jr., Elastic moduli of silicon vs hydrostatic pressure at 25.0 C and – 195.8 C, *J. Appl. Phys.* 35 (7) (1964) 2161–2165.
- [127] Y. Cheng, et al., The fabrication of hydrophone based on epitaxial PZT film for acoustic device applications, in: *Physics and Mechanics of New Materials and Their Applications*, 2013, pp. 373–381.
- [128] M. Shevtsova, Finite element based investigation of sandwich design and membrane-type piezoelectric transducers, *Piezoelectr. Related Mat.* (2011) 79–116.
- [129] S. Shevtsov, et al., Multiobjective pareto-based optimization of pMUT hydrophone with piezoelectric active diaphragm, in: *Engineering Systems Design and Analysis*, American Society of Mechanical Engineers, 2014.
- [130] S. Suzuki, P. Gerner, P. Lirk, 20 - Local anesthetics, in: H.C. Hemmings, T.D. Egan (Eds.), *Pharmacology and Physiology for Anesthesia*, 2nd ed., Elsevier, Philadelphia, 2019, pp. 390–411.
- [131] R. Guo, C.A. Wang, A. Yang, Piezoelectric properties of the 1–3 type porous lead zirconate titanate ceramics, *J. Am. Ceram. Soc.* 94 (6) (2011) 1794–1799.
- [132] Hong-Juan, H. Lian, J. chen, Two-dimensional combined vector hydrophone of the resonant-column type, in: *2012 International Conference on Computing, Measurement, Control and Sensor Network*, Taiyuan, China, 2012, pp. 179–182.
- [133] S. Chen, et al., A novel MEMS single vector hydrophone, *Acta Armamentarii* 29 (6) (2008) 673–677.
- [134] M. Liu, et al., Design of MEMS bionic vector hydrophone based on NBR sound-transparent cap, *Sens. Rev.* 35 (3) (2015) 303–309.
- [135] O. Sapozhnikov, et al., 3B-3 calibration of PVDF hydrophones using a broad focus electromagnetic lithotripter, in: *2007 IEEE Ultrasonics Symposium Proceedings*, New York, NY, USA: IEEE, 2007.
- [136] G.R. Harris, R.C. Preston, A.S. DeReggi, The impact of piezoelectric PVDF on medical ultrasound exposure measurements, standards, and regulations, *IEEE Trans. Ultrason. Ferroelectr. Freq. Control* 47 (6) (2000) 1321–1335.
- [137] G.R. Harris, et al., Interlaboratory evaluation of hydrophone sensitivity calibration from 0.1 to 2 MHz via time delay spectrometry, *Ultrasonics* 42 (1–9) (2004) 349–353.
- [138] H. Li, et al., Design parameters of a miniaturized piezoelectric underwater acoustic transmitter, *Sensors* 12 (7) (2012) 9098–9109.
- [139] W. Li-kun, et al., A cylindrical hydrophone with built-in amplifier, in: *2009 International Conference on Mechatronics and Automation*, Changchun, China: IEEE, 2009.
- [140] C. Hill, Calibration of ultrasonic beams for bio-medical applications, *Phys. Med. Biol.* 15 (2) (1970) 241.
- [141] P. Lewin, R. Chivers, Two miniature ceramic ultrasonic probes, *J. Phys. E Sci. Instrum.* 14 (12) (1981) 1420.
- [142] Q.P. Wang, et al., Features and technology of piezoelectric hydrophone, in: *Advanced Materials Research*, Trans Tech Publ., 2011.
- [143] R. Guo, C.-A. Wang, A. Yang, Effects of pore size and orientation on dielectric and piezoelectric properties of 1–3 type porous PZT ceramics, *J. Eur. Ceram. Soc.* 31 (4) (2011) 605–609.
- [144] T. Arai, et al., Properties of hydrophone with porous piezoelectric ceramics, *J. Appl. Phys.* 30 (9S) (1991) 2253.
- [145] P. Guillaussier, C. Audoly, D. Boucher, Porous lead zirconate titanate ceramics for hydrophones, *Ferroelectrics* 187 (1) (1996) 121–128.
- [146] D.-m. Lu, *Principles of Underwater Sound Transducer*, China Ocean University Press, QingDao, 2001.
- [147] A. Safari, E.K. Akdogan, *Piezoelectric and Acoustic Materials for Transducer Applications*, 1st ed., Springer Science & Business Media, 2008, 482.
- [148] H. Zhang, et al., Study on a high sensitivity tangential polarized acoustic-pressure hydrophone, in: *2012 Symposium on Piezoelectricity, Acoustic Waves, and Device Applications (SPAWDA)*, Shanghai, China: IEEE, 2012.
- [149] C.H. Sherman, J.L. Butler, *Transducers and Arrays for Underwater Sound*, vol. 4, Springer, New York, NY, 2007, pp. 610.
- [150] S. Alkoy, et al., Miniature piezoelectric hollow sphere transducers (BBs), *IEEE Trans. Ultrason. Ferroelectr. Freq. Control* 44 (5) (1997) 1067–1076.
- [151] D. Teng, H. Yang, G. Zhu, Design and test about high sensitivity thin shell piezoelectric hollow sphere hydrophone, in: *OCEANS 2017-Anchorage*, IEEE: Anchorage, AK, USA, 2017, pp. 1–6.
- [152] A.A. Anan'eva, *Ceramic Acoustic Detectors*, 1st ed., Springer US, 1965, 122.
- [153] A. Dogan, et al., The cymbal-like electromechanical actuator, in: *ISAF96*. Proceedings of the Tenth IEEE International Symposium on Applications of Ferroelectrics, East Brunswick, NJ, USA: IEEE, 1996.
- [154] J. Fernandez, et al., Tailoring the performance of ceramic-metal piezocomposite actuators,'cymbals', *Sens. Actuators A Phys.* 65 (2–3) (1998) 228–237.
- [155] J.F. Tressler, et al., Finite element analysis of the cymbal-type flextensional transducer, *IEEE Trans. Ultrason. Ferroelectr. Freq. Control* 45 (5) (1998) 1363–1369.
- [156] J. Zhang, et al., A class V flextensional transducer: the cymbal, *Ultrasonics* 37 (6) (1999) 387–393.
- [157] R. Newham, et al., Size effects in capped ceramic underwater sound projectors, in: *OCEANS'02 MTS/IEEE*, Biloxi, MI, USA: IEEE, 2002.
- [158] J. Fernandez, et al., Hollow piezoelectric composites, *Sens. Actuators A Phys.* 51 (2–3) (1995) 183–192.
- [159] J. Pons, A comparative analysis of piezoelectric and magnetostrictive actuators in smart structures, *Boletin de la Sociedad Espanola de Ceramica y Vidrio* 44 (3) (2005) 146–154.
- [160] C. Kannan, et al., Effect of manufacturing procedure on the miniaturized Flextensional Transducers (Cymbals) and hydrophone array performance, in: *OCEANS 2011 IEEE-Spain*, IEEE: Santander, Spain, 2011, pp. 1–5.
- [161] Z. Li, et al., Finite element analyzing of underwater receiving sensitivity of PMN-0.33 PT single crystal cymbal hydrophone, *Ultrasonics* 44 (2006) e759–e762.
- [162] S. Chen, G.-c. Lin, Testing an improved cymbal hydrophone, *J. Mar. Sci. Appl.* 8 (4) (2009) 328.
- [163] H. Chua, B. Kok, H. Goh, Modelling and design analyses of a piezoelectric cymbal transducer (PCT) structure for energy harvesting application, *Energy Sustain.* 186 (2014) 103.
- [164] A. Feeney, M. Lucas, Smart cymbal transducers with nitinol end caps tunable to multiple operating frequencies, *IEEE Trans. Ultrason. Ferroelectr. Freq. Control* 61 (10) (2014) 1709–1719.
- [165] K. Shotton, D. Bacon, R. Quilliam, A PVDF membrane hydrophone for operation in the range 0.5 MHz to 15 MHz, *Ultrasonics* 18 (3) (1980) 123–126.

- [166] M. Platte, A polyvinylidene fluoride needle hydrophone for ultrasonic applications, *Ultrasonics* 23 (3) (1985) 113–118.
- [167] H. Chan, et al., Piezoelectric copolymer hydrophones for ultrasonic field characterization, *Rev. Sci. Instrum.* 62 (1) (1991) 203–207.
- [168] B. Zhu, et al., Solid state MOSFET-based hydrophone, in: smart structures and materials 2000: smart electronics and MEMS, *Int. Soc. Opt. Photon.* (2000) 368–377.
- [169] H. Chan, et al., Nanocomposite ultrasonic hydrophones, *Sens. Actuators A Phys.* 75 (3) (1999) 252–256.
- [170] H. Ohta, N. Shimizu, T. Kamakura, Diffusive hydrophone for ultrasonic measurements, *J. Appl. Phys.* 40 (5S) (2001) 3570.
- [171] S. Lau, et al., Ferroelectric lead magnesium niobate–lead titanate single crystals for ultrasonic hydrophone applications, *Mater. Sci. Eng. B* 111 (1) (2004) 25–30.
- [172] H. Kitsunai, et al., Development of miniature needle-type hydrophone with lead zirconate titanate polycrystalline film deposited by hydrothermal method, *J. Appl. Phys.* 45 (5S) (2006) 4688.
- [173] M. Ito, et al., High sensitivity ultrasonic sensor for hydrophone applications, using an epitaxial Pb (Zr, Ti) O₃ film grown on SrRuO₃/Pt/γ-Al₂O₃/Si, *Sens. Actuators A Phys.* 145 (2008) 278–282.
- [174] S. Robinson, et al., PVDF reference hydrophone development in the UK—from fabrication and lamination to use as secondary standards, *IEEE Trans. Ultrason. Ferroelectr. Freq. Control* 47 (6) (2000) 1336–1344.
- [175] R. Preston, et al., PVDF membrane hydrophone performance properties and their relevance to the measurement of the acoustic output of medical ultrasonic equipment, *J. Phys. E Sci. Instrum.* 16 (8) (1983) 786.
- [176] M.B. Moffett, J.M. Powers, J.C. McGrath, A p c hydrophone, *J. Acoust. Soc. Am.* 80 (2) (1986) 375–381.
- [177] S. Bauer, F. Bauer, Piezoelectric polymers and their applications, in: *Piezoelectricity*, Springer, 2008, pp. 157–177.
- [178] J.A. McConnell, Analysis of a compliantly suspended acoustic velocity sensor, *J. Acoust. Soc. Am.* 113 (3) (2003) 1395–1405.
- [179] A. Nehorai, E. Paldi, Vector-sensor array processing for electromagnetic source localization, *Ieee Trans. Signal Process.* 42 (2) (1994) 376–398.
- [180] R. Romashko, et al., Laser adaptive fiber-optic hydrophone, *Bull. Lebedev Phys. Inst.* 42 (7) (2015) 201–205.
- [181] Y.C. Lee, J.-M. Yu, S.W. Huang, Fabrication and characterization of a PVDF hydrophone array transducer, *Key Eng. Mater.* 270–273 (2004) 1406–1413.
- [182] D.-s. Ju, Z. Zhou, J.-p. Ou, Study on strain-sensing of PVDF films, *J. Funct. Mater.* 35 (2004) 450–452.
- [183] J. Xu, et al., AlN-on-SOI platform-based micro-machined hydrophone, *Appl. Phys. Lett.* 109 (3) (2016) 032902.
- [184] R. Kressmann, New piezoelectric polymer for air-borne and water-borne sound transducers, *J. Acoust. Soc. Am.* 109 (4) (2001) 1412–1416.
- [185] L. Medeiros, et al., Multi-layer piezoelectret hydrophone for ultrasonic applications, in: 2012 IEEE International Ultrasonics Symposium, IEEE: Dresden, Germany, 2012, pp. 1–4.
- [186] H. Kara, et al., Porous PZT ceramics for receiving transducers, *IEEE Trans. Ultrason. Ferroelectr. Freq. Control* 50 (3) (2003) 289–296.
- [187] K. Ina, et al., Hydrophone sensitivity of porous Pb (Zr, Ti) O₃ ceramics, *J. Appl. Phys.* 33 (9S) (1994) 5381.
- [188] A. Perry, et al., PZT-Polymer composites for hydrophones: production and modelling, *Adv. Compos. Mater. Struct.* 206–213 (2002) 1505–1508.
- [189] W.A. Smith, A. Shaulov, B. Auld, Tailoring the properties of composite piezoelectric materials for medical ultrasonic transducers, in: *IEEE 1985 Ultrasonics Symposium*, IEEE, 1985, pp. 642–647.
- [190] S.T. Lau, et al., PT/P(VDF-TrFE) nanocomposites for ultrasonic hydrophone applications, *Ferroelectrics* 263 (1) (2001) 205–210.
- [191] J.-l. Zhu, Y.-q. Wei, Y.-l. Li, Shear-polarized cylinder hydrophone using 0–3 PZT/P (VDF-TFE) piezocomposite, *Electron. Comp. Mater.* 24 (8) (2005) 35–37.
- [192] Z. Yang, et al., Dynamic modeling of 1–3 piezoelectric composite hydrophone and its experimental validation, *Compos. Struct.* 150 (2016) 246–254.
- [193] R. Ramesh, H. Kara, C. Bowen, Finite element modelling of dense and porous piezoceramic disc hydrophones, *Ultrasonics* 43 (3) (2005) 173–181.
- [194] D.-h. Li, et al., 1-3 piezocomposites tubular hydrophone, *J. Funct. Mater. Devices* 7 (2) (2001) 125–129.
- [195] Y. Xinsheng, G. Qiqi, Design of low minor lobe underwater sound transducer with 1-3 piezocomposite materials, *J.-Ocean Univ. Qingdao-Chin. Ed.* 33 (5) (2003) 747–752.
- [196] M. Avellaneda, P.J. Swart, Calculating the performance of 1–3 piezoelectric composites for hydrophone applications: an effective medium approach, *J. Acoust. Soc. Am.* 103 (3) (1998) 1449–1467.
- [197] Z. Qi, K. LAN, Y. Li, Research on 1-3 piezocomposite broad-band underwater transducers, *Acta Acust.* 36 (6) (2011) 631–637.
- [198] S.-E. Park, T.R. Shrout, Characteristics of relaxor-based piezoelectric single crystals for ultrasonic transducers, *IEEE Trans. Ultrason. Ferroelectr. Freq. Control* 44 (5) (1997) 1140–1147.
- [199] S.-E. Park, T.R. Shrout, Relaxor based ferroelectric single crystals for electro-mechanical actuators, *Mater. Res. Innov.* 1 (1) (1997) 20–25.
- [200] J. Chen, R. Panda, Review: commercialization of piezoelectric single crystals for medical imaging applications, in: *IEEE Ultrasonics Symposium*, 2005, IEEE: Rotterdam, Netherlands, 2005, pp. 235–240.
- [201] M. Zipparo, C. Oakley, Finite element modeling of PZN-PT and PMN-PT single crystal materials, in: *2001 IEEE Ultrasonics Symposium. Proceedings*. An International Symposium (Cat. No. 01CH37263), IEEE, 2001.
- [202] K.C. Cheng, et al., Single crystal PMN-0.33 PT/epoxy 1-3 composites for ultrasonic transducer applications, *IEEE Trans. Ultrason. Ferroelectr. Freq. Control* 50 (9) (2003) 1177–1183.
- [203] J.A. Brown, et al., A single-crystal acoustic hydrophone for increased sensitivity, *Proceedings of Meetings on Acoustics ICA2013* (2013) 070056.
- [204] W.A. Smith, Optimizing electromechanical coupling in piezocomposites using polymers with negative Poisson's ratio, in: *IEEE 1991 Ultrasonics Symposium*, IEEE: Orlando, FL, USA, 1991, pp. 661–666.
- [205] J. Ueda, T.W. Secord, H.H. Asada, Large effective-strain piezoelectric actuators using nested cellular architecture with exponential strain amplification mechanisms, *IEEE/ASME Trans. Mechatron.* 15 (5) (2009) 770–782.
- [206] S. Iyer, M. Alkhader, T. Venkatesh, Electromechanical behavior of auxetic piezoelectric cellular solids, *Scr. Mater.* 99 (2015) 65–68.
- [207] K. Challagulla, T. Venkatesh, Electromechanical response of piezoelectric foams, *Acta Mater.* 60 (5) (2012) 2111–2127.
- [208] J. Bauer, et al., High-strength cellular ceramic composites with 3D microarchitecture, *Proc. Natl. Acad. Sci. U. S. A.* 111 (7) (2014) 2453–2458.
- [209] P. Fang, et al., Cellular polyethylene-naphthalate ferroelectrets: foaming in supercritical carbon dioxide, structural and electrical preparation, and resulting piezoelectricity, *Appl. Phys. Lett.* 90 (19) (2007) 192908.
- [210] H.N. Wadley, Multifunctional periodic cellular metals, *Philos. Trans. Math. Phys. Eng. Sci.* 364 (1838) (2006) 31–68.
- [211] O. Sigmund, S. Torquato, I.A. Akbay, On the design of 1–3 piezocomposites using topology optimization, *J. Mater. Res.* 13 (4) (1998) 1038–1048.
- [212] E.N. Silva, J.O. Fonseca, N. Kikuchi, Optimal design of piezoelectric microstructures, *Comput. Mech.* 19 (5) (1997) 397–410.
- [213] K.A. Khan, M.A. Khan, 3-3 piezoelectric metamaterial with negative and zero Poisson's ratio for hydrophones applications, *Mater. Res. Bull.* 112 (2019) 194–204.
- [214] H.R. Ansari, Z. Kordrostami, Development of a low stress RF MEMS double-cantilever shunt capacitive switch, *Microsyst. Technol.* 26 (8) (2020) 2739–2748.
- [215] H. Ghoddus, Z. Kordrostami, P. Amiri, Performance enhancement of MEMS-guided four beam piezoelectric transducers for energy harvesting and acceleration sensing, *Int. J. Mod. Phys. B* 33 (18) (2019) 1950192.
- [216] Z. Kordrostami, S. Roozbehzadeh, Particle swarm approach to the optimisation of trenched cantilever-based MEMS piezoelectric energy harvesters, *IET Sci. Meas. Technol.* 13 (4) (2019) 582–588.
- [217] H. Ghoddus, Z. Kordrostami, Harvesting the ultimate electrical power from MEMS piezoelectric vibration energy harvesters: an optimization approach, *IEEE Sens. J.* 18 (21) (2018) 8667–8675.
- [218] Z. Kordrostami, S. Roozbehzadeh, A groove engineered ultralow frequency piezomems energy harvester with ultrahigh output voltage, *Int. J. Mod. Phys. B* 32 (20) (2018) 1850208.
- [219] K. Hassanli, Z. Kordrostami, A. Akbarian, MEMS piezoresistive pressure sensor with patterned thinning of diaphragm, *Microelectron. Int.* 37 (3) (2020) 147–153.
- [220] P. Amiri, Z. Kordrostami, H. Ghoddus, Design and simulation of a flat cap mushroom shape microelectromechanical systems piezoelectric transducer with the application as hydrophone, *Int. Sci. Meas. Technol.* 14 (2) (2020) 157–164.
- [221] P. Amiri, Z. Kordrostami, Sensitivity enhancement of MEMS diaphragm hydrophones using an integrated ring MOSFET transducer, *IEEE Trans. Ultrason. Ferroelectr. Freq. Control* 65 (11) (2018) 2121–2130.
- [222] R. Wang, et al., Wide-frequency-bandwidth whisker-inspired MEMS vector hydrophone encapsulated with parylene, *J. Phys. D Appl. Phys.* 49 (7) (2016) 07LT02.
- [223] M.R. Arshad, Recent advancement in sensor technology for underwater applications, *Indian J. Geo-Mar. Sci. (IJMS)* 38 (3) (2009), p. 267–27.
- [224] L.F. Yeung, G. Nian, Z. Choujun, Effects of the transducer dynamics in underwater acoustic communication, *Appl. Acoust.* 71 (3) (2010) 276–281.
- [225] T. Al Mahruz, et al., Material and performance analysis of MEMS piezoresistive pressure sensor, *Int. J. Eng. Trends Technol. (IJETT)* 31 (1) (2016) 10–14.
- [226] M.R. Naik, U. Kempaiah, U. Kushal, Analysis of MEMS piezoelectric hydrophone at high sensitivity for underwater application, *Mater. Today Proc.* 4 (10) (2017) 10803–10809.
- [227] D.-n. Li, et al., Design and analysis of a novel mems piezoelectric accelerometer for vector hydrophone, in: *2019 Symposium on Piezoelectricity, Acoustic Waves and Device Applications (SPAWDA)*, IEEE: Harbin, China, 2019, pp. 1–6.
- [228] C. Li-jie, A design of novel piezoresistive vector hydrophone, *Appl. Acoust.* 25 (5) (2006) 273–278.
- [229] J. Bernstein, A micromachined condenser hydrophone, in: *Technical Digest IEEE Solid-State Sensor and Actuator Workshop*, IEEE, 1992.
- [230] H.K. Rockstad, et al., A microfabricated electron-tunneling accelerometer as a directional underwater acoustic sensor, *AIP Conference Proceedings* (1996).
- [231] Z. Fan, et al., Design and fabrication of artificial lateral line flow sensors, *J. Micromech. Microeng.* 12 (5) (2002) 655.
- [232] L. Guan, et al., Advancements in technology and design of NEMS vector hydrophone, *Microsyst. Technol.* 17 (3) (2011) 459.

- [233] S.-Y. Li, et al., A novel design of piezo-resistive type underwater acoustic sensor using SOI wafer, in: OCEANS 2006-Asia Pacific, IEEE, 2006.
- [234] C.L.-J.Y. Shi-E, A design of novel piezoresistive vector hydrophone, *Appl. Acoust.* 5 (2006).
- [235] G. Uma, et al., Design and simulation of PVDF-MOSFET based MEMS hydrophone, *Instrum. Sci. Technol.* 35 (3) (2007) 329–339.
- [236] S. Choi, H. Lee, W. Moon, A micro-machined piezoelectric hydrophone with hydrostatically balanced air backing, *Sens. Actuators A Phys.* 158 (1) (2010) 60–71.
- [237] L. Guan, et al., Design of T-shape vector hydrophone based on MEMS, *Sens. Actuators A Phys.* 188 (2012) 35–40.
- [238] J. Kim, Y. Roh, Homogenization of PMN-PT/epoxy 1–3 piezocomposites by resonator measurements and finite element analysis, *Sens. Actuators A Phys.* 206 (2014) 97–106.
- [239] L. Linxian, et al., Package optimization of the cilium-type MEMS bionic vector hydrophone, *IEEE Sens. J.* 14 (4) (2013) 1185–1192.
- [240] L. Mengran, et al., Design of the monolithic integrated array MEMS hydrophone, *IEEE Sens. J.* 16 (4) (2015) 989–995.
- [241] G. Zhang, et al., Design and optimization of stress centralized MEMS vector hydrophone with high sensitivity at low frequency, *Mech. Syst. Signal Process.* 104 (2018) 607–618.
- [242] P. Zhang, X. Shi, H. Chen, Research on capacitance attitude self-correction vector hydrophone, 2013 International Conference on Optoelectronics and Microelectronics (ICOM) (2013).
- [243] J. Van Baar, et al., Arrays of cricket-inspired sensory hairs with capacitive motion detection, in: 18th IEEE International Conference on Micro Electro Mechanical Systems, 2005. MEMS 2005, IEEE, 2005.
- [244] Y. Ozaki, et al., An air flow sensor modeled on wind receptor hairs of insects, in: Proceedings IEEE Thirteenth Annual International Conference on Micro Electro Mechanical Systems (Cat. No. 00CH36308), IEEE, 2000.
- [245] L. Junhong, W. Jianhui, M. Jun, ZnO thin film piezoelectric micromachined vector hydrophone, *Acta Acust.* 41 (3) (2016) 273–280.
- [246] J. Chen, J. Engel, C. Liu, Development of polymer-based artificial haircell using surface micromachining and 3D assembly, in: TRANSDUCERS'03. 12th International Conference on Solid-State Sensors, Actuators and Microsystems. Digest of Technical Papers (Cat. No. 03TH8664), IEEE, 2003, pp. 1035–1038.
- [247] J. Li, et al., A low-noise MEMS acoustic vector sensor, in: 2013 International Conference on Optoelectronics and Microelectronics (ICOM), IEEE, 2013, pp. 121–124.
- [248] M. Tabib-Azar, A. Garcia-Valenzuela, Sensing means and sensor shells: a new method of comparative study of piezoelectric, piezoresistive, electrostatic, magnetic, and optical sensors, *Sens. Actuators A Phys.* 48 (2) (1995) 87–100.
- [249] C. Xue, et al., A novel vector hydrophone based on the piezoresistive effect of resonant tunneling diode, *IEEE Sens. J.* 8 (4) (2008) 401–402.
- [250] W.D. Zhang, et al., Research of DOA estimation based on single MEMS vector hydrophone, *Sensors* 9 (9) (2009) 6823–6834.
- [251] N. Guo, G.J. Zhang, W.D. Zhang, Design and experiment research on MEMS vector hydrophone vibration damping structure, in: Key Engineering Materials, Trans Tech Publ., 2015, pp. 931–941.
- [252] L. Beccai, et al., Design and fabrication of a hybrid silicon three-axial force sensor for biomechanical applications, *Sens. Actuators A Phys.* 120 (2) (2005) 370–382.
- [253] C. Barbier, et al., Design, fabrication and testing of a bioinspired hybrid hair-like fluid motion sensor array, ASME International Mechanical Engineering Congress and Exposition (2007).
- [254] L.-J. Hong, et al., Study on a medium three dimensional co-oscillating vector hydrophone, *J. Vib. Shock* 30 (3) (2011) 79–84.
- [255] J. Zhang, et al., Modeling and underwater characterization of cymbal transducers and arrays, *IEEE Trans. Ultrason. Ferroelectr. Freq. Control* 48 (2) (2001) 560–568.
- [256] Q.Q. Ge, A kind of minitype 2D vector hydrophone, in: Z. Du, B. Liu (Eds.), *Applied Mechanics and Materials*, Trans Tech Publ., 2012, pp. 273–278.
- [257] D.-n. Li, et al., Design and analysis of a novel mems piezoelectric accelerometer for vector hydrophone, in: 2019 Symposium on Piezoelectricity, Acoustic Waves and Device Applications (SPAUDA), Harbin, China: IEEE, 2019.
- [258] N. Maluf, An introduction to microelectromechanical systems engineering, *Meas. Sci. Technol.* 13 (2) (2002) 229.
- [259] J.J. Bhat, Investigations on low frequency Piezofilm Hydrophones with improved performance, Department of Electronics (1994), p. 201.
- [260] P.N. Célat, R.C. Preston, A. Hurrell, A theoretical model describing the transfer characteristics of a membrane hydrophone and validation, *Ultrasonics* 43 (5) (2005) 331–341.
- [261] S.H. Chang, et al., Structural optimization of MEMS-Based hydrophones with perforated active membrane, *Appl. Mech. Mater.* 300–301 (2013) 597–603.
- [262] J. Xu, et al., AlN-on-SOI platform-based MEMS hydrophone with ultra-low operation frequency and ultra-high noise resolution, in: 2016 IEEE 29th International Conference on Micro Electro Mechanical Systems (MEMS), IEEE, 2016.
- [263] R.G. Swartz, J.D. Plummer, Integrated silicon-PVF 2 acoustic transducer arrays, *IEEE Trans. Electron Devices* 26 (12) (1979) 1921–1931.
- [264] J.-H. Mo, et al., Improvement of integrated ultrasonic transducer sensitivity, *Sens. Actuators A Phys.* 22 (1–3) (1990) 679–682.
- [265] A. Fiorillo, et al., AP (VDF-TrFE)-based integrated ultrasonic transducer, *Sens. Actuators A Phys.* 22 (1–3) (1990) 719–725.
- [266] W. Munch, V. Thiemann, Pyroelector array with PVDF on silicon integrated circuit, *Sens. Actuators A Phys.* 25 (1–3) (1990) 167–172.
- [267] R.R. Reston, E.S. Kolesar, Robotic tactile sensor array fabricated from a piezoelectric polyvinylidene fluoride film, in: IEEE Conference on Aerospace and Electronics, Dayton, OH, USA, 1990, pp. 1139–1144.
- [268] W. Galbraith, G. Hayward, Development of a PVDF membrane hydrophone for use in air-coupled ultrasonic transducer calibration, *IEEE Trans. Ultrason. Ferroelectr. Freq. Control* 45 (6) (1998) 1549–1558.
- [269] R.G. Swartz, J. Plummer, On the generation of high-frequency acoustic energy with polyvinylidene fluoride, *IEEE Trans. Sonics Ultrason.* 27 (6) (1980) 295–302.
- [270] J.-H. Mo, et al., Micromachining for improvement of integrated ultrasonic transducer sensitivity, *IEEE Trans. Electron Devices* 37 (1) (1990) 134–140.
- [271] X. Zheng, et al., An integrated PVDF ultrasonic sensor with improved sensitivity using polyimide, *Sens. Actuators A Phys.* 63 (2) (1997) 147–152.
- [272] B. Zhu, V.K. Varadan, Integrated MOSFET-based hydrophone device for underwater applications, in: Smart Structures and Materials 2002: Smart Electronics, MEMS, and Nanotechnology, International Society for Optics and Photonics, San Diego, California, United States, 2002, pp. 101–110.
- [273] W. Kühnel, G. Hess, Micromachined subminiature condenser microphones in silicon, *Sens. Actuators A Phys.* 32 (1–3) (1992) 560–564.
- [274] M. Sung, K. Shin, W. Moon, A new transduction mechanism for hydrophones employing piezoelectricity and a field-effect transistor, *Sens. Actuators A Phys.* 233 (2015) 557–568.
- [275] M. Sung, K. Shin, W. Moon, A micro-machined hydrophone employing a piezoelectric body combined on the gate of a field-effect transistor, *Sens. Actuators A Phys.* 237 (2016) 155–166.
- [276] J.C. Shipps, K. Deng, A miniature vector sensor for line array applications, in: Oceans 2003. Celebrating the Past... Teaming Toward the Future (IEEE Cat. No. 03CH37492), IEEE, San Diego, CA, USA, 2003.
- [277] d.B. Hans-Elias, et al., The μ -flow: a novel device for measuring acoustic flows, *Sens. Actuators A Phys.* 54 (1–3) (1996) 552–557.
- [278] J.L. Butler, et al., Metallic glass velocity sensor, *AIP Conference Proceedings* (1996).
- [279] J.-q. Du, et al., Method of medical ultrasonic power measurement based on sound field scanning with hydrophone, in: 2011 Symposium on Piezoelectricity, Acoustic Waves and Device Applications (SPAUDA), IEEE, 2011.
- [280] S. Lianjin, Shengguoyang, D. Hong, Research on sound wave receiving theory of co-oscillating sphere type vector hydrophone, *Acta Acust.* 34 (1) (2009) 30–38.
- [281] M. Liu, et al., Realization of a composite MEMS hydrophone without left-right ambiguity, *Sens. Actuators A Phys.* 272 (2018) 231–241.
- [282] S. Park, S. He, Standing wave brass-PZT square tubular ultrasonic motor, *Ultrasonics* 52 (7) (2012) 880–889.
- [283] X. Bao, et al., Recent development in the distributed fiber optic acoustic and ultrasonic detection, *J. Light. Technol.* 35 (16) (2016) 3256–3267.
- [284] H.-Y. Chang, et al., Hydrophone based on a fiber Bragg grating, in: 2018 Progress in Electromagnetics Research Symposium (PIERS-Toyama), IEEE, 2018.
- [285] K.-S. Kim, Y. Mizuno, K. Nakamura, Fiber-optic ultrasonic hydrophone using short Fabry-Perot cavity with multilayer reflectors deposited on small stub, *Ultrasonics* 54 (4) (2014) 1047–1051.
- [286] J. Bucaro, H. Dardy, E. Carome, Fiber-optic hydrophone, *J. Acoust. Soc. Am.* 62 (5) (1977) 1302–1304.
- [287] J. Staudenraus, W. Eisenmenger, Optisches sondenhydrophon, *Biomed. Eng.* 33 (s2) (1988) 105–106.
- [288] J.T. Kringlebotn, H. Nakstad, M. Eriksrud, Fibre optic ocean bottom seismic cable system: from innovation to commercial success, 20th International Conference on Optical Fibre Sensors (2009) 75037U.
- [289] S.J. Maas, I. Buchan, Fiber optic 4C seabed cable for permanent reservoir monitoring, in: 2007 Symposium on Underwater Technology and Workshop on Scientific Use of Submarine Cables and Related Technologies, IEEE, 2007.
- [290] G. Wild, S. Hinckley, Acousto-ultrasonic optical fiber sensors: overview and state-of-the-art, *IEEE Sens. J.* 8 (7) (2008) 1184–1193.
- [291] I. Leung, et al., A distributed-feedback fiber-laser-based optical fiber hydrophone system with very high sensitivity, in: Advanced Sensor Systems and Applications II, International Society for Optics and Photonics, 2005, pp. 434–443.
- [292] S. Atique, et al., Detecting ultrasound using optical fibres, *J. Opt.* 33 (4) (2004) 241–255.
- [293] P.J. Nash, G.A. Cranch, D.J. Hill, Large-scale Multiplexed Fiber Optic Arrays for Geophysical Applications, in: Industrial Sensing Systems, International Society for Optics and Photonics, 2000, pp. 55–65.
- [294] G.R.C. Possetti, et al., Metrological evaluation of optical fiber grating-based sensors: an approach towards the standardization, *J. Light. Technol.* 30 (8) (2011) 1042–1052.
- [295] R. De Paula, J. Cole, J. Bucaro, Broad-band ultrasonic sensor based on induced optical phase shifts in single-mode fibers, *J. Light. Technol.* 1 (2) (1983) 390–393.
- [296] L.-Y. Shao, et al., High-frequency ultrasonic hydrophone based on a cladding-etched DBR fiber laser, *IEEE Photonics Technol. Lett.* 20 (8) (2008) 548–550.
- [297] A. Jamshidi-Rad, F. Ueberle, An optical hydrophone for the single-shot field measurements of high power pressure pulse fields, *Acta Phys. Pol. A* 127 (1) (2015) 69–71.

- [298] C. Peng, et al., Optimal tone detection for optical fibre vector hydrophone, *IET Radar Sonar Navig.* 12 (11) (2018) 1233–1240.
- [299] G.A. Cranch, P.J. Nash, C.K. Kirkendall, Large-scale remotely interrogated arrays of fiber-optic interferometric sensors for underwater acoustic applications, *IEEE Sens. J.* 3 (1) (2003) 19–30.
- [300] C. Peng, X. Zhang, A dynamic depth estimation method for towed optical fiber hydrophone array, *J. Acoust. Soc. Am.* 143 (5) (2018) EL399–EL404.
- [301] H. Wang, et al., A fiber DBR laser based vector hydrophone for ultrasonic medical applications, in: Photoelectronic Technology Committee of the Chinese Society of Astronautics 2014, International Society for Optics and Photonics., 2014, pp. 95220A.
- [302] F.-X. Launay, et al., Acoustic antenna based on fiber laser hydrophones, 23rd International Conference on Optical Fibre Sensors (2014) 91570Y.
- [303] J. De Freitas, Recent developments in seismic seabed oil reservoir monitoring applications using fibre-optic sensing networks, *Meas. Sci. Technol.* 22 (5) (2011) 052001.
- [304] M.S. Canney, et al., Acoustic characterization of high intensity focused ultrasound fields: a combined measurement and modeling approach, *J. Acoust. Soc. Am.* 124 (4) (2008) 2406–2420.
- [305] P. Morris, et al., A Fabry-Pérot fiber-optic ultrasonic hydrophone for the simultaneous measurement of temperature and acoustic pressure, *J. Acoust. Soc. Am.* 125 (6) (2009) 3611–3622.
- [306] W. Zhang, Y. Liu, F. Li, An optimized design of a fiber optic hydrophone based on a flat diaphragm and multilayer fiber coils: a theoretical approach, *Measurement* 42 (2) (2009) 171–174.
- [307] M. Klann, C. Koch, Measurement of spatial cross sections of ultrasound pressure fields by optical scanning means, *IEEE Trans. Ultrason. Ferroelectr. Freq. Control* 52 (9) (2005) 1546–1554.
- [308] J. Staudenraus, W. Eisenmenger, Fibre-optic probe hydrophone for ultrasonic and shock-wave measurements in water, *Ultrasonics* 31 (4) (1993) 267–273.
- [309] B. Shen, et al., Fiber-optic ultrasonic probe based on refractive-index modulation in water, 21st International Conference on Optical Fiber Sensors (OFS21) (2011) 77539W.
- [310] A.J. Rad, F. Ueberle, K. Krueger, Investigation on the comparability of the light spot hydrophone and the fiber optic hydrophone in lithotripter field measurements, *Rev. Sci. Instrum.* 85 (1) (2014) 014902.
- [311] M. Pang, W. Jin, Detection of acoustic pressure with hollow-core photonic bandgap fiber, *Opt. Express* 17 (13) (2009) 11088–11097.
- [312] O. Kilic, et al., Asymmetrical spectral response in fiber Fabry-Perot interferometers, *J. Light. Technol.* 27 (24) (2009) 5648–5656.
- [313] O. Kilic, et al., Photonic crystal slabs demonstrating strong broadband suppression of transmission in the presence of disorders, *Opt. Lett.* 29 (23) (2004) 2782–2784.
- [314] W. Yang, et al., High-resolution dual-polarization fiber laser hydrophone by using a corrugated diaphragm, Asia Communications and Photonics Conference (2016).
- [315] L.K. Cheng, D. de Bruijn, High sensitivity flattened mandrel hydrophone, in: Fiber Optic and Laser Sensors XI, International Society for Optics and Photonics, Boston, MA, United States, 1994, pp. 24–29.
- [316] D.A. Frederick, J.F. Cappi, Fiber optic hydrophone having rigid mandrel, 1997, Google Patents: Canada.
- [317] O.H. Waagaard, G. Wang, An investigation of the pressure-to-acceleration responsivity ratio of fiber-optic mandrel hydrophones, *J. Light. Technol.* 19 (7) (2001) 994.
- [318] D. Brown, T. Hofler, S. Garrett, High-sensitivity, fiber-optic, flexural disk hydrophone with reduced acceleration response, *Fiber Integr. Opt.* 8 (3) (1989) 169–191.
- [319] U.K. Chandrika, et al., Flow noise response of a diaphragm based fibre laser hydrophone array, *Ocean Eng.* 91 (2014) 235–242.
- [320] G. Dolgikh, A. Plotnikov, V. Shvets, Laser hydrophone, *Instrum. Exp. Tech.* 1 (2007) 159–160.
- [321] G. Dolgikh, et al., The laser-interference superlow-frequency hydrophone, in: Lasers for Measurements and Information Transfer 2006, International Society for Optics and Photonics, Petersburg, Russian Federation, 2006, pp. 659409.
- [322] B.H. Lee, et al., Interferometric fiber optic sensors, *Sensors* 12 (3) (2012) 2467–2486.
- [323] J. Posada-Roman, J.A. Garcia-Souto, J. Rubio-Serrano, Fiber optic sensor for acoustic detection of partial discharges in oil-paper insulated electrical systems, *Sensors* 12 (4) (2012) 4793–4802.
- [324] D. Hill, P. Nash, Fiber-optic hydrophone array for acoustic surveillance in the littoral, in: Photonics for Port and Harbor Security, International Society for Optics and Photonics, 2005, pp. 1–10.
- [325] J. Ma, Y. Yu, W. Jin, Demodulation of diaphragm based acoustic sensor using Sagnac interferometer with stable phase bias, *Opt. Express* 23 (22) (2015) 29268–29278.
- [326] F. Zhang, et al., DFB fiber laser hydrophone with an acoustic low-pass filter, *IEEE Photon. Technol. Lett.* 23 (17) (2011) 1264–1266.
- [327] F.-X. Launay, et al., Static pressure and temperature compensated wideband fiber laser hydrophone, Fifth European Workshop on Optical Fibre Sensors (2013) 87940K.
- [328] F. Zhang, et al., Study on the frequency response of static pressure compensated fiber laser hydrophone-theory and finite element simulation, 23rd International Conference on Optical Fibre Sensors (2014) 91571I.
- [329] R. Rajesh, et al., An eight element hydrophone array using DFB fiber laser with bender bar packaging, International Conference on Fibre Optics and Photonics (2016) Th3A_52.
- [330] M. Li, et al., Development of high sensitivity eight-element multiplexed fiber laser acoustic pressure hydrophone array and interrogation system, *Photonic Sens.* 7 (3) (2017) 253–260.
- [331] V. Pallayil, Ceramic and fibre optic hydrophone as sensors for lightweight arrays—A comparative study, in: OCEANS 2017-Anchorage, IEEE, 2017.
- [332] S. Lau, et al., Characterization of a fibre grating laser-based hydrophone for detection of high frequency medical ultrasound: a comparison with PVDF membrane hydrophone, *Ferroelectrics* 333 (1) (2006) 115–120.
- [333] N.E. Fisher, et al., Ultrasonic hydrophone based on short in-fiber Bragg gratings, *Appl. Opt.* 37 (34) (1998) 8120–8128.
- [334] N. Takahashi, et al., Development of an optical fiber hydrophone with fiber Bragg grating, *Ultrasonics* 38 (1–8) (2000) 581–585.
- [335] D.C. Betz, et al., Acousto-ultrasonic sensing using fiber Bragg gratings, *Smart Mater. Struct.* 12 (1) (2003) 122.
- [336] W. Zhang, Y. Liu, F. Li, Fiber Bragg grating hydrophone with high sensitivity, *Chin. Opt. Lett.* 6 (9) (2008) 631–633.
- [337] Y.-N. Tan, Y. Zhang, B.-O. Guan, Hydrostatic pressure insensitive dual polarization fiber grating laser hydrophone, *IEEE Sens. J.* 11 (5) (2010) 1169–1172.
- [338] A. Rosenthal, D. Razansky, V. Ntziachristos, High-sensitivity compact ultrasonic detector based on a pi-phase-shifted fiber Bragg grating, *Opt. Lett.* 36 (10) (2011) 1833–1835.
- [339] M. Moccia, et al., Opto-acoustic behavior of coated fiber Bragg gratings, *Opt. Express* 19 (20) (2011) 18842–18860.
- [340] Z. Guo, et al., Doppler noise in the inline FBG-based interferometric hydrophone array, in: 2017 16th International Conference on Optical CommUunications and Networks (ICOON), IEEE, 2017.
- [341] A.R. Karas, et al., A passive optical fibre hydrophone array utilising fibre bragg grating sensors, in: Photonic Instrumentation Engineering V, International Society for Optics and Photonics, California, United States, 2018, pp. 105390H.
- [342] E.Z. Zhang, P.C. Beard, Characteristics of optimized fibre-optic ultrasound receivers for minimally invasive photoacoustic detection, in: Photons Plus Ultrasound: Imaging and Sensing 2015, International Society for Optics and Photonics, San Francisco, California, United States, 2015, pp. 932311.
- [343] H. Liao, et al., Phase demodulation of short-cavity Fabry-Perot interferometric acoustic sensors with two wavelengths, *IEEE Photon. J.* 9 (2) (2017) 1–9.
- [344] S. Dass, R. Jha, Cascaded taper mach-zehnder interferometer based hydrophone, International Conference on Fibre Optics and Photonics (2016).
- [345] D. Gallego, H. Lamela, High-sensitivity ultrasound interferometric single-mode polymer optical fiber sensors for biomedical applications, *Opt. Lett.* 34 (12) (2009) 1807–1809.
- [346] M.Y. Plotnikov, et al., Thin cable fiber-optic hydrophone array for passive acoustic surveillance applications, *IEEE Sens. J.* 19 (9) (2019) 3376–3382.
- [347] N.E. Fisher, et al., In-fibre Bragg gratings for ultrasonic medical applications, *Meas. Sci. Technol.* 8 (10) (1997) 1050.
- [348] W. Moray, Distributed fiber grating sensors, 7th Optical Fibre Sensors Conference (OFS'90) (1990) 285.
- [349] G. Cranch, et al., Acoustic performance of a large-aperture, seabed, fiber-optic hydrophone array, *J. Acoust. Soc. Am.* 115 (6) (2004) 2848–2858.
- [350] G.A. Cranch, P.J. Nash, Large-scale multiplexing of interferometric fiber-optic sensors using TDM and DWDM, *J. Light. Technol.* 19 (5) (2001) 687–699.
- [351] K. Saijyou, et al., Method for intrinsic crosstalk reduction on a serial array of interferometric optical fiber hydrophones based on fiber Bragg gratings, *Acoust. Sci. Technol.* 36 (4) (2015) 366–369.
- [352] H. Chen, et al., A high-frequency hydrophone using an optical fiber microknot resonator, *Opt. Commun.* 446 (2019) 77–83.
- [353] A.I. Azmi, et al., Fiber laser based hydrophone systems, *Photonic Sens.* 1 (3) (2011) 210–221.
- [354] J. Ma, et al., Low cost, high performance white-light fiber-optic hydrophone system with a trackable working point, *Opt. Express* 24 (17) (2016) 19008–19019.
- [355] W. Weise, V. Wilkens, C. Koch, Frequency response of fiber-optic multilayer hydrophones: experimental investigation and finite element simulation, *IEEE Trans. Ultrason. Ferroelectr. Freq. Control* 49 (7) (2002) 937–946.
- [356] V. Wilkens, Characterization of an optical multilayer hydrophone with constant frequency response in the range from 1 to 75 MHz, *J. Acoust. Soc. Am.* 113 (3) (2003) 1431–1438.
- [357] B.T. Cox, P.C. Beard, The frequency-dependent directivity of a planar Fabry-Perot polymer film ultrasound sensor, *IEEE Trans. Ultrason. Ferroelectr. Freq. Control* 54 (2) (2007) 394–404.
- [358] V. Wilkens, C. Koch, Fiber-optic multilayer hydrophone for ultrasonic measurement, *Ultrasonics* 37 (1) (1999) 45–49.
- [359] F. Guo, et al., High-sensitivity, high-frequency extrinsic Fabry-Perot interferometric fiber-tip sensor based on a thin silver diaphragm, *Opt. Lett.* 37 (9) (2012) 1505–1507.
- [360] F. Xu, et al., Fiber-optic acoustic pressure sensor based on large-area nanolayer silver diaphragm, *Opt. Lett.* 39 (10) (2014) 2838–2840.
- [361] R.V. Romashko, et al., Laser adaptive holographic hydrophone, *Quantum Electron.* 46 (3) (2016) 277.
- [362] Y. Léguillon, et al., Phase sensitivity to axial strain of microstructured optical silica fibers, in: 21st International Conference on Optical Fiber Sensors,

- International Society for Optics and Photonics: Ottawa, Canada, 2011, p. 77533S.
- [363] W. Jin, H. Xuan, H. Ho, Sensing with hollow-core photonic bandgap fibers, *Meas. Sci. Technol.* 21 (9) (2010) 094014.
- [364] A. Abdallah, C.Z. Zhang, Z. Zhong, Model analysis of underwater acoustic sensing with hollow-core photonic bandgap fiber, in: *Applied Mechanics and Materials*, Trans Tech Publ., 2014.
- [365] B.-O. Guan, et al., Polarimetric heterodyning fiber grating laser sensors, *J. Light. Technol.* 30 (8) (2011) 1097–1112.
- [366] C. Lyu, et al., Polarimetric heterodyning fiber laser sensor for directional acoustic signal measurement, *Opt. Express* 21 (15) (2013) 18273–18280.
- [367] J. De Freitas, T. Birks, M. Rollings, Optical micro-knot resonator hydrophone, *Opt. Express* 23 (5) (2015) 5850–5860.
- [368] X. Jiang, et al., All-fiber add-drop filters based on microfiber knot resonators, *Opt. Lett.* 32 (12) (2007) 1710–1712.
- [369] I.S. Maksymov, A.D. Greentree, Plasmonic nanoantenna hydrophones, *Sci. Rep.* 6 (1) (2016) 1–12.
- [370] Z. Jia, Design and characteristics of a resonant-sphere type three-dimensional vector hydrophone, *Appl. Acoust.* 20 (4) (2001) 15–20.
- [371] G.J. Krijnen, et al., MEMS based hair flow-sensors as model systems for acoustic perception studies, *Nanotechnology* 17 (4) (2006) S84.
- [372] Y.I. Wu, K.T. Wong, S.-K. Lau, The acoustic vector-sensor's near-field array-manifold, *IEEE Trans. Signal Process.* 58 (7) (2010) 3946–3951.
- [373] R. Amarasinghe, et al., Development of miniaturized 6-axis accelerometer utilizing piezoresistive sensing elements, *Sens. Actuators A Phys.* 134 (2) (2007) 310–320.
- [374] Z.Y. Zhang, Achievements of sonar technology in recent years, *MPDERN Ships* 2 (1994) 26–28.
- [375] J.C. Shipp, B.M. Abraham, Vector Sensors Secure Shore-based Manufacturing Plants, 2004.
- [376] H. Schau, A. Robinson, Passive source localization employing intersecting spherical surfaces from time-of-arrival differences, *IEEE Trans. Acoust. Speech Lang. Signal Process.* 35 (8) (1987) 1223–1225.
- [377] M.-J.D. Rendas, J.M. Moura, Cramer-Rao bound for location systems in multipath environments, *IEEE Trans. Signal Process.* 39 (12) (1991) 2593–2610.
- [378] Z. Wang, et al., Design considerations and performance of MEMS acoustoelectric ultrasound detectors, *IEEE Trans. Ultrason. Ferroelectr. Freq. Control* 60 (9) (2013) 1906–1916.
- [379] C.-G. Fan, et al., Ultrasonic testing experiment based on the PVDF piezoelectric film sensor, *Nondestruct. Test.* 34 (1) (2012) 27–30.
- [380] T. He, Z. Xu, Piezoelectric composite standard reference hydrophone for the frequency range 100 k–500 kHz, *Appl. Acoust.* 29 (2010) 302–305.
- [381] M.-x. Huo, et al., Micro-vibration sensors fabricated by bulk silicon technology, *J. Harbin Inst. Technol.* 36 (8) (2004) 1092–1094.
- [382] J. Ahmadi-Shokouh, H. Keshavarz, A vector-hydrophone~'s minimal composition for finite estimation-variance in direction-finding near a rigid reflecting boundary, in: *GLOBECOM'05. IEEE Global Telecommunications Conference, 2005*, IEEE: St. Louis, MO, USA, 2005, pp. 2179–2183.
- [383] K.T. Wong, H. Chu, Beam patterns of an underwater acoustic vector hydrophone located away from any reflecting boundary, *IEEE J. Ocean. Eng.* 27 (3) (2002) 628–637.
- [384] A. Nehorai, E. Paldi, Acoustic vector-sensor array processing, *IEEE Trans. Signal Process.* 42 (9) (1994) 2481–2491.
- [385] L.-g. GUAN, et al., Estimation of the underwater target based on NEMS vector hydrophone, *Ocean Technology* 28 (2009) 43–46.
- [386] M.R. Liu, et al., Experiment research on array grouped by MEMS vector hydrophone, *Key Eng. Mater.* 609 (2014) 927–931.
- [387] P. Wang, et al., Engineering application of mems vector hydrophone and self-adapting root-music algorithm, in: *2011 16th International Solid-State Sensors, Actuators and Microsystems Conference*, IEEE, 2011.
- [388] J.D. Maynard, E.G. Williams, Y. Lee, Nearfield acoustic holography: I. Theory of generalized holography and the development of NAH, *J. Acoust. Soc. Am.* 78 (4) (1985) 1395–1413.
- [389] T.-J. Shan, M. Wax, T. Kailath, On spatial smoothing for direction-of-arrival estimation of coherent signals, *IEEE Trans. Acoust. Speech Lang. Signal Process.* 33 (4) (1985) 806–811.
- [390] R.T. Williams, et al., An improved spatial smoothing technique for bearing estimation in a multipath environment, *IEEE Trans. Acoust. Speech Lang. Signal Process.* 36 (4) (1988) 425–432.
- [391] S.U. Pillai, B.H. Kwon, Forward/backward spatial smoothing techniques for coherent signal identification, *IEEE Trans. Acoust. Speech Lang. Signal Process.* 37 (1) (1989) 8–15.
- [392] E.G. Williams, et al., Interior near-field acoustical holography in flight, *J. Acoust. Soc. Am.* 108 (4) (2000) 1451–1463.
- [393] S. Sha, et al., A surveillance detection algorithm based on target passing characteristic, *Meas. Control Technol.* 32 (2013) 131–134.
- [394] C. Han, et al., Double vector hydrophones positioning of underwater moving sources, in: *2014 7th International Congress on Image and Signal Processing*, IEEE, 2014.
- [395] C. Han, et al., Experimental study on single vector hydrophone positioning, in: *2017 10th International Congress on Image and Signal Processing, BioMedical Engineering and Informatics (CISP-BMEI)*, IEEE: Shanghai, 2017, pp. 1–5.
- [396] R. Schmidt, Multiple emitter location and signal parameter estimation, *IEEE Trans. Antennas Propag.* 34 (3) (1986) 276–280.
- [397] K.W. Lo, B.G. Ferguson, Surface craft motion parameter estimation using multipath delay measurements from hydrophones, in: *2011 Seventh International Conference on Intelligent Sensors, Sensor Networks and Information Processing*, IEEE, 2011.
- [398] R. Roy, T. Kailath, ESPRIT-estimation of signal parameters via rotational invariance techniques, *IEEE Trans. Acoust. Speech Lang. Signal Process.* 37 (7) (1989) 984–995.
- [399] K.-M. Kim, et al., Passive-range estimation using dual focused beamformers, *IEEE J. Ocean. Eng.* 27 (3) (2002) 638–641.
- [400] Y. Zhang, D. Sun, Y. Lu, Analysis of lication precision when using a dual subsurface-buoy system with a vector hydrophone, *J. Harbin Eng. Univ.* 31 (7) (2010) 868–871.
- [401] Q. Wang, Y. Wang, G. Zhu, Matched field processing based on least squares with a small aperture hydrophone array, *Sensors* 17 (1) (2017) 71.
- [402] J. Xin, A. Sano, Computationally efficient subspace-based method for direction-of-arrival estimation without eigendecomposition, *IEEE Trans. Signal Process.* 52 (4) (2004) 876–893.
- [403] K.T. Wong, M.D. Zoltowski, Closed-form underwater acoustic direction-finding with arbitrarily spaced vector hydrophones at unknown locations, *IEEE J. Ocean. Eng.* 22 (4) (1997) 649–658.
- [404] K.T. Wong, M.D. Zoltowski, Extended-aperture underwater acoustic multisource azimuth/elevation direction-finding using uniformly but sparsely spaced vector hydrophones, *IEEE J. Ocean. Eng.* 22 (4) (1997) 659–672.
- [405] K.T. Wong, M.D. Zoltowski, Root-MUSIC-based azimuth-elevation angle-of-arrival estimation with uniformly spaced but arbitrarily oriented velocity hydrophones, *IEEE Trans. Signal Process.* 47 (12) (1999) 3250–3260.
- [406] K.T. Wong, M.D. Zoltowski, Self-initiating velocity-field beamspace MUSIC for underwater acoustic direction-finding with irregularly spaced vector-hydrophones, in: *1997 IEEE International Symposium on Circuits and Systems (ISCAS)*, IEEE, 1997.
- [407] P. Tichavsky, K.T. Wong, M.D. Zoltowski, Near-field/far-field azimuth and elevation angle estimation using a single vector hydrophone, *IEEE Trans. Signal Process.* 49 (11) (2001) 2498–2510.
- [408] H. Chen, J. Zhao, Coherent signal-subspace processing of acoustic vector sensor array for DOA estimation of wideband sources, *Signal Process.* 85 (4) (2005) 837–847.
- [409] B. Zhang, et al., Modeling and characterization of a micromachined artificial hair cell vector hydrophone, *Microsyst. Technol.* 14 (6) (2008) 821–828.
- [410] X. Ni, Y. Zhao, J. Yang, Research of a novel fiber Bragg grating underwater acoustic sensor, *Sens. Actuators A Phys.* 138 (1) (2007) 76–80.
- [411] P. Dawson, et al., Positions of the sub-band minima in GaAs (AlGa) As quantum well heterostructures, *Superlattices Microstruct.* 1 (3) (1985) 231–235.
- [412] W. Jian, et al., Pressure effects in AlAs/In_{1-x}As/GaAs resonant tunneling diodes for application in micromachined sensors, *Chin. Phys.* 16 (4) (2007) 1150–1154.
- [413] G.J. Zhang, et al., MEMS bionic vector hydrophone, *Key Eng. Mater.* 503 (2012) 114–117.
- [414] L. Liu, et al., Design of a novel MEMS resonant-column type bionic vector hydrophone, in: *2012 International Conference on Computing, Measurement, Control and Sensor Network*, IEEE, 2012.
- [415] R. Bashir, et al., On the design of piezoresistive silicon cantilevers with stress concentration regions for scanning probe microscopy applications, *J. Micromech. Microeng.* 10 (4) (2000) 483.
- [416] S. Firdaus, et al., Enhancing the sensitivity of a mass-based piezoresistive micro-electro-mechanical systems cantilever sensor, *Micro Nano Lett.* 5 (2) (2010) 85–90.
- [417] S. Firdaus, et al., Half cut stress concentration (HCSC) region design on MEMS piezoresistive cantilever for sensitivity enhancement, in: *2008 33rd IEEE/CPMT International Electronics Manufacturing Technology Conference (IEMT)*, IEEE, 2008.
- [418] D.-q. MEI, Y.-c. WANG, Z.-c. CHEN, Design of piezoresistive micro-cantilever with stress concentration regions, *Nanotechnol. Precis. Eng.* (4) (2007) 12.
- [419] Q. Li, et al., Design simulation of micro-cantilever with high sensitive SCR, *Transd. Microsyst. Technol.* 32 (2013) 95–98.
- [420] G.J. Zhang, P. Zhao, W.D. Zhang, Advancements in micro-structure with multiple stress concentration region for bionic vector hydrophone, in: *Key Engineering Materials*, Trans Tech Publ., 2015.
- [421] J.S. Han, et al., Bio-inspired piezoelectric artificial hair cell sensor fabricated by powder injection molding, *Smart Mater. Struct.* 24 (12) (2015) 125025.
- [422] Y. Liu, et al., "Lollipop-shaped" high-sensitivity Microelectromechanical Systems vector hydrophone based on Parylene encapsulation, *J. Appl. Phys.* 118 (4) (2015) 044501.
- [423] S.G. Prabhu, S. Nagabhushana, Design and simulation of underwater acoustic mems sensor, in: *COMSOL Conference*, Pune, 2015.
- [424] W. Xu, et al., Development of cup-shaped micro-electromechanical systems-based vector hydrophone, *J. Appl. Phys.* 120 (12) (2016) 124502.
- [425] X. Zhang, et al., Design and analysis of a multiple sensor units vector hydrophone, *AIP Adv.* 8 (8) (2018) 085124.
- [426] Q. Xu, et al., Design and implementation of two-component cilia cylinder MEMS vector hydrophone, *Sens. Actuators A Phys.* 277 (2018) 142–149.
- [427] R. Singh, et al., Design and optimization of MEMS-based Four beam vector hydrophone for direction of arrival, *International Workshop on the Physics of Semiconductor and Devices*, IWPSD 2017: The Physics of Semiconductor Devices (2017) 753–761.
- [428] L. Zhang, et al., Design and fabrication of a multipurpose cilia cluster MEMS vector hydrophone, *Sens. Actuators A Phys.* 296 (2019) 331–339.

- [429] Q. Xu, et al., New insight into contradictive relationship between sensitivity and working bandwidth of cilium MEMS bionic vector hydrophone, *J. Micromech. Microeng.* 29 (11) (2019) 115016.
- [430] G.J. Zhang, et al., Design of a monolithic integrated three-dimensional MEMS bionic vector hydrophone, *Microsyst. Technol.* 21 (8) (2015) 1697–1708.
- [431] R. Wang, et al., A ‘fitness-wheel-shaped’MEMS vector hydrophone for 3D spatial acoustic orientation, *J. Micromech. Microeng.* 27 (4) (2017) 045015.
- [432] J. Song, et al., A monolithic integration bio-inspired three-dimensional MEMS vector hydrophone, *IEEE Access* 7 (2019) 102366–102376.
- [433] G. Skrebnev, *Combined Underwater Acoustic Receiver*, Elmor, St. Petersburg, 1997.
- [434] M. Liu, et al., Array MEMS vector hydrophone oriented at different direction angles, *Sensors* 19 (19) (2019) 4282.
- [435] L. Zhu, F. Li, D. Chen, Study of vector noise field characteristics in shallow water by fiber optical vector hydrophone, *Tech. Acoust.* 32 (2016) 101–108.
- [436] L. Ding shan, C. Jia nian, L. Yun tao, Reduction of acceleration sensitivity of fiber optic hydrophone, *J. Harbin Eng. Univ.* 6 (2001).
- [437] Ji. Im, Design and evaluation of noise suppressing hydrophone, *Proceedings of the Korean Magnetics Society Conference* (2000) 546–560.
- [438] M. Kahn, A. Dalzell, B. Kovel, PZT ceramic-air composites for hydrostatic sensing, *Adv. Ceram. Mater.* 2 (4) (1987) 836–840.
- [439] P.R. Anderson, Low noise transducer system, in: Google patent. 1993, Westinghouse Electric Corp.
- [440] J.J. Eynck, Acoustic decoupler for a sonar array, in: Google patent. 1991, Westinghouse Electric (United States).
- [441] H.C. Hemond and W.H. Ezell, Sonar vibration isolation transducer mount, in: Google patent. 1984, Texas Instruments Inc.
- [442] M. Kahn, Noise-suppressing hydrophones, in: Google patent. 1990, The United States of America as represented by the Secretary of the Navy Washington DC.
- [443] J.-i. Im, Y. Roh, Design and evaluation of noise suppressing tonpilz hydrophone structures, *Jpn. J. Appl. Phys.* 39 (2R) (2000) 517.
- [444] S. Tao, et al., New algorithm design of micro-vibration isolation platform’s robust controller, ICECC’ 12: Proceedings of the 2012 International Conference on Electronics, Communications and Control (2012).
- [445] X. Zhang, et al., Study on aging of an elastomeric gasket material in simulated PEMFC environments, *Chin. J. Power Sources* 4 (2015) 759–762.
- [446] Y. Tao, et al., A sponge cover approach to reducing flow noise of hydrophone, in: *Oceans 2014-TAIPEI*, IEEE, Taipei, Taiwan, 2014, pp. 1–4.
- [447] J.-l. SONG, et al., Modeling and simulation of MEMS vector hydrophone for suppressing vibration output, 2018 International Conference on Applied Mechanics, Mathematics, Modeling and Simulation (AMMMS 2018) (2018).
- [448] J. Song, et al., A bionic micro-electromechanical system piezo-resistive vector hydrophone that suppresses vibration noise, *J. Micromech. Microeng.* 29 (11) (2019) 115007.
- [449] L. Guan, J. Xu, Design of T-shape hydrophone, *IEEE Trans. Prof. Commun.* 45 (2004) 2485–2495.
- [450] L. Guan, et al., Design of T-shape vector hydrophone based on MEMS, in: 2011 16th International Solid-State Sensors, Actuators and Microsystems Conference, IEEE, 2011.
- [451] B.A. Ganji, M.S. Nateri, M. Dardel, Design and modeling of a novel high sensitive MEMS piezoelectric vector hydrophone, *Microsyst. Technol.* 24 (4) (2018) 2085–2095.
- [452] B. Liu, J. Lei, *Principles of Underwater Sound*, Harbin Engineering University Press, Harbin, China, 2010.
- [453] S. Shengguo, *Research on Vector Hydrophone and Its Application for Underwater Platform*, Harbin Engineering University, 2006.
- [454] Z. Jia, Novel sensor technology for comprehensive underwater acoustic information-vector hydrophones and their applications, *Physics* 38 (3) (2009) 157–168.
- [455] De-Sen, S. Sheng, G. Yang, Effects of elastic elements on velocity hydrophone with co-oscillating sphere, *Appl. Acoust.* 23 (5) (2004) 21–26.
- [456] T.-J. Zhao, H.-J. Chen, H. Zhang, Simulation study on very low frequency vector hydrophone application platform’s suspension system, in: 2013 Symposium on Piezoelectricity, Acoustic Waves, and Device Applications, IEEE, 2013.
- [457] P. Wang, Y.Q. Du, Research on a Co-vibrating vector hydrophone with central fixed structure, *Adv. Mat. Res.* 346 (2012) 835–841.
- [458] T.-J. Zhao, et al., Analysis of the characteristic of vector hydrophone’s inner sound field, in: Proceedings of the 2014 Symposium on Piezoelectricity, Acoustic Waves, and Device Applications, Beijing, China: IEEE, 2014.
- [459] Q.-d. Sun, X.-j. Sun, Design and manufacture of combined co-vibrating vector hydrophones, in: Proceedings of the 2014 Symposium on Piezoelectricity, Acoustic Waves, and Device Applications, IEEE, 2014.
- [460] X. Lurton, *An Introduction to Underwater Acoustics: Principles and Applications*, Springer Science & Business Media, 2002.
- [461] Y. Brelet, et al., Underwater acoustic signals induced by intense ultrashort laser pulse, *J. Acoust. Soc. Am.* 137 (4) (2015) EL288–EL292.
- [462] S. Soloviev, *History and Prospects of Marine Seismology Development*, Nauka, Moscow, 1985.
- [463] A. Ostrovsky, Generalized spectra of the bottom seismic noise in the world ocean, *Okeanologiya* 22 (6) (1982) 980–983.
- [464] L.M. Gray, D.S. Greeley, Source level model for propeller blade rate radiation for the world’s merchant fleet, *J. Acoust. Soc. Am.* 67 (2) (1980) 516–522.
- [465] S. Kutakov, I. Maslov, Use of the piezoelectric hydrophone for detecting infra-low-frequency seismoacoustic fields, *Phys. Wave Phenom.* 18 (1) (2010) 75–80.
- [466] C.S. McCreery, D.A. Walker, G.H. Sutton, Spectra of nuclear explosions, earthquakes, and noise from Wake Island bottom hydrophones, *Geophys. Res. Lett.* 10 (1) (1983) 59–62.
- [467] D.A. Walker, Deep ocean seismology, *Eos Trans. Am. Geophys. Union* 65 (1) (1984) 2–3.
- [468] E. Herrin, The resolution of seismic instruments used in treaty verification research, *Bull. Seismol. Soc. Am.* 72 (6B) (1982) S61–S67.
- [469] H. Chen, et al., Analysis on performance of an infrasound piezoelectric hydrophone, in: 2016 Symposium on Piezoelectricity, Acoustic Waves, and Device Applications (SPAUDA), IEEE: Xi'an, China, 2016, pp. 309–313.
- [470] Y.-j. Zheng, et al., Sensitivity analysis of the infrasound piezoelectric hydrophone of radially polarized cylindrical tube, in: 2016 Symposium on Piezoelectricity, Acoustic Waves, and Device Applications (SPAUDA), IEEE: Xi'an, China, 2016, pp. 189–192.
- [471] T. Krishtop, et al., High-sensitive ultra-low frequency hydrophone, in: The International Conference on Micro- and Nano-Electronics 2018, SPIE, 2019, vol. 11022.
- [472] D.L. Zaitsev, et al., Frequency response and self-noise of the MET hydrophone, *J. Sens. Sens. Syst.* 7 (2) (2018) 443–452.
- [473] N.C. Chaggares, O. Ivanytskyy, G. Pang, Design of a 30 μm aperture membrane hydrophone for the measurement and characterization of High frequency ultrasound, in: 2016 IEEE International Ultrasonics Symposium (IUS), IEEE, 2016.
- [474] S. Umchid, et al., Development of calibration techniques for ultrasonic hydrophone probes in the frequency range from 1 to 100 MHz, *Ultrasonics* 49 (3) (2009) 306–311.
- [475] H.J. Bleeker, P.A. Lewin, A novel method for determining calibration and behavior of PVDF ultrasonic hydrophone probes in the frequency range up to 100 MHz, *IEEE Trans. Ultrason. Ferroelectr. Freq. Control* 47 (6) (2000) 1354–1362.
- [476] IEC, IEC (2007 B) 62127-2 – Part 2 – Calibration for Ultrasonic fields up to 40 MHz, International Electro-technical Commission, Geneva, 2007.
- [477] IEC, IEC (2007 C) 62127-3 – Part 3 – Properties of Hydrophones for Ultrasonic fields up to 40 MHz, International Electro-technical Commission, Geneva, 2007.
- [478] S.M. Nagle, et al., Challenges and regulatory considerations in the acoustic measurement of high-frequency (> 20 MHz) ultrasound, *J. Ultrasound Med.* 32 (11) (2013) 1897–1911.
- [479] P.C. Beard, A.M. Hurrell, T.N. Mills, Characterization of a polymer film optical fiber hydrophone for use in the range 1 to 20 MHz: a comparison with PVDF needle and membrane hydrophones, *IEEE Trans. Ultrason. Ferroelectr. Freq. Control* 47 (1) (2000) 256–264.
- [480] B. Fay, et al., Frequency response of PVDF needle-type hydrophones, *Ultrasound Med. Biol.* 20 (4) (1994) 361–366.
- [481] A. Goldstein, D.R. Gandhi, W.D. O’Brien, Diffraction effects in hydrophone measurements, *IEEE Trans. Ultrason. Ferroelectr. Freq. Control* 45 (4) (1998) 972–979.
- [482] T. Henriquez, Diffraction constants of acoustic transducers, *J. Acoust. Soc. Am.* 36 (2) (1964) 267–269.
- [483] T. Huttunen, J.P. Kaipio, K. Hynynen, Modeling of anomalies due to hydrophones in continuous-wave ultrasound fields, *IEEE Trans. Ultrason. Ferroelectr. Freq. Control* 50 (11) (2003) 1486–1500.
- [484] L. Chen, S.J. Rupitsch, R. Lerch, Quantitative reconstruction of a disturbed ultrasound pressure field in a conventional hydrophone measurement, *IEEE Trans. Ultrason. Ferroelectr. Freq. Control* 60 (6) (2013) 1199–1206.
- [485] IEC, IEC 61102 Measurement and Characterization of Ultrasonic Fields Using Hydrophones in the Frequency Range 0.5 MHz to 15 MHz, International Electro-technical Commission, Geneva, 1991.
- [486] J. Saneyoshi, M. Okujima, M. Ide, Wide frequency calibrated probe microphones for ultrasound in liquid, *Ultrasonics* 4 (2) (1966) 64–66.
- [487] B. Fay, M. Rinker, P. Lewin, Thermoacoustic sensor for ultrasound power measurements and ultrasonic equipment calibration, *Ultrasound Med. Biol.* 20 (4) (1994) 367–373.
- [488] L. Retat, Characterisation of the Acoustic, Thermal and Histological Properties of Tissue Required for High Intensity Focused Ultrasound (HIFU) Treatment Planning, Institute of Cancer Research (University Of London), 2011.
- [489] R. Smith, Are hydrophones of diameter 0.5 mm small enough to characterise diagnostic ultrasound equipment? *Phys. Med. Biol.* 34 (11) (1989) 1593.
- [490] P. Filmore, R. Chivers, Measurements on batch produced miniature ceramic ultrasonic hydrophones, *Ultrasonics* 24 (4) (1986) 216–229.
- [491] M.B. Moffett, J.M. Powers, W.L. Clay Jr., Ultrasonic microprobe hydrophones, *J. Acoust. Soc. Am.* 84 (4) (1988) 1186–1194.
- [492] A.D. Maxwell, et al., Simulated and experimental analysis of PVDF membrane hydrophone low-frequency response for accurate measurements of lithotripsy shockwaves, in: 2008 IEEE Ultrasonics Symposium, IEEE, 2008.
- [493] C. Wurster, J. Staudenraus, W. Eisenmenger, The fiber optic probe hydrophone, in: 1994 Proceedings of IEEE Ultrasonics Symposium, IEEE, 1994.
- [494] P. Lewin, et al., Acousto-optic, point receiver hydrophone probe for operation up to 100 MHz, *Ultrasonics* 43 (10) (2005) 815–821.
- [495] B. Culshaw, et al., The detection of ultrasound using fiber-optic sensors, *IEEE Sens. J.* 8 (7) (2008) 1360–1367.

- [496] S. Campopiano, et al., Underwater acoustic sensors based on fiber Bragg gratings, *Sensors* 9 (6) (2009) 4446–4454.
- [497] Y. Uno, K. Nakamura, Pressure sensitivity of a fiber-optic microprobe for high-frequency ultrasonic field, *J. Appl. Phys.* 38 (55) (1999) 3120.
- [498] P. Beard, T. Mills, Miniature optical fibre ultrasonic hydrophone using a Fabry-Perot polymer film interferometer, *Electron. Lett.* 33 (9) (1997) 801–803.
- [499] J.J. Alcoz, C. Lee, H.F. Taylor, Embedded fiber-optic Fabry-Perot ultrasound sensor, *IEEE Trans. Ultrason. Ferroelectr. Freq. Control* 37 (4) (1990) 302–306.
- [500] C. Koch, Coated fiber-optic hydrophone for ultrasonic measurement, *Ultrasonics* 34 (6) (1996) 687–689.
- [501] Y. Zhou, et al., Measurement of high intensity focused ultrasound fields by a fiber optic probe hydrophone, *J. Acoust. Soc. Am.* 120 (2) (2006) 676–685.
- [502] J.E. Parsons, C.A. Cain, J.B. Fowlkes, Cost-effective assembly of a basic fiber-optic hydrophone for measurement of high-amplitude therapeutic ultrasound fields, *J. Acoust. Soc. Am.* 119 (3) (2006) 1432–1440.
- [503] F. Wu, et al., Extracorporeal focused ultrasound surgery for treatment of human solid carcinomas: early Chinese clinical experience, *Ultrasound Med. Biol.* 30 (2) (2004) 245–260.
- [504] D.L. Miller, et al., Overview of therapeutic ultrasound applications and safety considerations, *J. Ultrasound Med.* 31 (4) (2012) 623–634.
- [505] A. Shaw, G. ter Haar, Requirements for Measurement Standards in High Intensity Focused Ultrasound (HIFU) Fields, National Physics Laboratory, 2006, pp. 7–71.
- [506] K. Raum, W.D. O'Brien, Pulse-echo field distribution measurement technique for high-frequency ultrasound sources, *IEEE Trans. Ultrason. Ferroelectr. Freq. Control* 44 (4) (1997) 810–815.
- [507] B. Huang, K.K. Shung, Characterization of high-frequency, single-element focused transducers with wire target and hydrophone, *IEEE Trans. Ultrason. Ferroelectr. Freq. Control* 52 (9) (2005) 1608–1612.
- [508] S.M. Howard, C.I. Zanelli, HIFU transducer characterization using a robust needle hydrophone, in: Couissos Constantin-C. Gt. Haar (Eds.), 6th International Symposium on Therapeutic Ultrasound, American Institute of Physics: Oxford, United Kingdom, 2007, pp. 8–14.
- [509] Y. Ying, et al., A method of estimating pressure and intensity distributions of multielement phased array high intensity focused ultrasonic field at full power using a needle hydrophone, *AIP Conference Proceedings* (2011) 227–232.
- [510] V. Wilkens, S. Sonntag, O. Georg, Robust spot-poled membrane hydrophones for measurement of large amplitude pressure waveforms generated by high intensity therapeutic ultrasonic transducers, *J. Acoust. Soc. Am.* 139 (3) (2016) 1319–1332.
- [511] M. Shiiba, et al., Development of anti-cavitation hydrophone with hydrothermal PZT film, in: 2015 IEEE International Ultrasonics Symposium (IUS), IEEE, 2015.
- [512] N. Okada, M. Shiiba, S. Takeuchi, Developing of tough hydrophone for high intensity acoustic field at low frequency, in: 2016 IEEE International Ultrasonics Symposium (IUS), IEEE, 2016.
- [513] N. Okada, et al., Durability test and observation on non-linear distortion in output waveform of anti-cavitation hydrophone in high intensity ultrasound, in: 2014 IEEE International Ultrasonics Symposium, IEEE, 2014.
- [514] N. Okada, et al., Characterization of hydrophone with hydrothermal PZT thick film vibrator and Ti front layer for measurement in high intensity therapeutic ultrasound, in: 2013 IEEE International Ultrasonics Symposium (IUS), IEEE, 2013.
- [515] J. Haller, et al., A comparative evaluation of three hydrophones and a numerical model in high intensity focused ultrasound fields, *J. Acoust. Soc. Am.* 131 (2) (2012) 1121–1130.
- [516] O.A. Sapozhnikov, et al., Acoustic holography as a metrological tool for characterizing medical ultrasound sources and fields, *J. Acoust. Soc. Am.* 138 (3) (2015) 1515–1532.
- [517] J. Haller, V. Wilkens, Short-and longtime stability of therapeutic ultrasound reference sources for dosimetry and exposimetry purposes, *AIP Conference Proceedings* (2017) 180001.
- [518] IEC, IEC TS 62556 Ultrasonics - Field Characterization - Specification and Measurement of Field Parameters for High Intensity Therapeutic Ultrasound (HITU) Transducers and Systems, International Electrotechnical Commission Geneva, Geneva, 2014.
- [519] T.Y. Kwon, et al., Fabrication of stabilized piezoelectric thick film for silicon-based MEMS device, *Appl. Phys. A* 88 (4) (2007) 627–632.
- [520] G. Zhong, Y. Zhang, X. Cao, Conjugated polymer films for piezoresistive stress sensing, *IEEE Electron Device Lett.* 30 (11) (2009) 1137–1139.
- [521] R. Olafsson, et al., Cardiac activation mapping using ultrasound current source density imaging (UCSDI), *IEEE Trans. Ultrason. Ferroelectr. Freq. Control* 56 (3) (2009) 565–574.
- [522] R.H. Parmenter, The acousto-electric effect, *Phys. Rev.* 89 (5) (1953) 990.
- [523] L. Busse, J. Miller, Detection of spatially nonuniform ultrasonic radiation with phase sensitive (piezoelectric) and phase insensitive (acoustoelectric) receivers, *J. Acoust. Soc. Am.* 70 (5) (1981) 1377–1386.
- [524] S. Haider, A. Hrbek, Y. Xu, Magneto-acousto-electrical tomography: a potential method for imaging current density and electrical impedance, *Physiol. Meas.* 29 (6) (2008) S41.
- [525] R. Olafsson, et al., Ultrasound current source density imaging, *IEEE Trans. Biomed. Eng.* 55 (7) (2008) 1840–1848.
- [526] R.S. Witte, et al., Inexpensive acoustoelectric hydrophone for mapping high intensity ultrasonic fields, *J. Appl. Phys.* 104 (5) (2008) 054701.
- [527] Z. Wang, et al., Simulation-based optimization of the acoustoelectric hydrophone for mapping an ultrasound beam, in: Medical Imaging 2010: Ultrasonic Imaging, Tomography, and Therapy, International Society for Optics and Photonics, San Diego, California, United States, 2010.
- [528] O. Oralkan, et al., Capacitive micromachined ultrasonic transducers: next-generation arrays for acoustic imaging? *IEEE Trans. Ultrason. Ferroelectr. Freq. Control* 49 (11) (2002) 1596–1610.
- [529] A. Bhuyan, et al., Miniaturized, wearable, ultrasound probe for on-demand ultrasound screening, in: 2011 IEEE International Ultrasonics Symposium, IEEE, 2011.
- [530] P. Cristman, et al., A 2D CMUT hydrophone array: characterization results, in: 2009 IEEE International Ultrasonics Symposium, IEEE: Rome, Italy, 2009, pp. 992–995.
- [531] M. Shiiba, et al., Development of anti-cavitation hydrophone with hydrothermal PZT film-estimation of durability, *IEEE Proc. IUS2015* (2015) 21–24.
- [532] L. Filipczynski, Absolute measurements of particle velocity, displacement or intensity of ultrasonic pulses in liquids and solids, *Acta Acust. United With Acust.* 21 (3) (1969) 173–180.
- [533] J. Etienne, et al., Electromagnetic hydrophone for pressure determination of shock wave pulses, *Ultrasound Med. Biol.* 23 (5) (1997) 747–754.
- [534] Y. Sharf, G.T. Clement, K. Hyynen, Absolute measurements of ultrasonic pressure by using high magnetic fields, *IEEE Trans. Ultrason. Ferroelectr. Freq. Control* 46 (6) (1999) 1504–1511.
- [535] P. Grasland-Mongrain, et al., Electromagnetic hydrophone with tomographic system for absolute velocity field mapping, *Appl. Phys. Lett.* 100 (24) (2012) 243502.
- [536] P. Grasland-Mongrain, et al., Electromagnetic hydrophone for high-intensity focused ultrasound (HIFU) measurement, *Proceedings of Meetings on Acoustics ICA2013* (2013).
- [537] P. Grasland-Mongrain, et al., Lorentz-force hydrophone characterization, *IEEE Trans. Ultrason. Ferroelectr. Freq. Control* 61 (2) (2014) 353–363.
- [538] Z.E. Chen, et al., Design of low frequency hydrophone based on PVDF piezoelectric materials, *Appl. Mech. Mater.* 513–517 (2014) 3085–3089.
- [539] G. Cranch, G. Miller, C. Kirkendall, Fiber-optic, cantilever-type acoustic motion velocity hydrophone, *J. Acoust. Soc. Am.* 132 (1) (2012) 103–114.
- [540] M. Sung, K. Shin, W. Moon, A micro-machined hydrophone using piezoelectricity on gate of a field-effect transistor, in: 2015 Transducers-2015 18th International Conference on Solid-State Sensors, Actuators and Microsystems (TRANSDUCERS), IEEE: Anchorage, AK, USA, 2015, pp. 379–382.
- [541] V. Wilkens, W. Molkenstruck, Broadband PVDF membrane hydrophone for comparisons of hydrophone calibration methods up to 140 MHz, *IEEE Trans. Ultrason. Ferroelectr. Freq. Control* 54 (9) (2007) 1784–1791.
- [542] A. DeReggi, et al., Piezoelectric polymer probe for ultrasonic applications, *J. Acoust. Soc. Am.* 69 (3) (1981) 853–859.
- [543] F.M. Boechat, et al., Development of a PVDF needle-type hydrophone for measuring ultrasonic fields, in: 2018 13th IEEE International Conference on Industry Applications (INDUSCON), IEEE: Sao Paulo, Brazil, 2018, pp. 1004–1007.
- [544] D.R. Bacon, Characteristics of a PVDF membrane hydrophone for use in the range 1–100 MHz, *IEEE Trans. Sonics Ultrason.* 29 (1) (1982) 18–25.
- [545] IEC, IEC 61157 Standard Means for the Reporting of the Acoustic Output of Medicaldiagnostic Ultrasonic Equipment, International Electro-technical Commission, Geneva, 2013.
- [546] IEC, IEC (2007 A) 62127-1 Part 1-Measurement and Characterisation of Medical Ultrasonic fields up to 40 MHz, International Electro-technical Commission, Geneva, 2007.
- [547] P.K. Verma, V.F. Humphrey, F.A. Duck, Broadband measurements of the frequency dependence of attenuation coefficient and velocity in amniotic fluid, urine and human serum albumin solutions, *Ultrasound Med. Biol.* 31 (10) (2005) 1375–1381.
- [548] T. Kujawska, A. Nowicki, P.A. Lewin, Determination of nonlinear medium parameter B/A using model assisted variable-length measurement approach, *Ultrasonics* 51 (8) (2011) 997–1005.
- [549] B. Zeqiri, et al., On measurement of the acoustic nonlinearity parameter using the finite amplitude insertion substitution (FAIS) technique, *Metrologia* 52 (2) (2015) 406.
- [550] C. Koch, W. Molkenstruck, Primary calibration of hydrophones with extended frequency range 1 to 70 MHz using optical interferometry, *IEEE Trans. Ultrason. Ferroelectr. Freq. Control* 46 (5) (1999) 1303–1314.
- [551] D.R. Bacon, Primary calibration of ultrasonic hydrophone using optical interferometry, *IEEE Trans. Ultrason. Ferroelectr. Freq. Control* 35 (2) (1988) 152–161.
- [552] P. Lum, et al., High-frequency membrane hydrophone, *IEEE Trans. Ultrason. Ferroelectr. Freq. Control* 43 (4) (1996) 536–544.
- [553] M.R. Mahlooji, J. Koohsorkhi, Micro-sensor design considerations for desired operational range based on piston coupled diaphragm, *IEEE Sens. J.* 19 (3) (2019) 852–859.
- [554] H. Gharaei, J. Koohsorkhi, Design and characterization of high sensitive MEMS capacitive microphone with fungous coupled diaphragm structure, *Microsyst. Technol.* 22 (2) (2016) 401–411.
- [555] O. Lotsberg, J. Hovem, B. Aksum, Experimental observation of subharmonic oscillations in Infusor bubbles, *J. Acoust. Soc. Am.* 99 (3) (1996) 1366–1369.

- [556] L. De Medeiros, et al., Piezoelectret-based hydrophone: an alternative device for vibro-acoustography, *Meas. Sci. Technol.* 26 (9) (2015) 095102.
- [557] G. Hayward, J.A. Hossack, Unidimensional modeling of 1-3 composite transducers, *J. Acoust. Soc. Am.* 88 (2) (1990) 599–608.
- [558] J. Bennett, G. Hayward, Design of 1-3 piezocomposite hydrophones using finite element analysis, *IEEE Trans. Ultrason. Ferroelectr. Freq. Control* 44 (3) (1997) 565–574.
- [559] M. Haun, R. Newnham, An experimental and theoretical study of 1-3 AND 1-3-0 piezoelectric PZT-Polymer composites for hydrophone applications, *Ferroelectrics* 68 (1) (1986) 123–139.
- [560] A.A. Shaulov, W.A. Smith, R.Y. Ting, Modified-lead-titanate/polymer composites for hydrophone applications, *Ferroelectrics* 93 (1) (1989) 177–182.
- [561] S. Marselli, et al., Porous piezoelectric ceramic hydrophone, *J. Acoust. Soc. Am.* 106 (2) (1999) 733–738.
- [562] W.A. Smith, Modeling 1-3 composite piezoelectrics: hydrostatic response, *IEEE Trans. Ultrason. Ferroelectr. Freq. Control* 40 (1) (1993) 41–49.
- [563] L. Gibiansky, S. Torquato, On the use of homogenization theory to design optimal piezocomposites for hydrophone applications, *J. Mech. Phys. Solids* 45 (5) (1997) 689–708.
- [564] R.Y. Ting, Evaluation of new piezoelectric composite materials for hydrophone applications, *Ferroelectrics* 67 (1) (1986) 143–157.
- [565] R. Chivers, P. Lewin, The voltage sensitivity of miniature piezoelectric plastic ultrasonic probes, *Ultrasonics* 20 (6) (1982) 279–281.
- [566] P. Lewin, R. Chivers, Voltage sensitivity of miniature ultrasonic probes, *Ultrasonics* 21 (6) (1983) 282–283.
- [567] D.-p. Zeng, et al., Sensitivity characteristics of 1-3 piezoelectric composite hydrophones over a wide frequency range, in: 2017 Symposium on Piezoelectricity, Acoustic Waves, and Device Applications (SPAWDA), IEEE: Chengdu, China, 2017, pp. 251–254.
- [568] A. Butler, et al., Multimode directional telesonar transducer, in: OCEANS 2000 MTS/IEEE Conference and Exhibition. Conference Proceedings (Cat. No. 00CH37158), IEEE, 2000.
- [569] S.M. Covich, J.L. Butler, Rare-earth iron"square ring" dipole transducer, *J. Acoust. Soc. Am.* 72 (2) (1982) 313–315.
- [570] S. Ehrlich, Spherical acoustic transducer, in Google Patents. 1973, Raytheon Co: United States.
- [571] S.H. Ko, G.A. Brigham, J.L. Butler, Multimode spherical hydrophone, *J. Acoust. Soc. Am.* 56 (6) (1974) 1890–1898.
- [572] S.H. Ko, H.L. Pond, Improved design of spherical multimode hydrophone, *J. Acoust. Soc. Am.* 64 (5) (1978) 1270–1277.
- [573] R.S. Gordon, L. Parad, J.L. Butler, Equivalent circuit of a ceramic ring transducer operated in the dipole mode, *J. Acoust. Soc. Am.* 58 (6) (1975) 1311–1314.
- [574] J.L. Butler, S.L. Ehrlich, Superdirective spherical radiator, *J. Acoust. Soc. Am.* 61 (6) (1977) 1427–1431.
- [575] A. Butler, et al., A trimodal directional modem transducer, in: Oceans 2003. Celebrating the Past... Teaming Toward the Future (IEEE Cat. No. 03CH37492), IEEE, San Diego, CA, USA, 2003, pp. 1554–1560.
- [576] Y. Lim, et al., Design of a multimode type ring vector sensor, *J. Acoust. Soc. Korea* 32 (6) (2013) 484–493.
- [577] Y. Lim, Y. Roh, Incidence angle estimation by the Tonpilz type underwater acoustic vector sensor with a quadrupole structure, *J. Acoust. Soc. Korea* 31 (8) (2012) 569–579.
- [578] Y. Lim, Y. Roh, Fabrication and characterization of an underwater acoustic Tonpilz vector sensor for the estimation of sound source direction, *J. Acoust. Soc. Korea* 34 (5) (2015) 351–359.
- [579] W.-J. Kim, et al., Direction-of-Arrival estimation for the ring-type multimode vector hydrophone based on the pressure gradient-acceleration relationship, *J. Acoust. Soc. Korea* 34 (1) (2015) 66–74.
- [580] J. Kim, S. Pyo, Y. Roh, Analysis of a thickness-shear mode vibrator for the accelerometer in vector hydrophones, *Sens. Actuators A Phys.* 266 (2017) 9–14.
- [581] Y. Roh, S. Pyo, S. Lee, Design of an accelerometer to maximize the performance of vector hydrophones, in: Nano-, Bio-, Info-Tech Sensors, and 3D Systems II, International Society for Optics and Photonics, Denver, Colorado, United States, 2018, pp. 1059707.
- [582] P.A. Włodkowski, K. Deng, M. Kahn, The development of high-sensitivity, low-noise accelerometers utilizing single crystal piezoelectric materials, *Sens. Actuators A Phys.* 90 (1-2) (2001) 125–131.
- [583] K.K. Deng, Underwater acoustic vector sensor using transverse-response free, shear mode, PMN-PT crystal, in Google Patents. 2006, Amphenol (maryland) Inc United States.
- [584] S. Pyo, et al., Development of vector hydrophone using thickness-shear mode piezoelectric single crystal accelerometer, *Sens. Actuators A Phys.* 283 (2018) 220–227.
- [585] K. Hyynen, et al., 500-element ultrasound phased array system for noninvasive focal surgery of the brain: a preliminary rabbit study with ex vivo human skulls, *Magn. Reson. Med.* 52 (1) (2004) 100–107.
- [586] J. White, G.T. Clement, K. Hyynen, Transcranial ultrasound focus reconstruction with phase and amplitude correction, *IEEE Trans. Ultrason. Ferroelectr. Freq. Control* 52 (9) (2005) 1518–1522.
- [587] J.J. Choi, et al., Noninvasive, transcranial and localized opening of the blood-brain barrier using focused ultrasound in mice, *Ultrasound Med. Biol.* 33 (1) (2007) 95–104.
- [588] E. Konofagou, et al., Ultrasound-induced blood-brain barrier opening, *Curr. Pharm. Biotechnol.* 13 (7) (2012) 1332–1345.
- [589] J.L. Robertson, et al., Accurate simulation of transcranial ultrasound propagation for ultrasonic neuromodulation and stimulation, *J. Acoust. Soc. Am.* 141 (3) (2017) 1726–1738.
- [590] C.I. Zanelli, S.M. Howard, A robust hydrophone for HIFU metrology, in: G.T. Clement, N.J. McDannold, K. Hyynen (Eds.), 5th International Symposium held 27–29 October 2005 in Boston, Massachusetts, American Institute of Physics, 2006, pp. 618–622.
- [591] A. Rahim, et al., Physical parameters affecting ultrasound/microbubble-mediated gene delivery efficiency in vitro, *Ultrasound Med. Biol.* 32 (8) (2006) 1269–1279.
- [592] J.A. Brown, et al., Fabrication and performance of a 40-MHz linear array based on a 1-3 composite with geometric elevation focusing, *IEEE Trans. Ultrason. Ferroelectr. Freq. Control* 54 (9) (2007) 1888–1894.
- [593] R.G. Holt, R.A. Roy, Measurements of bubble-enhanced heating from focused, MHz-frequency ultrasound in a tissue-mimicking material, *Ultrasound Med. Biol.* 27 (10) (2001) 1399–1412.
- [594] T. Giesecke, K. Hyynen, Ultrasound-mediated cavitation thresholds of liquid perfluorocarbon droplets in vitro, *Ultrasound Med. Biol.* 29 (9) (2003) 1359–1365.
- [595] C. Chandrana, et al., Design and analysis of MEMS based PVDF ultrasonic transducers for vascular imaging, *Sensors* 10 (9) (2010) 8740–8750.
- [596] A.D. Maxwell, et al., Cavitation clouds created by shock scattering from bubbles during histotripsy, *J. Acoust. Soc. Am.* 130 (4) (2011) 1888–1898.
- [597] W. Kreider, et al., Characterization of a multi-element clinical HIFU system using acoustic holography and nonlinear modeling, *IEEE Trans. Ultrason. Ferroelectr. Freq. Control* 60 (8) (2013) 1683–1698.
- [598] E. Vlaisavljevich, et al., Effects of ultrasound frequency and tissue stiffness on the histotripsy intrinsic threshold for cavitation, *Ultrasound Med. Biol.* 41 (6) (2015) 1651–1667.
- [599] A.D. Maxwell, et al., Fragmentation of urinary calculi in vitro by burst wave lithotripsy, *J. Urol.* 193 (1) (2015) 338–344.
- [600] D. Gross, E. Filoux, J.A. Ketterling, Multiple-frequency calibration of two-dimensional hydrophone arrays for instantaneous beam width measurements of shock-wave lithotripters, in: 2011 IEEE International Ultrasonics Symposium, IEEE: Orlando, FL, USA, 2011, pp. 1660–1663.
- [601] J.M. Mari, et al., Needle-tip localization using an optical fibre hydrophone, in: Optical Fibers and Sensors for Medical Diagnostics and Treatment Applications XIV, International Society for Optics and Photonics, San Francisco, California, United States, 2014, pp. 893804.
- [602] X. Song, et al., New Research on MEMS acoustic vector sensors used in pipeline ground markers, *Sensors* 15 (1) (2015) 274–284.
- [603] M. Chitre, S. Shahabudeen, M. Stojanovic, Underwater acoustic communications and networking: recent advances and future challenges, *Mar. Technol. Soc. J.* 42 (1) (2008) 103–116.
- [604] Z. Jian, et al., The design and research of intelligent search and rescue device based on sonar detection and Marine Battery, in: 2017 International Conference on Computer Network, Electronic and Automation (ICCNEA), IEEE: Xi'an, China, 2017, pp. 383–387.
- [605] J.E. Dusek, M.S. Triantafyllou, J.H. Lang, Piezoresistive foam sensor arrays for marine applications, *Sens. Actuators A Phys.* 248 (2016) 173–183.
- [606] S.G. Shock, et al., Buried object scanning sonar, *IEEE J. Ocean. Eng.* 26 (4) (2001) 677–689.
- [607] C.Y. Joh, G.C. Kim, O.C. Kwon, Supporting structure of hydrophones for towed array sonar system, in Google Patents. 2002, Agency for Defence Development United States.
- [608] C. Zhu, et al., Long-range automatic detection, acoustic signature characterization and bearing-time estimation of multiple ships with coherent hydrophone array, *Remote Sens. (Basel)* 12 (22) (2020) 3731.
- [609] M. Siderius, C.H. Harrison, M.B. Porter, A passive fathometer technique for imaging seabed layering using ambient noise, *J. Acoust. Soc. Am.* 120 (3) (2006) 1315–1323.
- [610] X. He, S. Shi, Measuring reflection coefficient of underwater acoustic materials with the vector hydrophone, in: 2011 International Conference of Information Technology, Computer Engineering and Management Sciences, IEEE, 2011.
- [611] C. Gervaise, et al., Passive geoaoustic inversion with a single hydrophone using broadband ship noise, *J. Acoust. Soc. Am.* 131 (3) (2012) 1999–2010.
- [612] M.K. Prior, et al., Long-range detection and location of shallow underwater explosions using deep-sound-channel hydrophones, *IEEE J. Ocean. Eng.* 36 (4) (2011) 703–715.
- [613] A. Cotrufo, et al., A hydrophone prototype for ultra high energy neutrino acoustic detection, *Nucl. Instrum. Methods Phys. Res. A* 604 (1-2) (2009) S219–S221.
- [614] N. Goujon, et al., Applications of piezoelectric materials in oilfield services, *IEEE Trans. Ultrason. Ferroelectr. Freq. Control* 59 (9) (2012) 2042–2050.
- [615] E.T. Küsel, et al., Marine mammal tracks from two-hydrophone acoustic recordings made with a glider, *Ocean. Sci.* 13 (2) (2017) 273–288.
- [616] W. Liu, et al., An experimental sonobuoy system based on fiber optic vector hydrophone, in: Hyperspectral Remote Sensing Applications and Environmental Monitoring and Safety Testing Technology, International Society for Optics and Photonics, Beijing, China, 2016, pp. 1015608.
- [617] S.A. Holt, Distribution of red drum spawning sites identified by a towed hydrophone array, *Trans. Am. Fish. Soc.* 137 (2) (2008) 551–561.

- [618] A. Young, J. Soli, G. Hickman, Self-localization technique for unmanned underwater vehicles using sources of opportunity and a single hydrophone, in: OCEANS 2017-Anchorage, IEEE, Anchorage, Alaska, United States, 2017, pp. 1–6.
- [619] J. Meunier, F. Huguet, P. Meynier, Reservoir monitoring using permanent sources and vertical receiver antennae: the Céré-la-Ronde case study, *Lead. Edge* 20 (6) (2001) 622–629.

Biographies

Hamid Saheban received the B.Sc. degree in electrical engineering from ITMC (Iranian Telecommunication Manufacturing Company (University of Applied Science and Technology, Shiraz, Iran, in 2016. He is currently pursuing the M.Sc. degree in electrical engineering with the Shiraz University of Technology, Shiraz, Iran, under

the supervision of Dr. Z. Kordrostami. His research interests include MEMS sensors and actuators, hydrophones, bio-sensors and optimization.

Zoheir Kordrostami received the B.Sc. degree in electrical engineering from the K.N. Toosi University of Technology, Tehran, Iran, in 2005, and the M.Sc. and Ph.D. degrees in electronics from Shiraz University, Shiraz, Iran, in 2007 and 2012, respectively. Since 2013, he has been an Assistant Professor with the Electrical and Electronic Engineering Department, Shiraz University of Technology, Shiraz. His research interests include nanoelectronics, solid-state electronic devices, MEMS, and sensors. Dr. Kordrostami received the best paper awards at the International Conference on Nanoscience and Technology (ChinaNano), Beijing, China, in 2009, the International Conference on Nanoscience and Nanotechnology, Shiraz, in 2010, and the International Conference on Nanostructures, Tehran, in 2018.